**Samina Arshid**

# Avaliação do efeito do précondicionamento isquêmico no proteoma e fosfoproteoma de neutrófilos de ratos após isquemia/reperfusão

SÃO PAULO

2016

Versão corrigida

Resolução CoPGr 6018/11, 01/11/2011

**Samina Arshid**

# Avaliação do efeito do précondicionamento isquêmico no proteoma e fosfoproteoma de neutrófilos de ratos após isquemia/reperfusão

Tese apresentada à Faculdade de Medicina
da Universidade de São Paulo para obtenção do título
de Doutor em Ciências
Programa de: Clínica Cirúrgica
Orientador: Prof. Dr. Belchor Fontes
Coorientador: Prof. Dr. Wagner Fontes

SÃO PAULO
2016

**Dados Internacionais de Catalogação na Publicação (CIP)**

Preparada pela Biblioteca da
Faculdade de Medicina da Universidade de São Paulo



Arshid, Samina
Avaliação do efeito do pré-condicionamento isquêmico no proteoma e fosfoproteoma de neutrófilos de ratos após isquemia/reperfusão / Samina Arshid. -- São Paulo, 2016.
Tese(doutorado)--Faculdade de Medicina da Universidade de São Paulo. Programa de Clínica Cirúrgica.
Orientador: Belchor Fontes.
Coorientador: Wagner Fontes.

Descritores: 1.Isquemia 2.Traumatismo por reperfusão 3.Precondicionamento isquêmico 4.Ativação de neutrófilo 5.Síndrome de resposta inflamatória sistêmica 6.Proteoma

USP/FM/DBD-260/16

# DEDICATION

**DEDICATION**

To my husband **Muhammad Tahir**, who has always been there for me in good and bad times, with patience and care, giving all the necessary support, unconditional love, patience and encouragement so that together we reached this point that is very important in our lives.

To my children **Ayan Tahir** and **Ahmad Tahir**, who are the greatest achievements of my life, for always making me smile and understanding times when I was busy. Without you no achievement is worth.

To my father **Arshid Mehmood** and Father in-law **Taj Merin** who have always served me as supporting persons with dedication and honesty.

To my mother **Farzana Iqbal** (Late), who dedicated her entire life for me and whose faith in me taught me to have faith in myself.

To all of my other family members without whom no event is special and complete in my life. They always guide and encourage me during every moment of my life.

# ACKNOWLEDGMENT

## ACKNOWLEDGMENT

To **Prof. Dr. Belchor Fontes**, for his kind supervision, useful suggestions, consistent encouragement, friendly behavior and dynamic supervision enabled me to perform my research work in ensuring my academic, professional and moral well-being.

To **Prof. Dr. Wagner Fontes,** as a co-supervisor, for his co-operation in providing me all possible facilities during my research at Laboratory of Biochemistry and Protein chemistry (LBQP), University of Brasilia (UnB). With all the help offered, availability, incredible scientific spirit, guidance and knowledge offered. Besides a great example of life, professionalism and dedication, he is also a great friend.

To **Prof. Dr. Edna Montero** for her support during research at LIM 62 and for all the opportunities offered for the surgical teaching procedures carried for this work.

To **Prof. Dr. Peter Roepstorff**, for all the opportunities offered at Southern University Denmark for the proteomics analysis and other professional support and help, who for me, will always serve as an example.

To **Prof. Veit Schwämmle** at Southern University Denmark, who guided in the analysis of the data sets provided his bioinformatics experience and expertise.

To **Dr. Simone Sidoli** at Southern University Denmark, who also helped in statisctical analysis of proteomic data.

To the **Prof. Dr. Vilma** for providing access to her lab to use the sonicator facility.

To the biologist **Dr. Muhammad Tahir**, for all the help offered, availability, incredible scientific spirit and all the guidance and knowledge offered. Without whom the success of this project was not possible.

To biologist **Ana Maria Heimbecker,** for providing practical experience as a research assistant, for the patience ad efforts in the surgical experiments from the beginning.

To **Marco Luna**, for his key role in enabling the experiments, impeccable organization and careful observation of animals.

To Biologist **Mario Itinoshi**, for all the help and availability from part of practice until the paperwork involving the project.

To pharmaceutical **Lucí Takasaka**, who kindly took turns in supporting surgical procedures and collection of materials.

To **Eliane Falconi Monico Gazetto**, in the office of graduate for the care, organization and who always answered my numerous questions with patience and kindness.

To **CAPES, CNPq** and **FAPDF** for financial support to run the project.

Esta tese está de acordo com as seguintes normas em vigor no momento da sua impressão:

Referências: Adaptado de *International Commitee of Medical Journals Editors (Vancouver)*.

Universidade de São Paulo. Faculdade de Medicina. Serviço de Biblioteca e Documentação. *Guia de apresentação de dissertações, teses e monografias*. Elaborado por Anneliese Carneiro da Cunha, Maria Júlia de A. L. Freddi, Maria F. Crestana, Marinalva de Souza Aragão, Suely Campos Cardoso, Valéria Vilhena. 2ª Ed. São Paulo: Serviço de Biblioteca e Documentação; 2005.

Abreviaturas dos títulos dos periódicos de acordo com *Listo f Journals Indexed in Index Medicus*.

## LIST OF ABBREVIATIONS

| | |
|---|---|
| Et al | And others |
| Fig | Figure |

**List of Symbols**

| | |
|---|---|
| Da | Dalton |
| g | Gravity |
| kg | Kilogram |
| mg | Milligram |
| ml | Milliliter |
| mM | Millimolar |
| rpm | Rotation per minute |

## List of Acronyms

| | |
|---|---|
| 1DE | One-dimensional gel electrophoresis |
| 2DE | Two-dimensional gel electrophoresis |
| 6PGDH | 6-phosphogluconate dehydrogenase |
| AA | Arachidonic acid |
| ACN | Acetonitrile |
| ADORA2B | Receptor, adenosine A2B |

| | |
|---|---|
| ALI | Acute lung injury |
| ARDS | Respiratory distress syndrome, adult |
| ATP | Adenosine triphosphate |
| BAL | Bronchoalveolar lavage |
| C3a | Complement C3 |
| CAMKS | Calcium-calmodulin-dependent protein kinases |
| CD11B | Antigens, cd11b |
| CID | Collision-induced dissociation |
| CINC-1 | Cytokine-induced neutrophil chemoattractant 1 |
| CXCR | Cxc chemokine receptors |
| DB3 | Dilution buffer 3 |
| DNA | Deoxyribonucleic acid |
| DOCK2 | Dedicator of cytokinesis 2 |
| ECS | Endothelial cells |
| EIF4B | Eukaryotic translation initiation factor 4b |
| ERK1/2 | Extracellular signal-regulated protein kinase-1/2 |
| ESI | Electrospray ionization |
| FAK | Focal adhesion kinase |
| FGR | Gardner-rasheed feline |
| FMLP | N-formylmethionyl-leucyl-phenylalanine |

| | |
|---|---|
| GCSF | Granulocyte-colony stimulating factor |
| GM-CSF | Granulocyte-macrophage colony-stimulating factor |
| GPS | Group-based prediction system |
| GRK2 | G protein-coupled receptor kinase 2 |
| H2O2 | Hydrogen peroxide |
| HCD | Higher-energy collisional dissociation |
| HILIC | Hydrophilic interaction chromatography |
| HO-1 | Heme-oxygenase-1 |
| HPLC | High performance liquid chromatography |
| HPLC | High performance liquid chromatography |
| IGPS | Gps algorithm with the interaction filter |
| ILS | Interlukeins |
| IMAC | Immobilized metal affinity chromatography |
| INPP5C | Inositol polyphosphate 5-phosphatase |
| INPP5D | Inositol polyphosphate-5-phosphatase D |
| IPC | Ischemic preconditioning |
| IR | Ischemic reperfusion |
| IRAK-4 | Interleukin-1 receptor-associated kinase-4 |
| ITRAQ | Isobaric tags for relative and absolute quantitation |
| KEGG | Kyoto encyclopedia of genes and genomes |

| | |
|---|---|
| LC-MS/MS | Liquid chromatography–mass spectrometry |
| LPS | Lipopolysaccharide |
| LIM-62 | Laboratory of Surgical Physiopathology, department of Surgery of FMUSP |
| LBQP | Laboratory of Biochemistry and Protein Chemistry of UnB |
| LTB4 | Leukotriene B4 |
| MALDI-MS | Matrix-assisted laser desorption/ionization |
| MAPK | Mitogen-activated protein kinases |
| MAPKAPK2 | MAPK activated protein kinase 2 |
| MCM | Mini-chromosome maintenance proteins |
| MOAC | Metal oxide affinity chromatography |
| MOF | Multiple organ failure |
| MPV | Mean platelet volume |
| MS | Mass spectrometer |
| MS/MS | Tandem mass spectrometry |
| NADPH | Nicotinamide adenine dinucleotide phosphate |
| NDR1 | Non-race specific disease resistance 1 |
| NF-KB | Nuclear factor kappa B |
| OXSR1 | Oxidative stress responsive 1 |
| PAF | Platelet-activating factor |
| PAK | P21 protein activated kinase |

| | |
|---|---|
| PCBP1 | Poly(rc)-binding protein 1 |
| PDCD4 | Programmed cell death protein 4 |
| PDW | Platelet distribution width |
| PECAM-1 | Platelet endothelial cell adhesion molecule |
| PIP2 | Phosphatidylinositol biphosphate |
| PK | Protein kinase |
| PKCδ | Protein kinase c delta |
| PKN1 | Serine/threonine-protein kinase n1 |
| PMNS | Polymorphonuclear neutrophils |
| PR3 | Proteinase 3 |
| PSGL-1 | P-selectin glycoprotein ligand 1 |
| PSSM | Position-specific scoring matrices |
| PTB | Phosphotyrosine-binding |
| PTM | Post translational modification |
| PTP | Phosphotyrosine phosphatase |
| PTPN6 | Tyrosine-protein phosphatase non-receptor type 6 |
| PTPRC | Receptor-type tyrosine-protein phosphatase C |
| RAC2 | Ras-related c3 botulinum toxin substrate 2 |
| RHOA | Ras homolog gene family, member A |
| RNA | Ribonucleic acid |

| | |
|---|---|
| ROS | Reactive oxygen species |
| RPS6 | Ribosomal protein s6 |
| RPS6KA2 | Ribosomal protein s6 kinase alpha-2 |
| RSK1 | Ribosomal s6 kinase 1 |
| SCOP | Structural classification of proteins |
| SDS | Sodium dodecyl sulfate |
| SDSPAGE | Sodium dodecyl sulfate polyacrylamide gel electrophoresis |
| SDU | University of Southern Denmark |
| SHIP | Sh2-containing inositol-5'-phosphatase 1 |
| SHP1 | Src homology region 2 domain-containing phosphatase-1 |
| SILAC | Stable isotope labeling with amino acids in cell culture |
| SIMAC | Sequential elution from IMAC |
| SIRS | Systemic inflammatory response syndrome |
| SLK | Ste20 like kinase |
| SMAO | Acute superior mesenteric artery occlusion |
| SOD | Superoxide dismutase |
| SPH | Serine phosphorylation |
| SPT16 | Component of the fact complex |
| STK38 | Serine/threonine-protein kinase 38 |
| STY | Serine, threonine or tyrosine residues |

| | |
|---|---|
| SYK | Spleen tyrosine kinase, |
| TEAB | Triethylammonium bicarbonate |
| TEC | Tyrosine-protein kinase |
| TIO2 | Titanium dioxide |
| TLR | Toll-like receptors |
| TNF | Tumor necrosis factor |
| TOF | Time of flight |
| U2AF2 | U2 small nuclear auxiliary factor 2 |

## LIST OF FIGURES

## LIST OF GRAPHS

## LIST OF TABLES

# TABLE OF CONTENTS

# Resumo

Arshid S. *Avaliação do efeito do précondicionamento isquêmico no proteoma e fosfoproteoma de neutrófilos de ratos após isquemia/reperfusão* [Tese]. São Paulo: Faculdade de Medicina, Universidade de São Paulo; 2016.

**Introdução**: O trauma é um fenômeno que cursa com lesão tecidual, sendo que o trauma cirúrgico (TC) apresenta a referida lesão como consequência de um ato cirúrgico. A isquemia seguida de reperfusão (IR) é um evento comum em várias condições patológicas, bem como em diversos procedimentos cirúrgicos, principalmente transplantes. É frequente o desenvolvimento de lesões teciduais locais e remotas após trauma e após a I/R, parte de um fenômeno conhecido como síndrome da resposta inflamatória sistêmica (SRIS), frequentemente seguida pela falência de múltiplos órgãos (FMO). Estudos provaram o envolvimento do neutrófilo em tais síndromes como resultado da ação de enzimas proteolíticas secretadas a partir de grânulos citoplasmáticos, radicais livres produzidos por explosão respiratória e citocinas liberadas após a infiltração nos tecidos. Nesse contexto, foi provado que o pré-condicionamento isquêmico (PCI), definido como curtos episódios de isquemia precedendo a IR, protege contra essas lesões, com menor ativação de neutrófilos. No entanto, o conhecimento a respeito dos mecanismos operantes nos neutrófilos após o trauma cirúrgico, a isquemia seguida de reperfusão ou o pré-condicionamento isquêmico, ainda são preliminares. **Objetivo**: Analisar com maior profundidade o impacto dessas condições (TC, IR e PCI) no proteoma e fosfoproteoma do neutrófilo. Métodos: Foi realizada a análise de parâmetros hematológicos juntamente com a análise proteômica e fosfoproteômica de neutrófilos de ratos submetidos a TC, IR e PCI, comparados ao grupo controle. A análise proteômica foi realizada em sistema de nLC-MS/MS orbitrap de alto desempenho, usando marcação com iTRAQ, enriquecimento de fosfopeptídios e pré-fracionamento por HILIC. A análise estatística baseada em clusters utilizando scripts em R mostrou proteínas com abundância relativa diferencial em todas as condições. **Resultados**: A avaliação dos parâmetros hematológicos antes e depois de TC, IR e IPC demonstrou alterações no número, forma e tamanho de linfócitos, hemácias, plaquetas e, principalmente, neutrófilos (granulócitos). Observou-se um claro aumento na contagem de neutrófilos após TC e IR, sendo que tal aumento foi prevenido pelo PCI. Um total de 393 proteínas foram determinadas como reguladas para

abundância relativa entre o grupo controle e o grupo TC. A maioria das proteínas encontradas como reguladas em comum nos grupos TC e IR estão relacionadas à apoptose (caspase-3), motilidade celular (PAK2), transdução de sinal (IL-5, IL-6 e TNF) e degradação pelo sistema proteassoma no neutrófilo. Maior produção de espécies reativas de oxigênio e disfunção da migração direcional de neutrófilos (PKC-delta) com aumento do tempo de vida dos neutrófilos são eventos iniciais importantes que podem resultar em mais dano tecidual e em infecção. A análise proteômica de neutrófilos de ratos após PCI levou à identificação de 2437 grupos de proteínas atribuídos a 5 clusters diferentes, contendo proteínas de abundância relativa significativamente aumentada ou diminuída em IR e PCI. O estudo de vias desses clusters baseado no KEGG revelou aumento nas vias de fagocitose mediada por Fc-gama R, sinalização por quimiocinas, adesão focal e migração transendotelial, citoesqueleto de actina, metabolismo e diminuição nas vias ribossomais, de transporte de RNA, de processamento de proteínas. A regulação da fosforilação de proteínas após IR e PCI mostrou algumas vias como quimiocinas, Fc-gama, GPCR, migração celular e vias pró e antiapoptóticas, sendo que a via de splicing alternativo foi a que apresentou regulação mais evidente ($p<0.0001$). A regulação da abundância, bem como da fosforilação, presença de motivos e de domínios levou à identificação de fosfatases, como Fgr, GRK2, PKC delta, ptpn6 e ptprc reguladas por IR, bem como stk38, pkn1, syk e inpp5d reguladas por PCI. A interação mais marcante entre proteínas foi demonstrada como sendo entre os receptores de Fgr e Ptp. **Conclusão**: Concluímos que as alterações causadas por TC, IR e PCI levaram a intenss alterações na abundância de algumas proteínas e em eventos de fosforilação em neutrófilos, levando ao efeito destrutivo observado após a IR e ao efeito protetor consequente ao PCI.

**Descritores:** Isquemia, Traumatismo por reperfusão, Precondicionamento isquêmico, Ativação de neutrófilo, Síndrome de resposta inflamatória sistêmica, Proteoma.

# Abstract

Arshid S. *Evaluation of the effect of ischemic preconditioning on the proteome and phosphoproteome of rat neutrophils after ischemia/reperfusion* [Thesis]. São Paulo: "Faculdade de Medicina, Universidade de São Paulo": 2016.

**Introduction:** Trauma is a phenomenon that involves tissue injury, whereas the surgical trauma (ST) has such injury as a consequence of a surgery. Ischemia reperfusion is common event in many surgical procedures, especially in transplants, as well as in many pathological conditions. Local and remote tissue injuries usually develop after trauma and ischemic reperfusion, part of a phenomenon known as systemic inflammatory response syndrome, frequently followed by multiple organ failure (MOF). Studies have proven the involvement of the neutrophil in all these injuries as a result of proteolytic enzymes secreted from cytoplasmic granules, free radicals produced by respiratory burst, cytokines released after tissue infiltration. In that context, ischemic preconditioning (IPC), that are short episodes of ischemia before ischemia reperfusion, was proved to be protective against these injuries with less activation of neutrophils. However the knowledge about the underlying mechanism operating in the neutrophil after surgical trauma, ischemia reperfusion and preconditioning is preliminary. **Objective:** To deeply analyze the impact of these conditions (ST, IR and IPC) on the neutrophil proteome and phosphoproteome. **Methodology:** We did hematological analysis along proteomics and phospho proteomics through high throughput nLC-MS/MS analysis by orbitrap using iTRAQ labeling, phospho peptide enrichments, and HILIC pre-fractionation. Neutrophils from control, ST, IR and IPC conditions after extraction were processed for proteomic analysis. Statistical package using R based on cluster analysis led to the detection of differentially regulated proteins in all conditions. **Results:** The evaluation of the hematological parameters before and after ST, IR or IPC on blood cells stated alteration in size, number and shape of lymphocytes, RBCs, platelets and specially neutrophils (granulocytes). In the analysis, a clear increase in neutrophil count after ST and IR with such increase prevented by IPC. A total of 393 proteins were found differentially regulated between control and trauma groups. Most of the common proteins found regulated in trauma and IR seem to be related to apoptosis (caspase-3), cell motility (PAK2) and signal transduction in IL5, IL6 and TNF

and proteasomal degradation in neutrophil. Higher oxygen species production and dysfunction of directional neutrophil migration (PKC delta) with increase in the life span of neutrophils are early important events that can finally result into more tissue damage and infection. The total proteomic analysis of rat neutrophils after IPC led to the identification of 2437 protein groups assigned to five different clusters with significantly up and downregulated proteins in IR and IPC. Cluster based KEGG pathways analysis revealed up-regulation of chemokine signaling, focal adhesion, leukocyte transendothelial migration, actin cytoskeleton, metabolism and Fc gamma R mediated phagocytosis, whereas downregulation in ribosome, spliceosome, RNA transport, protein processing in endoplasmic reticulum and proteasome, after intestinal ischemic preconditioning. The phosphoregulated proteins containing domains and motifs in the regulated peptides after IR and IPC led to the identification of some of important players such as chemokine, Fc gamma, GPCR, migration and pro/anti-apoptotic pathways. The phosphoproteins from alternative splicing was the pathway presenting the most remarkable regulation with a p-value of 0.0001. The regulation in expression as well as in phosphorylation, the presence of motifs and domains led to the identification of kinases and phosphatases including Fgr, GRK2, PKC delta, ptpn6 and ptprc in neutrophils after IR whereas stk38, pkn1, syk, and inpp5d in neutrophil due to IPC. The highest protein-protein interaction was shown by Fgr and Ptp receptors. **Conclusion:** We concluded that the changed stimulus produced after ST, IR and IPC led to the huge alteration in proteins expression and phosphorylation events in the neutrophil proteome as mentioned in our work, that leads to final destructive and protective phenotype of neutrophils respectively.

**Descriptors:** Ischemia, Reperfusion Injury, Ischemic preconditioning, Neutrophil activation, Systemic inflammatory response syndrome, Proteome.

# Introduction

# 1 INTRODUCTION

## 1.1 Neutrophils and trauma

Polymorphonuclear neutrophils [1] are part of the peripheral blood and play an important role in microbe clearance as a part of the innate immune system. Many studies showed an involvement of PMNs in the pathophysiology of trauma-related organ failure [3]. The surgical trauma (ST) is characterized as the tissue damage naturally consequent to any surgery, typically in an acute condition, varying in intensity and in physiological consequences, related to the characteristics of the surgical procedure. Abdominal surgery often alters the physical and immune function in human and animals [4,5]. An increase in neutrophil count and decrease in percentage of phagocytic neutrophils is an important event occurring after ST [6]. The increase in neutrophil life and released cytotoxic products at the site of injury may cause further damage [7]. The initial changes in neutrophil activation at proteomic level can be helpful for the better understanding of the underlying mechanisms followed by ST.

## 1.2 Neutrophils and intestinal ischemia/reperfusion injury

Ischemia is a common event during various traumatic and surgical events, especially in transplants, as well as in many pathological conditions. It often results in damage to active metabolic tissues whereas reperfusion to these ischemic tissues initiates events that aggravate tissue injury, a phenomenon called reperfusion injury [8]. In the tissue, mitochondria are the first intracellular sites of abnormality during ischemia due to the production of adenosine triphosphate (ATP) which is required for tissue recovery [9]. The mechanism underlying reperfusion injury is complicated and involves many factors. Among these, the generation of reactive oxygen species (ROS) produced upon the re-introduction of molecular oxygen during reperfusion. Other factors include an overload of calcium along with the opening of the mitochondrial permeability transition pore, hypoxanthine accumulation, endothelial dysfunction, expression of pro-inflammatory molecules like leukocyte adhesion molecules and cytokines production [10].

Ischemia/Reperfusion (IR) injury in the intestine can be caused by many clinical conditions like acute mesenteric ischemia, intestinal obstruction, small intestine

transplantation, neonatal necrotizing enterocolitis, incarcerated hernia, trauma, and shock that can result in severe clinical syndromes and even death [11,12]. For example, acute mesenteric ischemia has an overall mortality of 60% to 80%, and the reported incidence is increasing with time [13,14], the major reason for the high mortality rate is the continued difficulty in recognizing the conditions [14]. The intestinal reperfusion injury causes not only local acute inflammatory response, but also noteworthy pulmonary injury and systemic inflammatory changes [15]. Occurrence of the systemic inflammatory response syndrome [16] after IR is common and can develop into multiple organ failure (MOF) [17]. In such process, the pulmonary infiltration of neutrophils contributes to the development of acute respiratory distress syndrome (ARDS) and acute lung injury (ALI) [18].

During IR the intestinal mucosa starts producing various acute phase proteins [19], gut hormones [20], cytokines [21], reactive oxygen species [22], nitric oxide [23], arachidonic acid derivatives [24], cell adhesion molecules [25], nuclear factor-κB (NFκB) [20], granulocyte colony stimulating factor and IL-6 followed by polymorphonuclear neutrophil (PMNs) recruitment to the intestine [26].

Many studies showed an involvement of PMNs in the pathophysiology of IR. Intestinal reperfusion injury primarily takes place due to leukocytes and endothelial cells (ECs) interactions in the intestinal mucosa [27]. Depletion of PMNs from blood before reperfusion has shown to decrease effect of IR in the human small bowel [21]. Intra-vital microscopy studies of tissues following IR showed an acute inflammatory response due to increased protein efflux and PMNs adhesion in post capillary venules [28]. It was shown that after IR of the mouse intestine, both P- and E-selectins were overexpressed on neutrophils and ECs respectively. Blocking of P-selectins has reduced PMN rolling and adhesion so attenuating the injury [29]. PMNs cause damage by different ways like secretion of proteolytic enzymes from cytoplasmic granules [30], free radicals production by respiratory burst [31], and damage to microcirculation and extension of ischemia [15]. Pharmacological strategies which reduced neutrophil infiltration to tissues also reduced the ischemia/reperfusion injury (IRI) [32,33]. A study confirmed that PMNs are the initial source of free radicals in a rat model of IRI of the intestine [34]. The exact

mechanism by which neutrophils take part in IRI is still unknown.

### 1.3 Neutrophil and ischemic preconditioning (IPC)

The phenomenon of short episodes of ischemia and reperfusion before a long ischemia and reperfusion is known as Ischemic preconditioning (IPC). It was first described almost 30 years ago and has been proved to protect organs against IR injury [35]. After that the role of IPC has been tested in many animals and in human [36,37], in many organs including skeletal muscle [38], brain [39], spinal cord [40], kidney [41], intestine [42], lung [43], retina [44], and liver [45]. It is evident from the studies that IPC was also beneficial in the human heart [46] and the liver [41].

In 1996, the effect of IPC was checked in the intestine [47] and later studies have confirmed this phenomenon. One of the positive effects of IPC on the intestine was the decreased bacterial translocation from the intestine in rats [48]. The effects of IPC can be divided into two phases depending on time frames and mechanisms. An early phase starting immediately after ischemia and lasts 2–3 hours followed by a late phase beginning after 12–24 hours from the ischemia and lasting for about 3–4 days. The early phase starts within minutes and leads to changes in specific cell functions, whereas the late phase activates multiple stress response genes and new proteins synthesis [49,50]. However, the protective mechanism underlying IPC is also not clear yet.

The initial signals that are released from intestine and surgical sites (or other trauma sites) could be similar in the form of pro-inflammatory cytokines, such as TNF-alpha [51]. These alarm signals can be secreted by healthy cells or released by necrotic cells, which are present at the site of injury. The response of PMNs depends on both, the type of alarm signals and type of tissue (intestinal mucosa, other abdominal tissues or blood). These signals comprise mediators like cytokines, chemokines and complement [2, 4, 5]. Additionally, IL-10, an anti-inflammatory cytokine seemed to be protective either administrated or endogenously produced after IPC [52]. The protective effects of IPC on the small intestine has been correlated with the inhibition of epithelial cell apoptosis, involvement of several mediators like adenosine, nitric oxide (NO), oxidative stress, heme-oxygenase-1 and protein kinase C (PKC) [53]. Few studies explained the

changes in neutrophil behavior after IPC. A study done in vivo showed that IR caused profound and sustained endothelial dysfunction due to systemic neutrophil activation with elevated CD11b expression and formation of neutrophil-platelet complex, however IPC attenuated both effects [54]. Similarly, in patients having partial liver resection after 10 minutes of ischemic preconditioning resulted into less activation of PMNs with reduced cytokine plasma levels and superoxide anion production but increased $\beta_2$-integrin and IL8 [50]. Therefore, the down-regulation of cytotoxic functions of PMNs through an unknown mechanism might be an important step in mediating protection by ischemic preconditioning.

The blocking or depletion of neutrophils in experimental models results in a reduction of organ failure in the pro-inflammatory (early) phase. However, later, an increased incidence of organ failure was caused by severe infections during the anti-inflammatory [51] phase [55]. It seems more favorable to regulate the neutrophil behavior instead of shutting down this important defense mechanism. For the regulation of neutrophil activation, a more detailed knowledge of signal transduction pathways is necessary. IPC has shown to alter the neutrophil biology but the mechanism underlying was unknown. In this work we have tried to find the initial impact of these stimuli secreted from intestine on PMNs proteome after abdominal surgery, IR and IPC to provide a database for the future investigations.

### 1.4 Hematological analysis before and after IR and IPC

Hematological analyses, such as the complete blood count (CBC), can provide information regarding changes in patient's health. During illness, the CBC is useful in characterizing the severity of a disease whether it is a primary or secondary hematologic abnormality. Nowadays, automated hematology analyzers used in veterinary and human medicine provide complete, fast, accurate, and precise data as a result of advancements in technology [56]. The stimuli in form of cytokines and chemokines secreted by the intestine during ST, IR or IPC can directly affect the production of blood cell components such as erythrocytes, leukocytes and thrombocytes originated from stem cells in the bone marrow. The hematological parameters analyzed in this study were determination of the total erythrocyte count (RBC), total white blood cell count (WBC),

hematocrit (HCT), hemoglobin [57] concentration, erythrocyte indices (MCV, MCH, MCHC), and white blood cell differential count. In this way we have gathered the information about the neutrophils (granulocytes) along with RBCs and platelets. During various disease states, changes in size, shape and number of lymphocytes, monocytes, and neutrophils can also be analyzed. Additional hematologic parameters including red blood cell distribution width, mean platelet volume, platelet distribution width, and several others provide quantitative morphologic information about red blood cells and platelets that are helpful in discovering the cause to some hematologic abnormalities seen routinely in human and veterinary medicine [58]. Therefore evaluation the hematological parameters helped us to monitor the changes occurring before and after ST, IR or IPC on blood cells in rats [59]

## 1.5 Proteomic Analysis of Neutrophils (PMNs)

As the molecular mechanisms behind trauma, IR and IPC are not clear, our goal was to identify neutrophil proteins that present relative abundance changes between these conditions. In that sense, proteomic analysis of neutrophils with and without IPC was done. Although there are previous studies about neutrophil proteomics, there is still no study available on proteomic analysis of neutrophil after Intestinal Ischemic Preconditioning. For a deeper understanding of the neutrophil proteins taking part in molecular pathways involved in all of these conditions mentioned above such as trauma, IR and IPC, we also studied the phosphoproteome of rat neutrophils using iTRAQ for labeling peptides, both SIMAC and TiO2 for enrichment of phospho peptides, HILIC for the peptide fractionation and Orbitrap MSMS for quantification.

### 1.5.1 The neutrophil and quantitative proteomic studies after IR and IPC in intestine

There is need to identify protein expression of cells since not all the genes are translated into proteins, which is also true for neutrophils, where the correlation between mRNA and protein expression is inconsistent. There are limited proteomic studied of neutrophils particularly explaining the effect of the inflammatory response on the neutrophil proteome [60].

The first global analysis of the rat neutrophil proteins was done by two-dimensional gel electrophoresis (2DE) and MS approaches and identified 52 proteins [61]. Later 250 proteins were identified through a combination of 1DE followed by ESI-MS/MS from bovine neutrophils. Proteins identified belong to cell metabolism, cell motility, immune response, protein synthesis, cell signaling and membrane trafficking [62].

Proteomic analysis of gelatinase, specific, and azurophil granules by 2DE and MALDI-TOF identified 87 proteins including one membrane-spanning protein. Although the resolving ability of 2DE was limited this study identified differential expression of actin associated with all granules [63]. Cytoskeletal, structural, and membrane fusion proteins (247 proteins) were identified from human neutrophil azurophil granules lipid rafts by 10% SDS-PAGE and LC-MS/MS [64]. A similar study identified total of 23 proteins from plasma membrane lipid rafts using gradient gel electrophoresis and MALDI-MS/MS. Nine of the proteins belonging to the cytoskeleton were common to a previous study of human neutrophil azurophil granules lipid rafts [65]. Fessler et al. [66] identified 1200 proteins from neutrophil after exposure to lipopolysaccharide (LPS) for 4 h and found 100 upregulated proteins and another 100 downregulated proteins. 2DE followed by MALDI-TOF-MS identified substrates for MMP2 and MMP9 from the BAL fluid of mice. These substrates include Ym1, S100A8, and S100A9 that showed chemotactic activity [67]. Proteomic analysis of rat intestinal mucosa after ischemic preconditioning in IRI model identified 10 proteins using 2DE in combination with MALDI-TOF-MS and these proteins were involved in anti-oxidation, apoptosis inhibition and energy metabolism. This study also revealed up-regulation of aldehyde dehydrogenase and aldose reductase in IPC group [68]. A similar study used 2-DE combined with MALDI-MS to analyze the proteome of intestinal mucosa subjected to I/R injury in the absence or presence of IPC pretreatment in rats. In total 16 proteins were diferentially expressed attributed to cellular energy metabolism, anti-oxidation and anti-apoptosis of which aldose reductase that removes ROS, was significantly downregulated in IR and upregulated in IPC [49].

### 1.5.2 Neutrophils and the Phosphoproteomic studies

Protein phosphorylation, an essential and the most common post-translational modification (PTM) that affects most cellular activities including signal transduction, cell cycle progression, gene expression, and many other biological functions [69]. It is a reversible PTM that can induce conformational changes in the structure of proteins, leading to their activation or deactivation. The enzymes responsible for the transfer of a phosphoryl group from energy-rich organic compounds (like adenosine triphosphate, ATP) to the side chain of serine, threonine, or tyrosine are known as protein kinases, a family of proteins presenting over 500 members. Kinases have been predicted to encompass 1.7% of the human genes [70]. The estimated relative abundances of phosphoserine, phosphothreonine, and phosphotyrosine found in the human proteome was 90%, 10%, and 0.05%, respectively [71]. By hydrolysing the covalent phosphoester bond, protein phosphatases catalyse the enzymatic removal of these added phosphate groups from proteins, returning them to their non-phosphorylated state [72].

The complex dynamics of protein phosphorylation regulated by kinases and phosphatases can be disrupted in many diseases like cancer, diabetes, neurodegenerative and autoimmune diseases [73]. The detailed knowledge of phosphorylation and dephosphorylation on proteins taking place in different conditions is necessary to clearly understand the molecular mechanisms regulating such conditions, as well as to identify novel therapeutic targets and biomarkers. Various mechanisms including mutations, deregulation in the expression of kinases or phosphatases with increased or decreased enzymatic activity, substrate availability and epigenetic modifications can be involved during diseases [74].

As mentioned above, the phosphorylation-induced conformational changes regulate protein functions [74]. However sometimes it can disrupt the surfaces for protein-substrate interactions without inducing any conformational changes and can also create substrate -binding surface without inducing conformational changes [75].

Protein kinases (PK) can recognize their physiological substrates in cells with specificity due to the following two types of interactions. The first is between the active

site of the protein kinase and the consensus phosphorylation sequence of the substrate protein. The second is the distal binding between the kinase domain and the docking motif in the substrate. Both domain (in the kinase) and motif (in the substrate) are located distally from the active site and phosphorylation sequence respectively [76].

The identification of potential substrate for PK can be done with the knowledge of the structural basis of these interactions. Similarly, protein phosphatases have specificity for substrate due to specific interactions between interaction motifs or domains and distal docking motifs in protein substrates (other than the active site and phosphorylation site) [77]. The knowledge of specific dephosphorylation of the substrate due to the interaction between the active site of protein phosphatases with protein substrates is not complete. The dephosphorylation sequences of several protein tyrosine phosphatases have been defined by using the oriented phosphopeptide library approach [78]. The substrate trapping mutant approach allowed the identification of physiological protein substrates of many phosphatases. With the advances in bioinformatics and MS identification of phosphosites, a better understanding of the motifs surrounding such sites resulted into the development of the methodology for the extraction of motifs through the comparison to a dynamic statistical background. The identification of dozens of the novel known phosphorylation motifs for S\T\Y phosphorylation, along with consensus sequences of identified and unidentified kinases have been done [78].

Nowadays, Mass spectrometry (MS) being widely used for the quantitation and qualification of thousands of proteins and protein phosphorylations in a single run. The low stoichiometry, wide dynamic range, and the presence of various isoforms of phosphorylated proteins in the biological samples make it difficult. Luckily, these problems can be solved by using a combination of multidimensional separation methods, pre-fractionation and enrichment techniques before MS analysis [79].

## 1.6 Quantitative Phosphoproteomics

MS-based quantitative proteomics is used for biological and clinical research like the identification of functional modules and pathways or monitoring of disease biomarkers. The use of MS-based proteomic approaches is increasing day by day due to

sensitivity, mass accuracy and faster data analysis. Especially with the advancements in the residue specific stable isotope labelling methods, the quantification of proteins in different conditions is now possible in a single run with higher reproducibility [80-82]. Among the many labeling methods, iTRAQ allowed simultaneous relative and absolute labelling quantitation of four or eight samples and is independent of protein synthesis [83,84].

The isobaric labels used for primary amines (N-terminus and the ε-amino group of the lysine side chain) have a total mass of 145 Da composed by a unique reporter group, a peptide reactive group, and a neutral balance group (Fig-1). During peptide fragmentation in MS/MS, reporter groups separate from isobaric tags and produce distinguishable ions with m/z 114, 115, 116 and 117. In this way, the relative intensities of the reporter ions give the relative abundances of each peptide in the samples. This MS/MS fragmentation of tagged peptides also produces strong y- and b-ion signals for more confident identification [85].

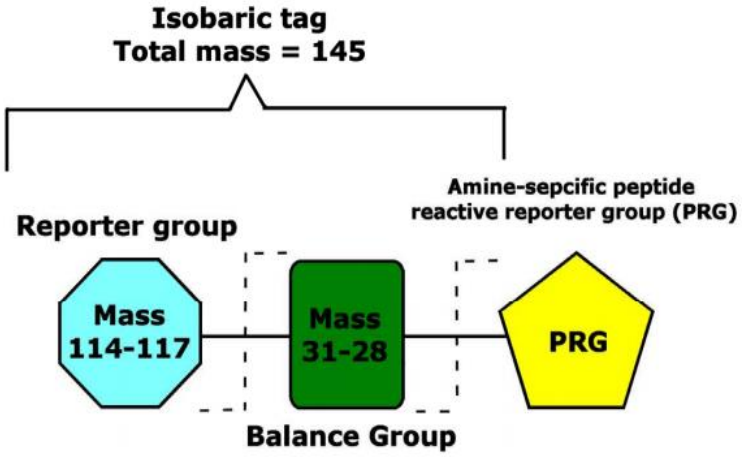


**Figure 1** Structure of the iTRAQ reagents. Adapted from [84].

In a workflow for bottom-up phosphoproteomic analysis, the protein extraction from samples is followed by digestion, enrichment and separation of peptides fractions. The analysis of separated phosphopeptides from each fraction, takes place by LC-MS/MS (tandem mass spectrometry). At the end of the process, confident assignment of the site localization for identified phosphopeptides takes place through a database search algorithm. During sample preparation, the use of specific protease and

phosphatase inhibitors during the cell lysis step is important to avoid phosphorylation/dephosphorylation unrelated to the biological condition. Trypsin is the most widely used protein digestion enzyme in phosphoproteomic workflows [13]. Although collision-induced dissociation (CID) is the most widely used fragmentation method for peptide sequencing, it preferentially fragments at the phosphate group. During fragmentation, it produces a non-sequenced neutral precursor and charged losses from product ions that limit the process of identification and localization of phosphopeptides and phosphosites respectively [16.] However high-energy collision dissociation (HCD) was shown to identify more phosphopeptides and phosphorylation sites as it produces less abundant neutral loss and more informative product ions [20, 21]. Studies have shown a considerable reduction in the number of phosphopeptides identified using CID and HCD peptide fragmentation after labeling with iTRAQ tags due to significant increase in the average ion charge state of phosphopeptides. Using ammonia vapor sprayed showed an improvement in identification perpendicular to the electrospray needle during ionization associated with an overall decrease in the average charge states of phosphopeptides [86].

### 1.6.1 Post Translational Modifications (PTM) Enrichment

A variety of PTM enrichment techniques have been developed like immunoprecipitation (IP), chemical modification, immobilized metal affinity chromatography (IMAC), and metal oxide affinity chromatography (MOAC) [3, 29] (Fig-2). Using different combinations of these methods, large-scale phosphoproteomics have uncovered thousands of phosphorylated sites in proteins [87,88].

#### 1.6.1.1 Titanium dioxide affinity chromatography-$TiO_2$

Metal oxide affinity chromatography (MOAC) has shown better results than IMAC due to better tolerance to low pH loading and washing buffers that efficiently protonate carboxyl groups leaving the negatively charged phosphorylated peptides [89]. The affinity for the oxygen present in metal oxides of the resin ($TiO_2$, $ZrO_2$, $Fe_3O_4$, $SnO_2$, $HfO_2$ and $CeO_2$) helps in the enrichment of peptides containing phosphate groups (fig-2). The titanium dioxide $TiO_2$, has the ability to form an ionic and steric interaction

with the phosphate groups and hence used in microcolumns. Such columns bind to the phopshopeptides, are wshed by low pH buffers to remove the non-binding peptides, which are then eluted by high pH buffers. This approach is cheap, fast, reproducible and MS compatible [90,91]. The optimization of the ratio between the amount of titanium and the concentration of peptides is required for higher efficiency [92]. Also acidic pH (2,5-dihydroxybenzoic acid (DHB), phthalic acid, glycolic acid, TFA of loading buffer make the peptides neutral leaving a negative charge on the phospho groups. In addition, $TiO_2$ chromatography of phosphorylated peptides is extremely tolerant to most biological buffers [93].

$TiO_2$ has the ability to enrich both the multi and monophosphorylated peptides however, the multiply phosphorylated peptides having higher binding affinity are difficult to elute. This problem can be solved by a pre-separation of mono- and multiphosphorylated peptides at different high pH conditions [89].

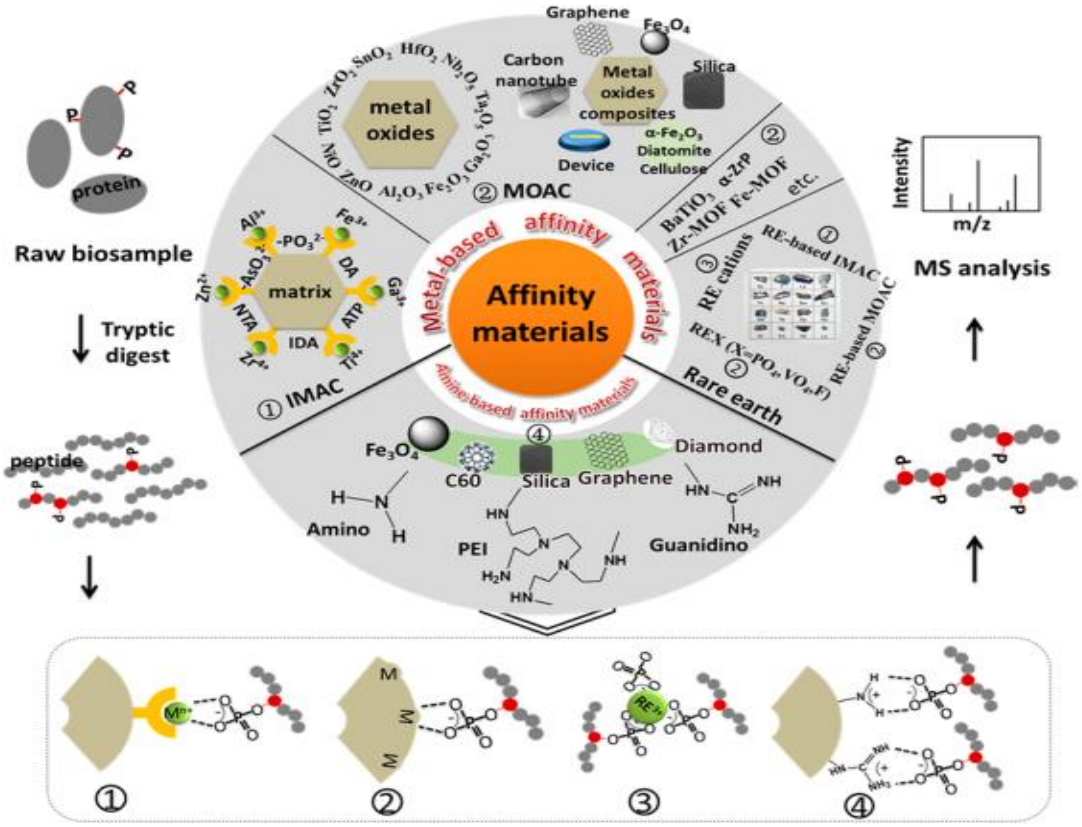


**Figure 2** Schematic illustrations of phosphopeptides enrichment for MS detection using diverse affinity materials. The numbers "①②③④" represent the main enrichment mechanisms for different affinity materials where ① represents Metal Cation-Immobilized Affinity materials, ② represents Metal Oxide (MO)-Based Materials for MOAC, ③ represents Rare Earth cations and ④ represents amine-based materials. The pie chart summarizes the affinity materials [94,95].

### 1.6.1.2 Sequential elution from IMAC (SIMAC)

SIMAC is a combined method for phosphopeptide-enrichment using both MOAC and IMAC [96]. It separates both multiply and mono phosphorylated peptides by using first acidic conditions (1% TFA, 20% acetonitrile, pH 1.0), followed by basic elution (ammonium hydroxide, pH 11.3) respectively. Then monophosphorylated peptides along with the flow through pass on $TiO_2$-MOAC and are analyzed by tandem mass spectrometry [97]. The second enrichment helps to discard non-phosphorylated peptides from the first elution and to collect phosphorylated peptides from the first flow-through [98]. SIMAC led to the identification of a greater amount of phosphopeptides than MOAC only and is more efficient for multiply phosphorylated peptides enrichment [99]. The sequential elution lead to greater amount of less complex

phosphopeptide fractions and greater probability of their ionization and identification by MS [100].

### 1.6.2 Pre-fractionation techniques

The effectively enriched thousands of phosphopeptides from samples by using $TiO_2$ and SIMAC cannot be analyzed in deep by a single step chromatography before MS. Therefore, pre-fractionation with one or multiple LC methods before routine RPLC-MS/MS analysis reduces sample complexity. The most common pre-fractionation methods include strong cation exchange chromatography (SCX), hydrophilic interaction chromatography (HILIC), electrostatic repulsion hydrophilic interaction chromatography (ERLIC), high pH RPC and capillary electrophoresis (CE).

#### 1.6.2.1 Hydrophilic interaction chromatography (HILIC)

Hydrophilic interaction chromatography (HILIC) has been used for fractionation of phosphopeptides due to suitable orthogonality [100]. Here samples are loaded at high organic solvent concentration and the polarity of the mobile phase increases during elution. Because of considerable hydrophilicity, multiphosphorylated peptides are retained in HILIC columns and elute in the same fraction. Recently, HILIC was implemented into the workflow of sequential elution from (SIMAC) to improve the selectivity of downstream TiO2 enrichment [99].

### 1.6.3 Phosphorylation of neutrophil Proteins

In the past, proteomic of neutrophil was done for the better understanding of protein expression, structure and function. Many proteins were identified under resting and dynamic conditions (after activation), providing information on protein relative abundance quantification of neutrophil proteins. However, in spite of advances, the complete knowledge of expression, structure and function of neutrophil proteins in pathological conditions remained a challenge. In that scenario, MS has the ability to identify many PTMs (phosphorylation, methylation, acetylation, ubiquitination, glycosylation, and proteolysis), however most of the focus was on the kinases due to

their role in cellular functional responses. The knowledge of signaling networks for the kinases and phosphatases of neutrophil phosphoproteome is still limited [101].

Eight substrates for MAPKAPK2 in the p38 MAPK pathway were identified by in vitro phosphorylation, using one-dimensional SDS-PAGE, and MADLI-TOF MS, [64]. Later 2DE and immunoblotting analysis were applied to confirm 14-3-3ζ as a substrate for MAPKAPK2 upon fMLP stimulation of neutrophils and PP2A phosphatase treatment partially reversed the pI shift indicating incomplete dephosphorylation or fMLP stimulation of other negatively charged post-translational modifications [102]. Another study using a combination of 2DE and MALDI-MS identified the p16-Arc subunit of the Arp2/3 complex as a MAPKAPK2 substrate [103]. Later, calcium binding protein myeloid-related protein-14 was also identified as a target of p38 MAPK phosphorylation in neutrophils stimulated by fMLP [104].

The RhoGTPase regulator, LyGDI, was found tyrosine phosphorylated during fibronectin-accelerated TNF-α-mediated neutrophil apoptosis in an experiment using 2DE, immunobloting and MS/MS. Phosphorylation was followed by increased caspase-3-mediated LyGDI cleavage, and this cleavage was identified as part of a signaling event in TNF-α-mediated apoptosis [105]. LC-MS/MS analysis of neutrophil lysates separated by SDS-PAGE showed interleukin-1 receptor-associated kinase-4 (IRAK-4) in downstream of TLR-4 with phosphorylation of serine and threonine residues on $p47^{phox}$ (a component of the NADPH oxidase) which results into enhanced NADPH oxidase activity [106].

Using phosphoprotein-specific gel staining (Pro-Q Diamond), changes in expression and phosphorylation of L-plastin, meosin, cofilin, and strathmin proteins were found [107]. The phosphorylation on Ser345 of p47 phox, was confirmed in extracellular signal-regulated protein kinase-1/2 (ERK1/2) in response to GM-CSF, and by p38 MAPK in response to TNF-α. This selective phosphorylation was found associated to a shift in MAPK signaling that primes the respiratory burst [108]. A combination of IMAC with ESI-MS/MS for analysis of specific granules from un-stimulated and fMLP stimulated human neutrophils identified 31 and 49 phopshopeptides respectively. One peptide that contained two phosphoserines was

identified as Slp homolog lacking C2 domains b (Slac2-b) presenting a known p38 MAPK phosphorylation motif and was considered to participate in the activation of granule exocytosis [109,110]. Recently in 2015 western blotting, phosphopeptide enrichment and mass spectrometric analyses of samples of fMLP-treated human neutrophils were performed by LC–MS/MS on an LTQ Orbitrap Velos mass spectrometer. In total, 770 ± 21 proteins (≥ 1 peptide) were identified using Poly MAC-Ti-enriched samples [111].

## 1.7 Motifs and domains in proteins

In eukaryotes, proteins contain two different types of functional and structural building blocks: protein domains and linear motifs respectively. The domains are larger units (usually with more than 30 residues) and evolutionary conserved that only change through divergent evolution [112]. Domains are related to specific functions. Whereas motifs are regions presenting conserved spatial structures and evolve more rapidly through convergent evolution [113]. Conserved motifs are not necessarily related to similar functions.

The different combinations of domains result in a variety of protein structures and bear the basic features of the entire protein. There are many specific functions associated with domains such as binding a ligand, DNA or RNA or interacting with other protein domains. The domains in protein give stability, compactness, hydrophobic core, and ability to fold independently. The domains have the ability to interact within domains itself or with other domains however the rate of interaction with its residues is more pronounced than with other domains [114]. Around one thousand distinct structural domains are represented by the unique folds in SCOP classification [115] or unique topologies in CATH classification [116]. The consistency of agreement among methods used for domain identification is 80% or less, some methods based exclusively, or partially, on the knowledge of human experts, while the some other are computational [117].

Post-translational modification of domains and motifs is a driving force behind directional and dynamic protein-interaction networks including enzyme-substrate

interactions [118]. In this regard, the role of domains in protein-tyrosine kinases (PTKs), the protein-tyrosine phosphatases (PTPs), and the proteins that recognize the phosphorylated ligand to specify downstream signaling events is a highly interdependent signaling process (Fig-3). Several modular interaction domains have the capability to bind to tyrosine-phosphorylated ligands. These include most Src homology 2 (SH2) domains, Pleckstrin homology domain (PH), a subset of phosphotyrosine-binding (PTB) domains, at least one C2 domain and the Hakai pTyr-binding domain. The SH2 domain is the largest domain family dedicated to pTyr recognition, with 111 proteins in the human participating in a diverse range of signaling networks as shown in figure 4 [119].

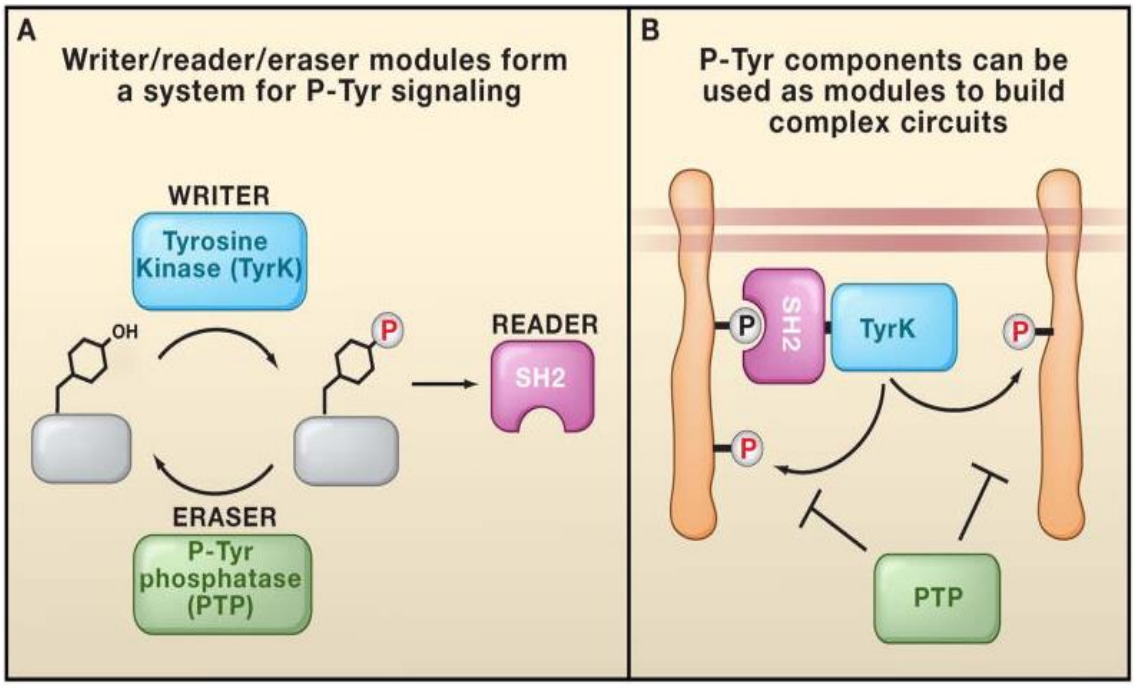


**Figure 3**-A The pTyr signaling, involving the tyrosine kinase (TyrK), Src Homology 2 (SH2), and phosphotyrosine phosphatase (PTP) domains interdependent signaling platform. This platform serves as the writer, reader, and eraser modules, respectively, for processing pTyr marks. (*B*) Components of pTyr signaling can be used to build complex circuits. As SH2-TyrK protein interaction with initiating pTyr site can lead to amplification of tyrosine phosphorylation through a positive feedback loop. Adapted from [120].

Similarly the Pleckstrin homology domain (PH) binds with affinity to phosphoinositides exerting a certain function in cell signaling, cytoskeletal reorganization or membrane trafficking [121].

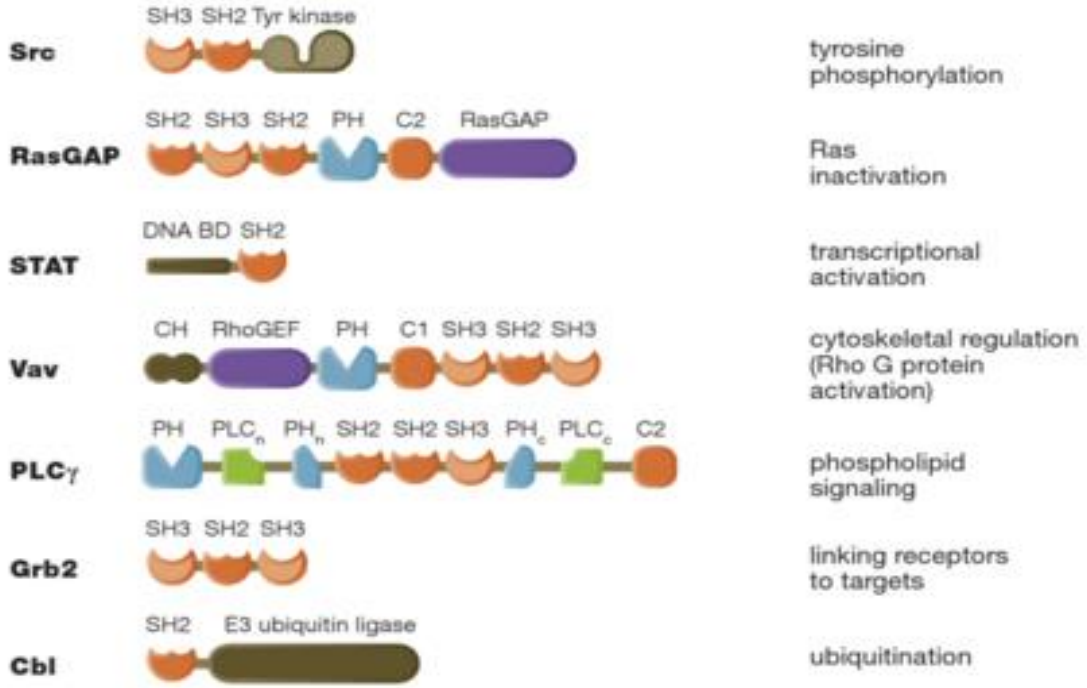


**Figure 4** The SH2 domains in various proteins with different functions. Adapted from [122].

Thousands of in vivo phosphorylation sites have been identified thanks to advances in mass-spectrometry techniques (8–11). However, the kinases responsible for phosphorylation of these sites along with the proteins recognizing these phosphorylated sites are often unknown (12). Linking these sites to the hundreds of protein kinase catalytic domains and motifs is a challenge for in-depth understanding of cellular signaling processes. Numerous methods have been developed to predict potential phosphorylation sites for specific kinases; like position-specific scoring matrices (PSSMs) derived from peptide libraries (13, 15–17), manually constructed sequence patterns (14, 18, 19), and a variety of machine-learning algorithms that have been trained on in vivo phosphorylation data (20–24). The motif-x algorithm is also advanced for computationally determining short linear motifs was first described by Schwartz and Gygi in 2005, [123] and an online implementation was made available by Chou and Schwartz at that time from MS data sets.

From our observations from the literature, the molecular mechanism by which

IPC offers protection through attenuation of neutrophil intestinal tissue infiltration is not clear. Proteomic research has been done for better understanding of the neutrophil biology in the past but there is still no study available on the proteomic analysis of neutrophil after intestinal ischemic preconditioning. For a deeper understanding of the neutrophil proteins and their phospshorylation patterns taking part in molecular pathways involved in surgical trauma, IR and PCI we performed quantitative iTRAQ and Phosphoproteomics in a rat models.

# Objectives

# 2 OBJECTIVE

The main objective of this research project was to evaluate the effect of IPC on the proteome and phosphoproteome of rat neutrophils.

## 2.1 Specific Objectives

- To evaluate the influence of IR and of IPC on the hematologic parameters;
- To analyse the changes in the proteome of neutrophils in response to ischemia and reperfusion preceded by ischemic preconditioning;
- To identify the enzyme and pathways underlying IPC.
- To identify significantly regulated kinases and phosphatases after IR and IPC.

# Experimental Design

# 3 MATERIALS AND METHODS

## 3.1 Experimental Subjects and Sample Collection:

Male Wistar rats with no inflammatory disease and weighing 250–350 g were collected from the animal house of the Faculty of Medicine University of Sao Paulo (FMUSP), Sao Paulo State, Brazil. The project was approved by the Ethics Committee of FMUSP (Protocol No. 8186) for the use of rats as experimental subjects. The animals had access to food and water *ad libitum* until the time of the experiment.

### 3.1.1 Experimental groups

Forty rats were randomly allocated into the following four groups (Fig. 5):

1- The control group (C) (n=10), without any surgical procedure.

2- The sham laparotomy group (LAP) (n=10), without the clamping of any artery, but receiving the same surgical procedure, except for the clamping.

3- Ischemia/reperfusion (IR) group (n=10), submitted to superior mesenteric artery occlusion (SMAO) for 45 min followed by 120 min of reperfusion.

4- Ischemic Preconditioning (IPC) group (n=10), submitted to a 10 min period of SMAO followed by a 10 min reperfusion immediately before 45 min of ischemia and 120 min of reperfusion, as in the IR group.

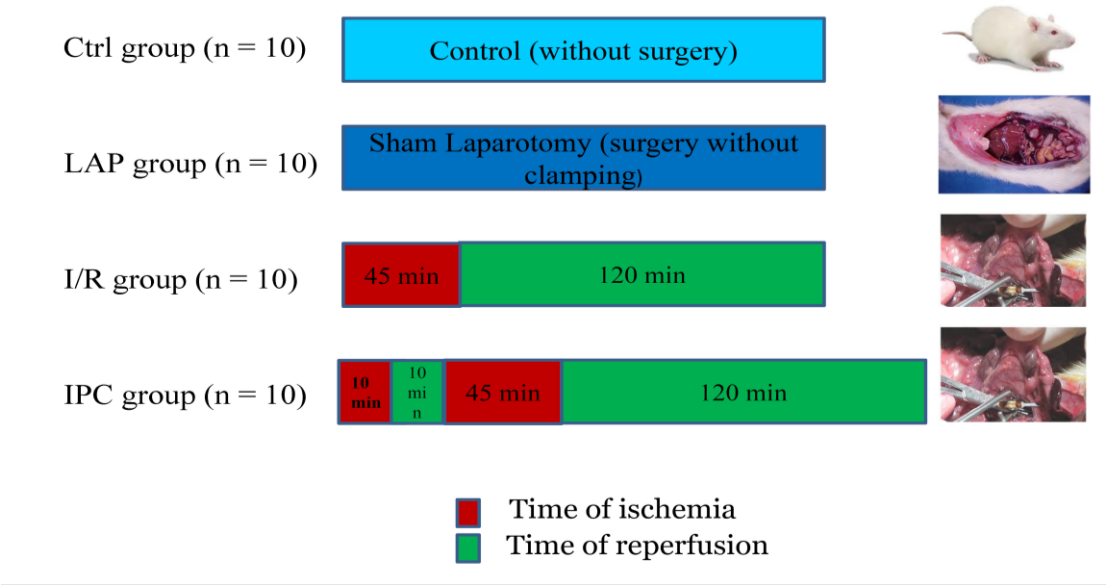


**Figure 5** Experimental groups and their times of ischemia and reperfusion.

## 3.2 Hematological analyses

We collected 20□l blood from the tails of all animals before and after surgery and injected the samples into a veterinary automated cell counter (BC-2800Vet, Shenzhen Mindray Bio-Medical Electronics Co., Nanshan, China). The hematimetric parameters analyzed included the determination of the total erythrocyte count (RBC), total white blood cell count (WBC), hematocrit (HCT), hemoglobin [124] concentration; erythrocyte indices as mean corpuscular volume (MCV), mean corpuscular hemoglobin (MCH), mean corpuscular hemoglobin concentration (MCHC); platelet (PLT) count, mean platelet volume (MPV), platelet distribution widths (PDW), plateletcrit (PCT) and white blood cell differential count [22, 23].

### 3.2.1 Surgical procedures:

The surgical procedures were performed in the Laboratory of Surgical Physiopathology (LIM-62), department of Surgery, FMUSP. Rats from all groups were anesthetized with intraperitoneal (i.p.) injections of sodium pentobarbital (45 mg/kg,)/Ketamine (80 mg/kg) + xylazine (7 mg/kg), and their core body temperatures were maintained at 37°C. After midline laparotomy, the superior mesenteric artery was

isolated near its aortic origin. During this procedure, the intestinal tract was placed between gauze pads that had been soaked with warmed 0.9% NaCl solution. In rats from the IR group, the superior mesenteric artery was clamped, resulting in the total occlusion of the artery for 45 min. After the time of occlusion, the clamps were removed, and blood samples were collected from the animal tail after 120 min of reperfusion. In the rats of the IPC group, the ischemic procedure described above was preceded by 10 min of clamping followed by 10 min of reperfusion.

### 3.2.2 Statistical Analysis

For statistical analysis, the data were first checked for normality by applying the D'Agostino & Pearson omnibus normality test. Data were normalized, and outliers were removed, based on the Thompson tau technique; then, normality was reconfirmed with the above-mentioned normality test. Variance analysis (One-way ANOVA) was used to determine the difference between the groups, and the Tukey-Kramer test was employed to compare and determine the means that differed significantly from each other, using the Graph Pad Prism program (V.6.0c). Values with $p<0.05$ were considered significant

## 3.3 Methodology used for Proteomic analysis

### 3.3.1 Experimental Subjects and Surgical Procedure

Male Wistar rats weighing 250-350 g with no inflammatory diseases were collected from the animal house of Faculty of Medicine, University of São Paulo (FMUSP), São Paulo state, Brazil. To use rats as experimental subjects, project was first approved by the ethical committee of FMUSP with protocol no. 8186. Twenty rats were divided randomly into two groups, the control group and surgical group and each group had 10 rats. Absence of inflammatory processes was confirmed by hemocytometric analysis before the rats were included in the experiment as described above. Rats from both the groups were anesthetized according to Tahir *et al.*, (16) and rats from the surgical group were subjected to the abdominal surgery. After midline abdominal surgical incision, the abdominal cavity was kept open for 45 minutes and the intestinal tract was placed between gauze pads soaked with warmed 0.9% NaCl solution to

simulate intra-abdominal manipulation. Then the intestines were placed back into the cavity, the abdominal wall was sutured and the animals observed for 120 minutes. The control group was anesthetized and kept under observation for the same period.

### 3.3.2 Sample Collection and Neutrophil Isolation

After 165 minutes of surgical procedures (or observation), about 10-12 mL of blood was collected from the heart (right ventricle catheter). Rat neutrophils were isolated by using Ficoll gradient protocol according to Russo Carbolante *et al.* (17) with minor modifications. Briefly, about 10 mL of blood were layered carefully upon equal amount of Ficoll in a Falcon tube and centrifuged at 400 rcf for 45 minutes. After centrifugation, the upper layer was discarded and the bottom layer (rich in erythrocytes and neutrophils) was mixed with 6% dextran solution in 0.15 M of NaCl. The final volume was increased to 14 mL by adding phosphate buffer saline (PBS) solution. The samples were homogenized and mixed well and incubated at 37°C for 20 minutes. The transparent supernatant layer was collected in a fresh falcon tube and centrifuged for 10 minutes at 270 rcf. The pellet was washed by adding 5 mL of milli-Q water for 15-20 seconds to lyse residual erythrocytes and then 5 mL of 2x PBS solution, mixed and centrifuged for 10 minutes at 500 rcf. After centrifugation, the neutrophil pellet was resuspended in 1 mL of 1x PBS solution to count under the microscope.

### 3.3.3 Neutrophil Lysis and Protein Digestion

After counting, $3x10^6$ neutrophils were lysed in 200 µLof lysis buffer (2% SDS, 20 mM TEAB, 100 mM DTT, Phosphatase and Protease Inhibitors Mix) by using tip-sonicator for 10 cycles with 15 seconds of each cycle and 1 minute of interval on ice. After sonication the samples were heated at 80°C for 10 minutes and then centrifuged and quantified for protein concentration by using Quant-iTTM Protein Assay Kit (Cat. No. Q33210). SDS was removed from the samples according to Wisniewski *et al.* (18) by using 30 KDa Vivacon spin filters. The DTT reduced samples were alkylated with 400 µLof iodoacetamide (IAA) buffer (50 mM IAA in 1% SDC and 20 mM TEAB solution) in the dark for 20 minutes at room temperature. Samples were washed with 400 µLof 1% SDC and 20 mM TEAB solution. Proteins were digested on the filters at

37°C overnight by using Promega Trypsin in 1:50 trypsin to sample ratio in 400 µLof 1% SDC and 20 mM TEAB solution. After digestion, the samples were acidified to a final concentration of 0.1% by adding TFA and filter units were shifted to new collection tubes, centrifuged at 14000 rcf for 20 minutes and filtrates having peptides were saved. Peptides were desalted by homemade microcolumns of Poros Oligo R2/R3 packed resins (1 cm long) in p200 tips (19). Peptide quantification was carried out by using Biochrome 30 amino acid composition analyzer (Cambridge, UK) as described in Laursen *et al.* (20).

### 3.3.4 iTRAQ Labeling and HILIC-Fractionation

Peptides from two rats of the same group were pooled together to make one biological replicate and we had five biological replicates for each of the two conditions. Biological replicates from each condition were iTRAQ labeled according to the manufacturer's instructions. Briefly, 100 µg of lyophilized, desalted digest from each replicate was resuspended individually in 30 µLof 300 mM TEAB and added to a vial with iTRAQ label resuspended in 70 µLof ethanol. The vials were mixed and incubated at room temperature for 2 hours. The labeled peptides were combined in 1:1 proportion based on the amino acid analysis quantification. Equal proportion combination and iTRAQ labeling was confirmed by MALDI-MS/MS analysis (Bruker Daltonics, Billerica, CA, USA). All replicates from the control group were labeled with iTRAQ-114 and surgical trauma replicates were labeled with iTRAQ-115. Prior to LC-MS/MS analysis, 20 µg of multiplexed iTRAQ-labeled peptides of each replicate were separated into 7 fractions by using hydrophilic interaction chromatography (HILIC) on an Agilent 1200 HPLC system (21). For that, lyophilized samples were resuspended in solvent B (90% acetonitrile, 0.1% TFA) and loaded into a TSK-gel Amide 80 HILIC HPLC column (length = 17 cm, inner diameter = 250 µm, particle size = 3 µm). Peptides were eluted at 6 µL/minute by a decreasing gradient of 90% ACN/0.1% TFA to 60% ACN/0.1% TFA over 35 minutes. Fractions were collected automatically in a microwell plate at 1 minute of intervals after UV detection at 210 nm. Collected fractions were combined in 7 fractions, based on the uniform distribution of the UV absorbance pattern, and lyophilized.

### 3.3.5 LC-MS/MS and Data Analysis

Dried fractions were resuspended in buffer-A (0.1% formic acid) and loaded onto a Proxeon Easy-nLC system (Thermo Fisher Scientific, Odense, Denmark), coupled online with LTQ-Orbitrap Velos mass spectrometer (Thermo Fisher Scientific, Bremen, Germany). Peptides were loaded into a picofrit 18 cm long fused silica capillary column (75 μm inner diameter) packed in-house with reversed-phase Repro-Sil Pur C18-AQ 3 μm resin. A gradient of 180 minutes was set for peptide elution from 0-34% buffer-B (95% ACN/0.1% formic acid) at a flow rate of 250 nL/min. The MS method was set up in a data-dependent acquisition (DDA) mode. For full MS scan, the mass range of 400-1200 *m/z* was analyzed in the Orbitrap at 30, 000 FWHM (400 *m/z*) resolution and 1x106 AGC target value. Each MS scan in the Orbitrap analyzer was followed by MS/MS of the seven most intense ions ($\geq$ 2+ charge state). Fragment ions were acquired in the Orbitrap using a resolution of 7,500 after high-energy collision dissociation (HCD) with energy set at 36 (22). Raw data were viewed in Xcalibur v.2.1 (Thermo Scientific).

For the resulting raw files Proteome Discoverer software (v.1.4.0.288, Thermo Fisher Scientific) was used to perform database searching and relative quantification. MS/MS spectra were searched against UniProt Rodents database (updated November 2013) by using an in-house MASCOT (v2.3, Matrix Science, London, UK) server. The searches were performed with the following parameters: oxidation (M) and deamidation $^{13}$ were set as variable modifications, while carbamidomethylation (C) was set as fixed modification. Precursor mass tolerance was 10 ppm; MS/MS tolerance was 0.05 Da. Trypsin was selected as digestion enzyme and up to two missed cleavages were allowed. Using Percolator as validator (23), results were filtered for 1% false discovery rate (FDR) and minimal of 2 peptides were accepted for protein identification using Proteome Discoverer. Protein iTRAQ ratios were log2 transformed and normalized by the average value to compensate for possible imprecisions during equal mixing of the samples. Proteins were considered for quantitative analysis only if present in at least two replicates. One-tail Student's t-test (p-value < 0.05) was used to assess statistical validation for significantly regulated proteins between conditions. Protein Center

(Thermo Scientific) was used to interpret annotation and statistical GO classification of the identified proteins. More detailed annotation and enzyme activity prediction and classification (Enzyme Commission numbers) were retrieved from the online UniProt database service. Functional analysis of the trauma relevant proteins clusters was carried out by Wikipathways using WEB-based GEne SeT AnaLysis Toolkit (WebGestalt) (24) whereas protein-protein interaction networks analysis was acquired from STRING with highest confidence score (0.900) (25).

Data availability mass spectrometer output files (Raw data) have been deposited in a public repository, the Peptide Atlas database (https://db.systemsbiology.net/sbeams/cgi/PeptideAtlas/PASS_View?identifier=PASS00790), under the identifier PASS00790.

### 3.4 Methodology used for Proteomics analysis of all four groups

#### 3.4.1 Experimental subject preparation and sample collection

Forty male Wistar rats weighing 250-350 g with no inflammatory disease were collected from the animal house of the Faculty of Medicine, University of São Paulo, Brazil. Rats were randomly allocated into four experimental groups with each group carrying 10 rats. The four experimental groups included the control group (Ctrl, without any surgical procedure), sham laparotomy group (Lap, without clamping of any artery but receiving the same surgical procedure), intestinal ischemia and reperfusion group (iIR, subjected to 45 min of superior mesenteric artery occlusion (SMAO) followed by 120 min of reperfusion), and intestinal ischemic preconditioning group (iIPC, subjected to 10 min of SMAO followed by 10 min of reperfusion immediately before 45 min of ischemia and 120 min of reperfusion as in iIR). All the surgical procedures and sample preparations were performed in Laboratory of Surgical Physiopathology (LIM-62), Department of Surgery, FMUSP, according to Fontes et al. (27). The ethical committee of FMUSP approved the project (Protocol No. 8186). Absence of pre-existing inflammatory responses was confirmed before the surgical procedures and sample collection by hemocytometric analysis using granulocytes concentration (%) as

selection criterion. About 10-12 ml of blood was collected from the heart and processed for neutrophil isolation.

### 3.4.2 Neutrophil separation and protein digestion

For neutrophil separation the collected blood was processed by using the Ficoll gradient protocol (28) with minor modifications as described above. Briefly, the total volume of blood collected from each rat was layered carefully upon an equal volume of Ficoll in a Falcon tube, centrifuged at 400 rcf for 45 min and the supernatant was discarded carefully. The bottom layer rich in RBCs and neutrophils was mixed with 6% dextran solution in 0.15M of NaCl and the final volume was adjusted to 14 ml by adding phosphate buffer saline solution (PBS). The sample was homogenized, mixed gently and incubated at 37°C for 20 min. The upper transparent layer was collected in a fresh falcon tube and centrifuged at 270 rcf for 10 min. Residual RBCs were removed by hypotonic lysis and neutrophils were washed in PBS. After counting, $3x10^6$ neutrophils were tip sonicated in 200 µL of lysis buffer (2% SDS, 20mM TEAB, 100mM DTT and Protease Inhibitor Mix). Following sonication, the protein samples were heated at 80oC for 10 min in water bath, centrifuged and quantified by using Quant-iT Protein Assay Kit (Thermo Scientific, MA, USA) and then combined in pools of two, so that samples from ten rats in each group were grouped to five biological replicates. Vivacon (Sartorius Stedim, CA, USA) spin filters of 30 KDa were used to remove SDS from the protein samples according to Wisniewski et al (29). The DTT reduced samples were alkylated in 400 µLof Iodoacetamide solution (50 mM IAA in 1% SDC and 20 mM TEAB solution) for 20 minutes in the dark at room temperature. Samples were washed with 400 µLof 1% SDC and 20 mM TEAB solution followed by on filter digestion in 1:50 trypsin to sample ratio in the same washing solution. After overnight digestion, the samples were acidified to a final concentration of 0.1% by adding TFA and the filters with peptides were shifted to new collection tubes, centrifuged at 14000 rcf for 20 min and the peptides were collected. Peptides were desalted in homemade microcolumns of Poros Oligo R2/R3 packed resins (~ 1 cm long) in p200 tips (30) and quantified by amino acid analysis on a Biochrome 30 amino acid composition analyzer (31).

### 3.4.3 iTRAQ labeling and peptide fractionation

After the peptide quantification, 100 μg of peptide solution was picked from each of the 4 biological conditions for all the 5 biological replicates into a new clean eppendorf tube. The samples were vacuum dried to label by 4-plex iTRAQ Reagent Kit. The dried peptides were reconstituted in 20 μLof dissolution buffer in accordance with manufacturer instructions. Peptides from the control group were labeled with 114, laparotomy with 115, intestinal ischemia and reperfusion with 116 and intestinal ischemic preconditioning with 117. Labeling was confirmed by MALDI-MS and, after that, the labeled digests were multiplexed in 1:1:1:1 ratio. About 20 μg of each iTRAQ labeled multiplexed replicate sample was HILIC fractionated into 7 fractions on an Agilent 1200 HPLC system (32). For fractionation, the lyophilized samples were reconstituted in 90% acetonitrile (ACN)/0.1% TFA solution and loaded into a TSK-gel Amide 80 HILIC HPLC column (length = 17 cm, particle size 3 μm). For peptides elution at 6 μl/minute a gradient of 90% ACN/0.1% TFA to 60% ACN/0.1% TFA over 35 min was used. Peptide fractions were collected automatically into a microwell plate at 1 min of interval after UV detection at 210 nm. Collected fractions were combined in 7 fractions based on the uniform distribution of the UV absorbance pattern and lyophilized.

### 3.4.4 Reversed phase nano-liquid chromatography tandem mass spectrometry (nano-LC-MS/MS)

Seven HILIC fractions from each of the 5 biological replicates were analyzed using an Easy-nLC system (Proxeon Biosystems, Odense, Denmark) coupled online with an LTQ Orbitrap Velos mass spectrometer (Thermo Scientific, Waltham, MA). The labeled peptides from each fraction were loaded onto an 18 cm homemade reversed-phase capillary column (75-μm inner diameter) packed with ResiproSil-Pur C18-AQ 3-μm resin (Dr. Maisch, GmbH, AmmerbucH, Germany). The peptides were eluted directly into an LTQ-Orbitrap Velos MS by using a gradient of 180 min from 0-34% buffer-A (95% ACN/0.1% formic acid) at 250 nl/min. The MS method was set up

in a data-dependent acquisition (DDA) mode and a full MS scan in the mass range of 400-1200 m/z in Orbitrap using a resolution of 30, 000 FWHM (400 m/z) with target value of 1x106 was performed. Each MS scan in the Orbitrap analyzer was followed by MS/MS of the seven most intense ions (≥ 2+ charge state) and fragmentation was performed by high-energy collision dissociation (HCD) using a resolution of 7, 500(33).

### 3.4.5 Database searching and Data Analysis

The resulting raw files were viewed in Xcalibur v.2.1 (ThermoScientific) and processed using Proteome Discoverer [125] v.1.4.0.288 (Thermo Scientific) for database searching and relative quantification. MS/MS spectra were searched against UniProt Rodents database (updated November 2013) by using an in-house MASCOT (v2.3, Matrix Science, London, UK) software. The parameters used for database searches were: precursor mass tolerance, 10 ppm; MS/MS tolerance, 0.05 Da; Methionine oxidation, deamidation [25], Lysine and peptide N-terminal iTRAQ tagging were set as variable modifications, whereas carbamidomethylation of cysteine residue was selected as fixed modification. Trypsin was selected as digestion enzyme and up to two missed cleavages were allowed. The number of proteins and protein groups were filtered for less than 1% false discovery rate (1% FDR), using Percolator as validator (34). A minimum of two peptides per protein was accepted for identification.

Identified proteins were grouped in clusters according to their relative abundance profiles. For cluster analysis, the mean over all five replicated values for each condition was calculated. Two validation indices Xie-Beni index (35) and minimal centroid distance (36) were used to assign the proteins in the best number of clusters in accordance with their expression regulation. After determining the value of the fuzzifier parameter, fuzzy c-means clustering (37-39) was applied and the number of clusters was obtained according to Schwämmle (36). For statistical analysis of the regulated proteins an in house program was developed in R (http://www.r-project.org/), where the iTRAQ intensity values were log-transformed and median normalized for all the five biological replicates. For the multiple measurements of the same peptide one peptide measurement was allowed in RRollup function of DanteR (40). The peptide values were converted into protein quantitation using the mean of a minimum of two peptides per protein

identification. The Limma test (41) and rank products (42) were used as they are more powerful in dealing with low replicate numbers and higher percentage of missing values (43). These statistical tests were applied on all protein ratios against label 114 (control) and corrected for multiple testing (44). From both statistical analysis, proteins with q-values less than 0.05 were considered regulated.

ProteinCenter (Thermo Scientific, Waltham, USA) was used to interpret the results at protein level, like, GO Slim classification with 5% false discovery rate (FDR). Prediction of enzyme activity and classification (Enzyme Commission (EC) numbers) of the identified proteins was carried out by using UniProt (http://www.uniprot.org/). KEGG pathways analysis was acquired by using WebGestalt with default parameters using Rattus norvegicus genome as reference set for enrichment analysis from KEEG pathways (45) whereas protein-protein interaction networks analysis were acquired by String 10 with highest confidence score (0.900) (46).

Data Availability—Mass spectrometer output files (Raw data), peptide and protein identification files (MSF and XLS files) have been deposited in a public repository, the PeptideAtlas database, under the dataset tag neutrophil_IPC and database identifier PASS00798.

### 3.5 Methodology used for Phodphoproteomics analysis

The animal model used also in study was male Wistar rat (*Rattus norvegicus*), weighing between 250 to 350 g from the animal house of the Faculty of Medicine University of Sao Paulo (FMUSP), Sao Paulo State, Brazil. The Ethics Committee of FMUSP (Protocol 8186) approved the project for the use of animals. All the rats used for experiments had access to food and water *ad libitum* in laboratory of LIM-62 (FMUSP).

As described above, the surgical procedures were performed in the Laboratory of Medical Investigation (LIM-62), department of Surgery, FMUSP. After hematological analysis and surgical procedure, 10-20ml of blood was collected directly from the heart for neutrophils separation from the rats (all 4 groups). Then proteins were extracted, followed by FASP method, and alkylation, trypsin digestion and amino acid

quantification of the purified peptides was performed. After that hundred microgram of peptides were labeled with 114 (Control group), 115 (Laparotomy), 116 (Ischemia reperfusion) and 117 (ischemic preconditioning) iTRAQ labeling reagents separately, confirmed by MALDI and digests from the four experimental groups were mixed in 1:1:1:1 ratio as previously described.

### 3.5.1 Enrichment of Phosphopeptides ($TiO_2$-SIMAC-HILIC procedure)

This procedure was performed in the following steps:

1. First $TiO_2$ purification
2. IMAC purification
3. Second $TiO_2$ purification to separate mono-phosphopeptides from deglycosylated peptides

#### 3.5.1.1 First TiO2 Purification

The purification of phosphorylated peptides was performed with little modifications in batch mode using Titanium dioxide chromatography as previously described [69,70,126]. Briefly, 400 µg of tryptic labeled digests (obtained after mixing 100 µg from each of the four iTRAQ labeled conditions) were reconstituted in 800 µl loading buffer (5% TFA (v/v), 1M Glycolic acid and 80% acetonitrile (v/v) (ACN)). These peptides were incubated in low binding polypropylene tubes containing 0.6 mg $TiO_2$ beads per 100 µg peptide solution with constant shaking at room temperature for 15min. The samples were centrifuged (6000 rpm for 30 sec), the supernatant was incubated with half of the amount of $TiO_2$ used in the first incubation in another low-binding tube. The process was repeated to recover as much phosphopeptides and sialylated glycopeptides as possible bound to the $TiO_2$ beads. The flow-through from $TiO_2$ incubations was collected in a low-binding eppendorf tube and saved for further analysis of unmodified and glycopeptides. The $TiO_2$ beads from all the four incubations were pooled using 100 µl loading buffer and transferred to a new low-binding eppendorf tube. The $TiO_2$ beads were washed with 50 µl washing buffer-1 (1% TFA (v/v) and 80% ACN (v/v)) and 50 µl washing buffer-2 (0.2% TFA (v/v) and 10% ACN (v/v)) and vacuum dried for 10min. The phosphopeptides and sialylated glycopeptides were eluted with elution buffer (60µl Ammonia solution (28%) in 940 µl $H_2O$, pH 11.3)

for 15min at constant shaking. Using small table centrifuge for about 1min the samples were centrifuged and the supernatant, containing phosphopeptides and sialylated glycopeptides, was passed through a C8 stage tip to remove TiO2 beads and lyophilized completely.

### 3.5.2 Enzymatic deglycosylation

As the lyophilized sample contained both phosphorylated and sialylated glycopeptides, in order to remove sialic acid from peptides the sample was re-dissolved in 50µl of 20 mM TEAB and 2µl of 1U/µl PNGase F [127] and 0.5µl of 1U Sialidase A. The enzymatic reaction was performed overnight at 37°C in a wet chamber [128].

### 3.5.3 IMAC Purification of the Multi-Phosphorylated Peptides

The de-sialylated solution was acidified by adding 1 µl 10% TFA (v/v) and diluted with 200µl of 50% ACN/10% TFA (v/v) and the pH was adjusted to 1.6-1.8 with 10% TFA. The IMAC beads (80 µl) were washed twice with 200µl of 50% ACN/0.1% TFA (v/v) and added to the peptides solution for 30min incubation at room temperature. Half of the supernatant IMAC flowthrough (IMAC-FT) was transferred to a new low-binding tube and the remaining solution with IMAC beads was passed through a 200µl GeLoader tip flat at the end to retain the IMAC beads with the help of a syringe to press the liquid through into the “IMAC-FT” eppendorf tube and pack the IMAC column. The IMAC beads in the GeLoader tip were washed with 50µl of 50%ACN/0.1% TFA, 70µl of 20% ACN/1% TFA and washes were collected in an eppendorf tube. The eluate was acidified with 8µl of 100% formic acid or 2µl 10% TFA and the multi-phosphorylated peptides from IMAC beads were eluted, using 80µl of ammonia elution buffer, directly down in a p200 stage tip with Poros R3 material (1-2 cm). The multi-phosphorylated peptides were washed with 60µl of 0.1% TFA, eluted with 60µl of 60% ACN/0.1% TFA and vacuum dried [127,129].

### 3.5.4 Second TiO2 Purification of the Mono-Phosphorylated Peptides

The IMAC-FT was resuspended in 200µl of 70% ACN/2% TFA. The $TiO_2$ beads were added in the same amount as in the first $TiO_2$ incubation. The $TiO_2$ beads were washed with 50 µl washing buffer-1 (1% TFA and 80% ACN (v/v)) and 50 µl

washing buffer-2 (0.2% TFA (v/v) and 10% ACN (v/v)) and vacuum dried for 10min. The phosphopeptides and sialylated glycopeptides were eluted with elution buffer (60µl Ammonia solution (28%) in 940µl $H_2O$, pH 11.3) for 15min with constant shaking. After twice $TiO_2$ incubation and constant shaking for 15min, the flow-through, containing all the deglycosylated peptides was saved. The $TiO_2$ beads were pooled using 100 µl 50% ACN/0.1% TFA and vacuum dried for 10min. The mono-phosphopeptides were eluted with ammonia buffer on a shaker for 15 min. The solution was spun for 1min and passed over a C8 stage tip to recover the liquid directly down in a p200 stage tip with R3 material. The Eluate was acidified with 8 µl of 100% formic acid or 2µl 10% TFA prior to R3 purification. The mono-phosphorylated peptides were purified on the R3 column, washed with 60µl 0.1% TFA, eluted with 60 µl 60% ACN/0.1% TFA and vacuum dried.

### 3.5.5 Sample Washing

The micro-columns were prepared by stamping out a small plug of C8 extraction disk and placed in the constricted end of the P200 tip. The reversed-phase resin (R3) was re-suspended in 100% ACN and packed by applying air pressure with the help of a syringe in the tip where the C8 stopped the leakage of the resin material. The vacuum dried samples were re-suspended in 100µl of 0.1% TFA. The micro-columns were equilibrated with 60µl of 0.1% TFA, samples were loaded onto the micro-columns, washed with 0.1% TFA and peptides were eluted with 60% ACN/0.1% TFA (v/v) and lyophilized. The mono-phosphorylated peptides were desalted twice with Poros R3 [128].

### 3.5.6 HILIC fractionation of Mono-phosphorylated and non-phosphorylated peptides

The HILIC fractionation of the mono-phosphorylated peptides from TiO2 enrichment and non-phosphorylated after desalting was performed [126]. The lyophilized peptides were reconstituted in 90% ACN/0.1% TFA and 40µl of the sample was injected onto an in-house packed TSK gel Amide-80 HILIC 320 um x 170 mm capillary HPLC column using an Agilent 1200 HPLC system. A gradient of elution buffer from 90% ACN/0.1% TFA to 60% ACN/0.1% TFA for 35min at flow rate of 6µl/min was used. The fractions were collected automatically in a microwell plate at 1min intervals

after UV detection at 210 nm and pooled in accordance with the UV detection. The fractions were then dried in speed vacuum.

### 3.5.7 Nano-Liquid Chromatography Tandem Mass Spectrometry (nano-LC-MS)

The phohopeptides fractions were analyzed by a Proxeon EASY-nLC system (Thermo Fisher Scientific, Odense, Denmark), coupled with mass spectrometry LTQ-Orbitrap Velos (ThermoScientific) by loading onto an 18cm homemade reversed-phase capillary column (75 um inner diameter) packed with ReproSil-Pur C18 AQ 3µm material (Dr. Maisch, Ammerbuch Entringen, Germany) in buffer-A (0.1% formic acid). The peptides were directly eluted into a LTQ-Orbitrap Velos MS, using 110-180 min gradients from 0-34% Buffer-B (95% ACN/0.1% formic acid) at 250 nl/min. The MS method was set up in a data-dependent acquisition (DDA) mode. A full MS scan was performed in the mass range of 400-1200 m/z in the Orbitrap using a resolution of 30,000 FWHM (400 m/z) and the target value of $1x10^6$ ions. For each full scan the seven most intense ions ($\geq 2^+$ charge states) were selected for higher energy collision dissociation (HCD) using a resolution of 7,500. The settings for the HCD were as following: threshold for the ion selection was 2000, the target value of ions for HCD 300ms, activation time of 0.1ms, isolation window of 2 m/z and normalized collision energy was 36.

### 3.5.8 Database Searching and Bioinformatics for proteomic data analysis

The raw files were processed using Proteome Discoverer version 1.4.0.288 (Thermo Fisher Scientific), tandem MS/MS spectra were converted to .mgf files and searched against the UniProt rodents database using Mascot (v2.3.2, Matrix Science, London, UK). The parameters used for database searches were: precursor mass tolerance 10ppm, fragment (MS/MS) mass tolerance 0.05Da, up to two missed cleavages and trypsin as digestion enzyme. The variable modifications included oxidation (M) and deamidation [130] for phosphopeptides (serine, threonine, tyrosine) were included. The carbamidomethylation on cystein residue was applied as a fixed modification and results were filtered for 1% false discovery rate (FDR) using Percolator as validator [99]. We applied further filters for the analysis of phosphopeptides by excluding all phosphopeptides with phosphoRS 3.0 probability lower than 95%.

For statistical approach an in house script developed under the the statistical package R software was used. The data of phosphopeptides fractions consisted of five biological replicates. The iTRAQ intensities values for each fraction were log-transformed and median-normalized. One peptide measurement was allowed by choosing "mean" instead of "median" in RRollup function of DanteR package for the multiple measurements of the same peptide [100]. Limma [114] and rank products [131] provided sufficient power to deal with low replicate numbers and additional missing values [132]. Both statistical tests were carried out on all phosphopeptides and protein ratios against label 114 and corrected for multiple testing [133]. From both statistical tests all the phosphopeptides and proteins with q-value below 0.05 (5% FDR) were considered regulated.

For the cluster analysis, we calculated the mean over all 5 replicated values for each condition. Phosphopeptides and proteins were merged into one data set. Fuzzy c-means clustering [134,135] was applied after determining the value of the fuzzifier and obtaining the number of clusters according to Schwämmle (2010) [136]. A standard principal component analysis (PCA) was performed by using R package to check the variability between different conditions and similarity among the biological replicates of the same group.

ProteinCenter (Thermo Scientific, Waltham, USA) was used to interpret the results at protein level, e.g, statistical GO Slim classification with 5% false discovery rate (FDR) and number of domains. For KEGG pathways analysis WebGestalt [137] was used with default parameters. STRING v9.1 [138] was used to check protein-protein interactions for phosphor proteins identified in a pathway. The predictions of kinase recognition sites on protein sequences were performed using GPS software [139] and *Rattus norvegicus* was the organism. For the kinase substrate prediction the significantly regulated phosphopeptides were up loaded to iGPS1.0. The searching database was used as *M. musculus* and prediction confidence was used as high and string/experiment was selected to find the interactions. The protein interaction network was generated by iGPS to see the possible kinase substrate interaction. Sequence motif enrichment analyses of phosphorylation sites were performed using the MotifX algorithm [78] with windows of

17 amino acids. The Rattus norvegicus database employed previously for protein identification was used as a background file. Phosphorylation in the regulating domains of kinases and phosphatases were checked manually in NCBI.

# Results

# 4 RESULTS

## 4.1 Hematological study

The hematological parameters of the control, laparotomy, ischemia/reperfusion and ischemic preconditioning groups are summarized in supplementary table 1.

All surgical groups (LAP, IR and IPC) produced a remarkably smaller amount of lymphocytes than the control group. Among the surgical groups, IR showed a decrease in lymphocyte counts (p=0.0021) when compared with the LAP group; however, an increase was noted in IPC (p=0.0171), compared with IR (Graph 1A).

White blood cell counts showed a significant increase in both the IR (p=0.0005) and the IPC (p=0.0074) group, compared with the control group (Graph 1B). The elevation in WBCs was more prominent in IR than IPC. A significant increase in the granulocyte count was observed in the LAP, IR and IPC groups compared with controls. There was an increase in the IR group compared with the LAP group (p=0.0015), and IPC promoted an important reduction (p=0.0168) compared with the IR group, almost approaching the LAP level (Graph 1C).

The platelets showed a significant difference between the IR and IPC groups. The platelet counts were higher (p=0.0340) in the IR group than in the IPC group (Graph 1D). The MPV showed a significantly increased value in the IR (p=0.0096) and IPC (p=<0.0001) groups, compared with the controls. In preconditioned rats, the MPV was higher than in the LAP (p=0.0004) and IR rats (p=0.0485) (Graph 1E). Platelet distribution widths were significantly higher in IPC rats compared with all other groups. The p-values for IPC as compared to control, Lap and IR are p= 0.0003, 0.0015 and 0.0011 respectively (Graph 1F).

**Graph 1** Box plot representing distribution of the hematimetric parameters in the four experimental groups. (A) Lymphocytes count, (B) White blood cells count (C) Granulocytes count, (D) Platelets count, (E) Mean Platelet Volume and (F) Platelet distribution width. (***P < 0.001; **P < 0.001 to 0.01; *P < 0.01 to 0.05)

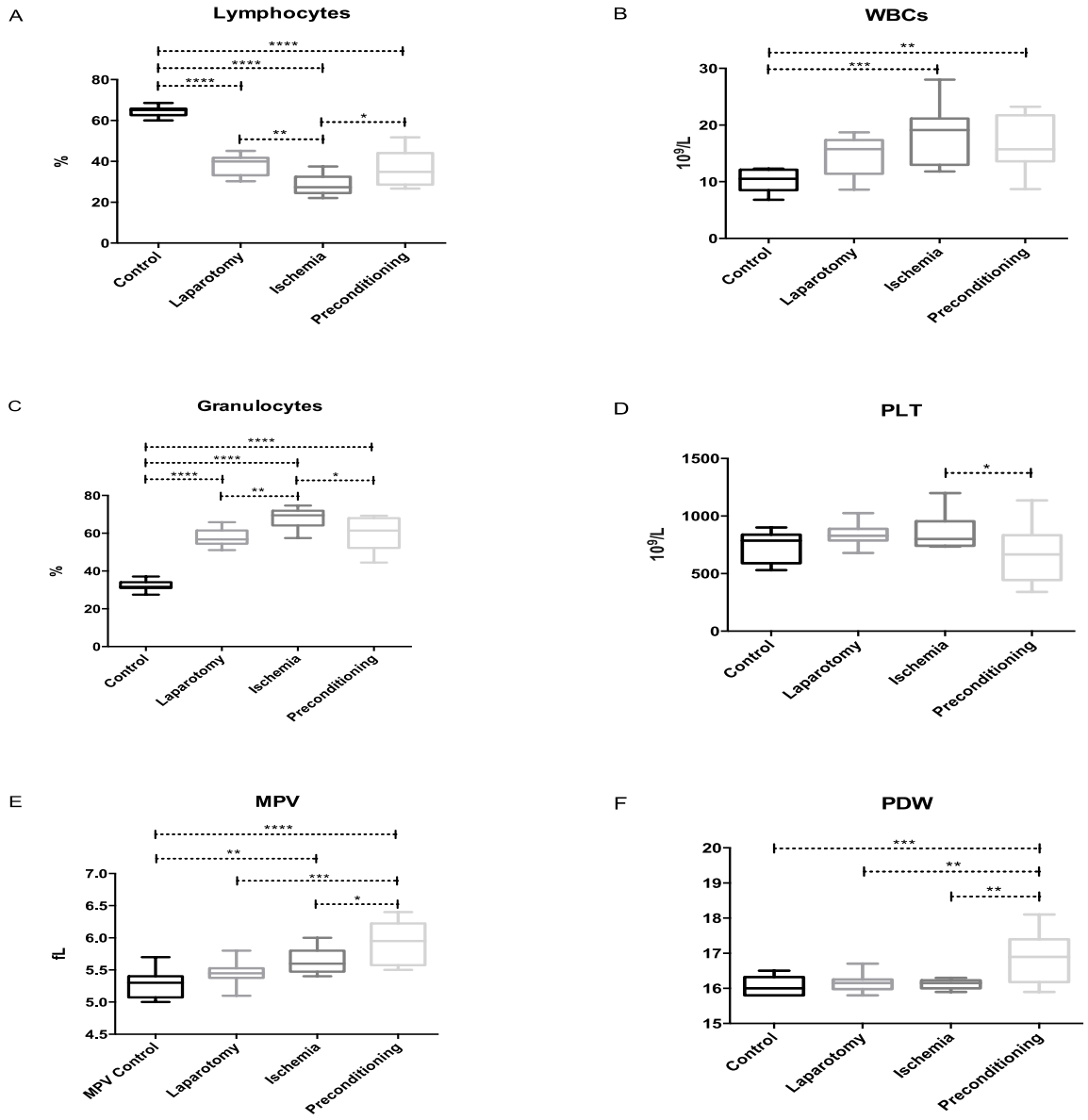


The monocytes, RBCs, Hb, MCV and MCH were not influenced significantly in any experimental group. The hematocrit (HCT) was increased (p=0.0082) in the IR group, compared with the control (supplementary graph 1). The mean corpuscular hemoglobin concentration (MCHC) was decreased in the IR group (p=0.0111) in comparison with the controls, while there was an increase in the MCHC value in the

IPC (p=0.0111), compared with the IR, returning the MCHC value to a normal level (Graph 1B, supplementary). The red cell deviation width was higher (p=0.0152) in the IPC group, compared with the controls; no other group showed a significant difference (Graph 1C, supplementary). Both IR and IPC had significant differences regarding their plateletcrit (PCT) levels, while the rest of the groups did not show any significance differences. The plateletcrit (PCT) was higher (p=0.0264) in IR as compared to IPC (Graph 1D supplementary).

## 4.2 Protein identification and relative protein expression analysis after surgical truma

In this study we performed a comprehensive comparative proteomic analysis of neutrophils from surgically traumatized rats to evaluate the early effect of surgical trauma on the rat neutrophil proteome compared to the control, neutrophils from rats anesthetized but not submitted to surgery. Each group of control and surgical trauma contained 10 rats and the neutrophils were isolated from blood by using Ficoll density gradient method. After neutrophil isolation, proteins were extracted from the neutrophils and quantified. Pooling of two rats protein samples was done followed by trypsin digestion on Vivacon filters. All experiments were performed in five biological replicates. The resulting peptides were identified and quantified using nLC-MS/MS with iTRAQ labeling. nLC-MS/MS was preceded by HILIC fractionation to improve the depth of the analysis (Fig. 6).

From the nLC-MS/MS analysis a total of 2924 rat neutrophil proteins were identified. Among the identified proteins, 393 (13.4% of the total identified proteins) were significantly different in terms of regulation (t-test P-value < 0.05) in the surgical trauma group as compared to the control. Out of 393 proteins, 190 proteins (~6.5%) showed significant up-regulation in surgical trauma whereas 203 proteins (6.94%) presented down-regulation as compared to the control group.

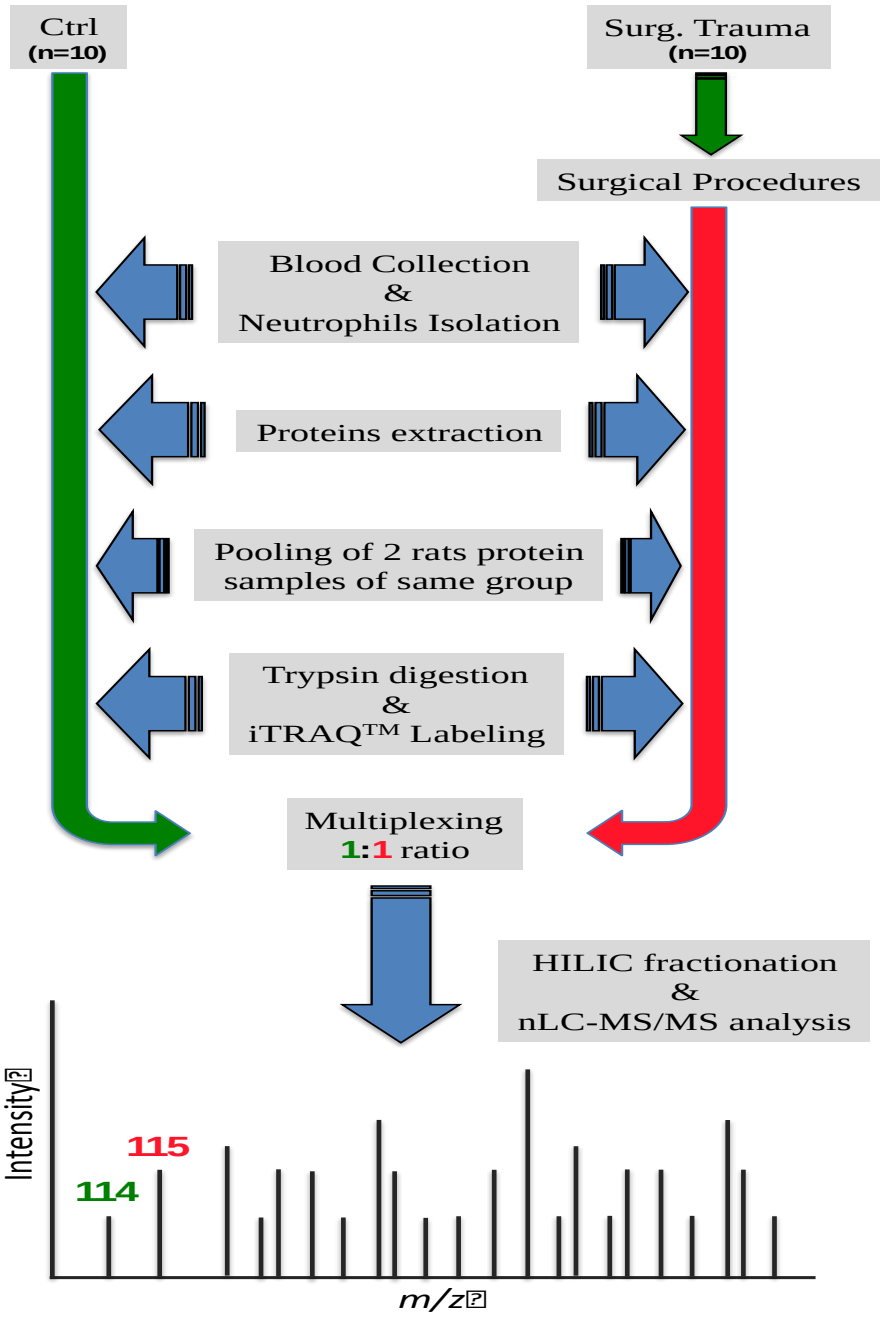


**Figure 6** Experimental workflow for the quantitative proteomic analysis of rat neutrophil subjected to surgical trauma

### 4.2.1 Gene Ontology analysis of differentially regulated protein after surgical truma

The gene ontology (GO) classification of the differentially regulated proteins according to their expected subcellular localization revealed that most of the proteins

belonged to cytoplasm, membrane, nucleus, cytoskeleton, organelle lumen and cytosol (Supplemental Graph 2). The cytoskeleton, membrane, nucleus and vacuole showed higher number of down-regulated proteins and cytosol, endoplasmic reticulum, mitochondrion had higher count of up-regulated proteins, whereas ribosomal proteins were only up-regulated or non-significant. Biological process analysis of the regulated proteins revealed most of the proteins involved in cell communication, cell organization and biogenesis, metabolic processes, response to stimuli and transport. Molecular function analysis further classifies most of the proteins with catalytic activity, and proteins with binding ability for nucleotide, RNA, proteins and metal ions.

### 4.2.2 Predicted enzyme activity for the Surgical Truma responsive proteins

Different enzymes have been linked to the neutrophil activation and function under different conditions and GOs term catalytic activity was found as enriched among the regulated proteins in this study. Therefore, the analysis of the proteins having enzyme activity will highlight the effect of surgical trauma on the neutrophil proteome and function. Enzyme activity prediction for the ST responsive proteins was carried out (Graph. 2) and we found that oxidoreductases and transferases are predominant among the down-regulated proteins whereas ligases were found more frequently within the proteins with significantly up-regulation from neutrophils after abdominal surgery in neutrophils. Table-1 shows all the differentially regulated proteins with their predicted enzyme activity.

**Graph 2** Predicted enzyme activities of proteins with differential regulation level in ST as compare to control.

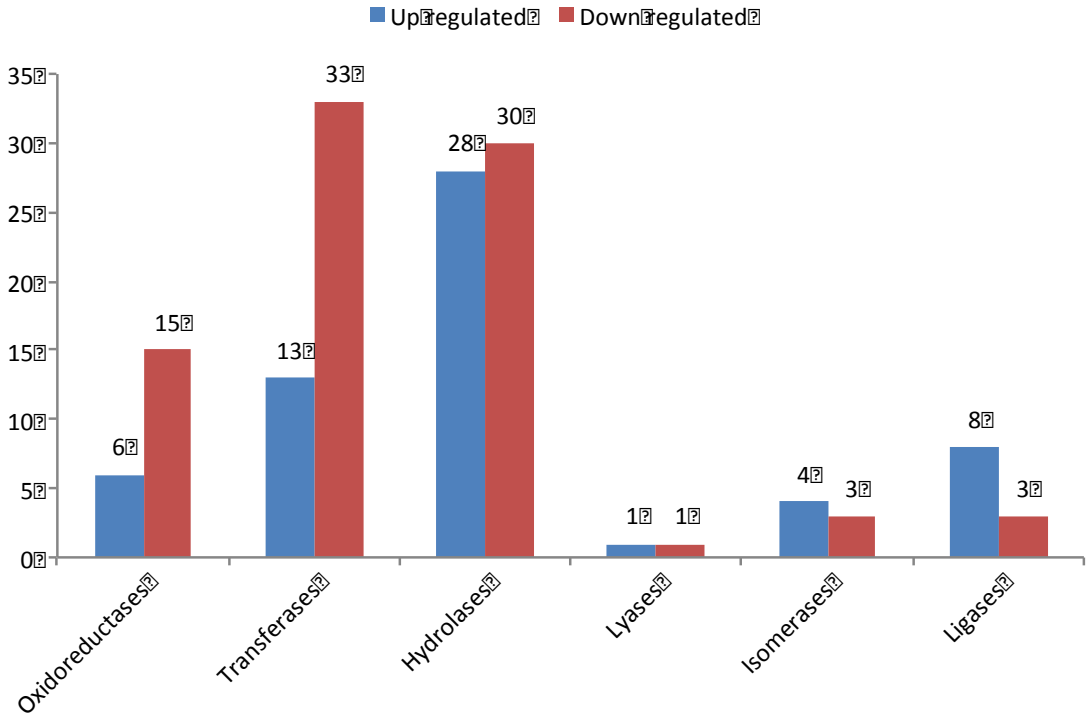

**Table 1** Predicted enzyme activities of the quantified proteins.

| Enzyme Description | EC Number | Accession | GENE Symbol | Sig. Abundance |
|---|---|---|---|---|
| **Oxidoreductases** | | | | |
| malate dehydrogenase, mitochondrial precursor | EC 1.1.1.37 | P04636 | Mdh2 | High |
| Thioredoxin-dependent peroxide reductase, mitochondrial | EC 1.11.1.15 | Q9Z0V6 | Prdx3 | High |
| fatty acyl-CoA reductase 1 isoform 1 | EC 1.2.1.n2 | Q922J9 | Far1 | High |
| biliverdin reductase A precursor | EC 1.3.1.24 | P46844 | Blvra | High |
| coproporphyrinogen-III oxidase, mitochondrial precursor | EC 1.3.3.3 | P36552 | Cpox | High |
| C-1-tetrahydrofolate synthase, cytoplasmic | EC 1.5.1.5 | P27653 | Mthfd1 | High |
| 3-hydroxyacyl-CoA dehydrogenase type-2 | EC 1.1.1.178 | O70351 | Hsd17b10 | Low |
| 3-hydroxyacyl-CoA dehydrogenase type-2 | EC 1.1.1.51 | O70351 | Hsd17b10 | Low |
| Arachidonate 15-lipoxygenase | EC 1.13.11.31 | Q02759 | Alox15 | Low |
| L-lactate dehydrogenase C chain | EC 1.1.1.27 | P19629 | Ldhc | Low |
| 3-hydroxyacyl-CoA dehydrogenase type-2 | EC 1.1.1.35 | O70351 | Hsd17b10 | Low |
| 6-phosphogluconate dehydrogenase, decarboxylating | EC 1.1.1.44 | P85968 | LOC100360180,Pgd | Low |
| eosinophil peroxidase precursor | EC 1.11.1.7 | P49290 | Epx | Low |
| Arachidonate 15-lipoxygenase | EC 1.13.11.33 | Q02759 | Alox15 | Low |
| arachidonate 5-lipoxygenase | EC 1.13.11.34 | P48999 | Alox5 | Low |
| protein-methionine sulfoxide oxidase MICAL1 | EC 1.14.13.- | D3ZBP4 | Mical1 | Low |
| leukotriene-B(4) omega-hydroxylase 2 | EC 1.14.13.3 | Q3MID2 | Cyp4f18 | Low |
| metalloreductase STEAP4 | EC 1.16.1.- | Q4V8K1 | Steap4 | Low |
| peroxisomal acyl-coenzyme A oxidase 1 | EC 1.3.3.6 | P07872 | Acox1 | Low |
| **Transferases** | | | | |
| lysophospholipid acyltransferase 5 | EC 2.3.1.23 | Q5FVN0 | Lpcat3 | High |
| nucleoside diphosphate kinase B | EC 2.7.13.3 | P19804 | Nme2 | High |
| lysophospholipid acyltransferase 5 | EC 2.3.1.- | Q5FVN0 | Lpcat3 | High |
| citrate synthase, mitochondrial precursor | EC 2.3.3.1 | Q8VHF5 | Cs | High |
| dolichol-phosphate mannosyltransferase subunit 1 | EC 2.4.1.83 | Q9WU83 | Dpm1 | High |
| dolichyl-diphosphooligosaccharide--protein glycosyltransferase 48 kDa subunit precursor | EC 2.4.99.18 | O54734 | Ddost | High |
| dolichyl-diphosphooligosaccharide--protein glycosyltransferase subunit STT3A | EC 2.4.99.18 | P46978 | Stt3a | High |
| dolichyl-diphosphooligosaccharide--protein glycosyltransferase subunit DAD1 | EC 2.4.99.18 | P61806 | Dad1 | High |
| Dolichyl-diphosphooligosaccharide--protein glycosyltransferase subunit STT3B | EC 2.4.99.18 | Q3TDQ1 | Stt3b | High |
| glycosaminoglycan xylosylkinase | EC 2.7.1.- | Q8VCS3 | Fam20b | High |
| galactokinase | EC 2.7.1.6 | Q9R0N0 | Galk1 | High |
| nucleoside diphosphate kinase B | EC 2.7.4.6 | P19804 | Nme2 | High |
| succinyl-CoA:3-ketoacid coenzyme A transferase 1, mitochondrial precursor | EC 2.8.3.5 | B2GV06 | Oxct1 | High |
| lysophosphatidylcholine acyltransferase 2 | EC 2.3.1.51 | Q8BYI6 | Lpcat2 | Low |
| lysophosphatidylcholine acyltransferase 2 | EC 2.3.1.67 | Q8BYI6 | Lpcat2 | Low |
| interferon-induced, double-stranded RNA-activated protein kinase | EC 2.7.1.2 | Q63184 | Eif2ak2 | Low |
| 5'-AMP-activated protein kinase catalytic subunit alpha-1 | EC 2.7.11.26 | P54645 | Prkaa1 | Low |
| 5'-AMP-activated protein kinase catalytic subunit alpha-1 | EC 2.7.11.27 | P54645 | Prkaa1 | Low |
| 5'-AMP-activated protein kinase catalytic subunit alpha-1 | EC 2.7.11.31 | P54645 | Prkaa1 | Low |
| UMP-CMP kinase | EC 2.7.4.6 | Q4KM73 | Cmpk1 | Low |
| Transketolase | EC 2.2.1.1 | P50137 | Tkt | Low |
| transaldolase | EC 2.2.1.2 | Q9EQS0 | Taldo1 | Low |
| lysophosphatidylcholine acyltransferase 2 | EC 2.3.1.23 | Q8BYI6 | Lpcat2 | Low |
| ATP-citrate synthase isoform 2 | EC 2.3.3.8 | Q91V92 | Acly | Low |
| nicotinamide phosphoribosyltransferase | EC 2.4.2.12 | Q80Z29 | Nampt | Low |
| glutathione S-transferase P | EC 2.5.1.18 | P04906 | Gstp1 | Low |
| phosphatidylinositol 5-phosphate 4-kinase type-2 alpha | EC 2.7.1.149 | Q9R0I8 | Pip4k2a | Low |
| diacylglycerol kinase zeta | EC 2.7.1.17 | O08560 | Dgkz | Low |
| tyrosine-protein kinase CSK | EC 2.7.1.2 | P32577 | Csk | Low |
| tyrosine-protein kinase BTK | EC 2.7.1.2 | P35991 | Btk | Low |
| protein-tyrosine kinase 2-beta | EC 2.7.1.2 | P70600 | Ptk2b | Low |
| NAD kinase 2, mitochondrial | EC 2.7.1.23 | Q1HCL7 | Nadk2,Nadkd1 | Low |
| STE20-like serine/threonine-protein kinase | EC 2.7.11.1 | O08815 | Slk | Low |
| Phosphoinositide 3-kinase regulatory subunit 4 | EC 2.7.11.1 | P0C0R5 | Pik3r4 | Low |
| 5'-AMP-activated protein kinase catalytic subunit alpha-1 | EC 2.7.11.1 | P54645 | Prkaa1 | Low |
| serine/threonine-protein kinase TAO3 | EC 2.7.11.1 | Q53UA7 | Taok3 | Low |
| interferon-induced, double-stranded RNA-activated protein kinase | EC 2.7.11.1 | Q63184 | Eif2ak2 | Low |
| Serine/threonine-protein kinase PAK 2 | EC 2.7.11.1 | Q64303 | Pak2,LOC100910732 | Low |
| serine/threonine-protein kinase 17B | EC 2.7.11.1 | Q91XS8 | Stk17b | Low |
| serine/threonine-protein kinase MST4 | EC 2.7.11.1 | Q99JT2 | 2610018G03Rik | Low |
| serine/threonine-protein kinase 4 | EC 2.7.11.1 | Q9JI11 | Stk4 | Low |
| serine/threonine-protein kinase WNK1 isoform B | EC 2.7.11.1 | Q9JIH7 | Wnk1 | Low |
| cAMP-dependent protein kinase catalytic subunit beta | EC 2.7.11.11 | P68180 | | Low |
| protein kinase C delta type | EC 2.7.11.13 | P09215 | Prkcd | Low |
| calcium/calmodulin-dependent protein kinase type 1 | EC 2.7.11.17 | Q63450 | Camk1 | Low |
| UMP-CMP kinase | EC 2.7.4.14 | Q4KM73 | Cmpk1 | Low |

Table 1 *(Continuous)*

| Enzyme Description | EC Number | Accession | GENE Symbol | Sig. Abundance |
|---|---|---|---|---|
| **Hydrolases** | | | | |
| C-1-tetrahydrofolate synthase, cytoplasmic | EC 6.3.4.9 | P27653 | Mthfd1 | High |
| ras GTPase-activating protein-binding protein 1 | EC 3.6.4.13 | P97855 | G3bp1 | High |
| isoamyl acetate-hydrolyzing esterase 1 homolog | EC 3.1.-.- | Q711G3 | Iah1 | High |
| peptidyl-tRNA hydrolase 2, mitochondrial isoform b | EC 3.1.1.29 | Q8R2Y8 | Ptrh2 | High |
| palmitoyl-protein thioesterase 1 precursor | EC 3.1.2.22 | P45479 | Ppt1 | High |
| myotubularin-related protein 6 | EC 3.1.3.- | Q8VE11 | Mtmr6 | High |
| 1-phosphatidylinositol 4,5-bisphosphate phosphodiesterase beta-3 | EC 3.1.4.11 | Q99JE6 | Plcb3 | High |
| N-acetylglucosamine-6-sulfatase precursor | EC 3.1.6.14 | Q8BFR4 | Gns | High |
| Tissue alpha-L-fucosidase | EC 3.2.1.51 | P17164 | Fuca1 | High |
| xaa-Pro aminopeptidase 1 | EC 3.4.11.9 | O54975 | Xpnpep1 | High |
| eukaryotic translation initiation factor 3 subunit F | EC 3.4.19.12 | Q9DCH4 | Eif3f | High |
| Myeloblastin | EC 3.4.21.76 | Q61096 | Prtn3 | High |
| pro-cathepsin H precursor | EC 3.4.22.16 | P00786 | Ctsh | High |
| Caspase-1 | EC 3.4.22.36 | P43527 | Casp1 | High |
| Cathepsin D | EC 3.4.23.5 | P24268 | Ctsd | High |
| inorganic pyrophosphatase | EC 3.6.1.1 | Q9D819 | Ppa1 | High |
| sarcoplasmic/endoplasmic reticulum calcium ATPase 2 isoform b | EC 3.6.3.8 | P11507 | Atp2a2 | High |
| SWI/SNF-related matrix-associated actin-dependent regulator of chromatin subfamily A member 5 | EC 3.6.4.- | Q91ZW3 | Smarca5 | High |
| DNA replication licensing factor MCM4 | EC 3.6.4.12 | P49717 | Mcm4 | High |
| DNA replication licensing factor MCM5 | EC 3.6.4.12 | P49718 | Mcm5 | High |
| DNA replication licensing factor MCM2 | EC 3.6.4.12 | P97310 | Mcm2 | High |
| DNA replication licensing factor MCM6 | EC 3.6.4.12 | P97311 | Mcm6 | High |
| ras GTPase-activating protein-binding protein 1 | EC 3.6.4.12 | P97855 | G3bp1 | High |
| chromodomain-helicase-DNA-binding protein 4 | EC 3.6.4.12 | Q6PDQ2 | Chd4 | High |
| putative pre-mRNA-splicing factor ATP-dependent RNA helicase DHX15 isoform 2 | EC 3.6.4.13 | O35286 | Dhx15 | High |
| eukaryotic initiation factor 4A-I isoform 1 | EC 3.6.4.13 | P60843 | Eif4a1 | High |
| ATP-dependent RNA helicase DDX3X | EC 3.6.4.13 | Q62167 | Ddx3x | High |
| transitional endoplasmic reticulum ATPase | EC 3.6.4.6 | P46462 | Vcp | High |
| inositol monophosphatase 1 | EC 3.1.3.94 | P97697 | Impa1 | Low |
| diphosphoinositol polyphosphate phosphohydrolase 2 | EC 3.6.1.- | Q8R2U6 | Nudt4 | Low |
| neutral cholesterol ester hydrolase 1 | EC 3.1.1.- | B2GV54 | Nceh1 | Low |
| platelet-activating factor acetylhydrolase 2, cytoplasmic | EC 3.1.1.47 | P83006 | Pafah2 | Low |
| Sialate O-acetylesterase | EC 3.1.1.53 | P82450 | Siae | Low |
| acyl-protein thioesterase 1 | EC 3.1.2.- | P70470 | Lypla1 | Low |
| eosinophil cationic protein precursor | EC 3.1.27.- | P70709 | LOC100361866,Ear11 | Low |
| ubiquitin-like domain-containing CTD phosphatase 1 | EC 3.1.3.16 | Q5FWT7 | Ublcp1 | Low |
| serine/threonine-protein phosphatase 6 catalytic subunit | EC 3.1.3.16 | Q9CQR6 | Ppp6c | Low |
| protein phosphatase 1F | EC 3.1.3.16 | Q9WVR7 | Ppm1f | Low |
| inositol monophosphatase 1 | EC 3.1.3.25 | P97697 | Impa1 | Low |
| phosphoserine phosphatase | EC 3.1.3.3 | Q5M819 | Psph | Low |
| receptor-type tyrosine-protein phosphatase C isoform 4 precursor | EC 3.1.3.48 | P04157 | Ptprc | Low |
| 1-phosphatidylinositol 4,5-bisphosphate phosphodiesterase gamma-2 | EC 3.1.4.11 | P24135 | Plcg2 | Low |
| beta-mannosidase precursor | EC 3.2.1.25 | Q4FZV0 | Manba | Low |
| Neutral alpha-glucosidase AB | EC 3.2.1.84 | Q8BHN3 | Ganab | Low |
| aminopeptidase N precursor | EC 3.4.11.2 | P15684 | Anpep | Low |
| tripeptidyl-peptidase 2 | EC 3.4.14.1 | Q64560 | Tpp2 | Low |
| Signal peptidase complex catalytic subunit SEC11A | EC 3.4.21.89 | P42667 | Sec11a | Low |
| caspase-3 | EC 3.4.22.56 | P55213 | Casp3 | Low |
| proteasome subunit alpha type-2 | EC 3.4.25.1 | P49722 | Psma2 | Low |
| adenosine deaminase | EC 3.5.4.4 | Q920P6 | Ada | Low |
| protein prune homolog | EC 3.6.1.1 | Q6AYG3 | Prune | Low |
| ectonucleoside triphosphate diphosphohydrolase 1 | EC 3.6.1.5 | P97687 | Entpd1 | Low |
| diphosphoinositol polyphosphate phosphohydrolase 2 | EC 3.6.1.52 | Q8R2U6 | Nudt4 | Low |
| m7GpppX diphosphatase | EC 3.6.1.59 | Q9DAR7 | Dcps | Low |
| E1A-binding protein p400 | EC 3.6.4.- | Q8CHI8 | Ep400 | Low |
| regulator of nonsense transcripts 1 isoform a | EC 3.6.4.- | Q9EPU0 | Upf1 | Low |
| fumarylacetoacetase | EC 3.7.1.2 | P25093 | Fah | Low |

Table 1 *(End)*

| Enzyme Description | EC Number | Accession | GENE Symbol | Sig. Abundance |
|---|---|---|---|---|
| **Lyases** | | | | |
| multifunctional protein ADE2 | EC 4.1.1.21 | P51583 | Paics | High |
| DNA-(apurinic or apyrimidinic site) lyase | EC 4.2.99.18 | P43138 | Apex1 | Low |
| **Isomerases** | | | | |
| peptidyl-prolyl cis-trans isomerase A | EC 5.2.1.8 | P17742 | Ppia | High |
| peptidyl-prolyl cis-trans isomerase F, mitochondrial precursor | EC 5.2.1.8 | P29117 | Ppif | High |
| peptidyl-prolyl cis-trans isomerase FKBP3 | EC 5.2.1.8 | Q62446 | Fkbp3 | High |
| thromboxane-A synthase | EC 5.3.99.5 | P49430 | Tbxas1 | High |
| ribose-5-phosphate isomerase | EC 5.3.1.6 | P47968 | Rpia | Low |
| glucose-6-phosphate isomerase | EC 5.3.1.9 | Q6P6V0 | Gpi | Low |
| DNA topoisomerase 2-beta | EC 5.99.1.3 | Q64399 | | Low |
| **Ligases** | | | | |
| Glycine--tRNA ligase | EC 6.1.1.14 | Q5I0G4 | Gars | High |
| succinyl-CoA ligase [ADP-forming] subunit beta, mitochondrial precursor | EC 6.2.1.5 | Q9Z2I9 | Sucla2 | High |
| E3 ubiquitin/ISG15 ligase TRIM25 | EC 6.3.2.19 | Q61510 | Trim25 | High |
| glutathione synthetase | EC 6.3.2.3 | P46413 | Gss | High |
| multifunctional protein ADE2 | EC 6.3.2.6 | P51583 | Paics | High |
| tRNA-splicing ligase RtcB homolog | EC 6.5.1.3 | Q99LF4 | D10Wsu52e,Rtcb | High |
| E3 ubiquitin/ISG15 ligase TRIM25 | EC 6.3.2.n3 | Q61510 | Trim25 | High |
| C-1-tetrahydrofolate synthase, cytoplasmic | EC 6.3.4.3 | P27653 | Mthfd1 | High |
| threonine--tRNA ligase, cytoplasmic | EC 6.1.1.3 | Q9D0R2 | Tars | Low |
| Lysine--tRNA ligase | EC 6.1.1.6 | P37879 | LOC100766627 | Low |
| lysine--tRNA ligase isoform 2 | EC 6.1.1.6 | Q99MN1 | Kars | Low |

### 4.2.3 Functional pathways and in silico protein-protein interactions analysis of trauma affected proteins

The functional pathways analysis of the trauma related proteins was carried out by wikipathways using web-based gene set analysis toolkit (webgestalt) (24). Table 2 lists the top ten pathways enriched for significantly up and downregulated proteins in st compared to control. We determined the pathways of a number of proteins regulated in ST rats, including protein biosynthesis and several other pathways related to the immune system, oxidative phosphorylation and energy metabolism like TCA and pentose phosphate pathway, proteasome degradation and regulation of actin cytoskeleton. Furthermore, protein-protein interaction analysis using string (fig. 7) facilitated the visualization of pathways where regulated proteins were enriched.

**Table 2** Predicted Wiki pathways analysis for the proteins with significantly differential regulation.

| Pathway Name | Overlaped Gene | Reference Genes | Ratio | Raw P-value | Adjusted P-value |
|---|---|---|---|---|---|
| **Pathways for more abundant proteins** | | | | | |
| Cytoplasmic Ribosomal Proteins | 12 | 86 | 36.06 | 9.15E-16 | 2.20E-14 |
| Translation Factors | 8 | 47 | 43.99 | 1.18E-11 | 1.42E-10 |
| Electron Transport Chain | 8 | 100 | 20.67 | 5.88E-09 | 4.70E-08 |
| mRNA processing | 8 | 130 | 15.9 | 4.65E-08 | 2.79E-07 |
| TNF-alpha NF-kB Signaling Pathway | 9 | 203 | 11.46 | 1.12E-07 | 5.38E-07 |
| DNA Replication | 4 | 40 | 25.84 | 1.78E-05 | 7.12E-05 |
| Oxidative phosphorylation | 4 | 58 | 17.82 | 7.81E-05 | 0.0003 |
| TCA Cycle | 3 | 28 | 27.69 | 0.0002 | 0.0005 |
| G1 to S cell cycle control | 4 | 73 | 14.16 | 0.0002 | 0.0005 |
| Cell cycle | 4 | 95 | 10.88 | 0.0005 | 0.0012 |
| **Pathways for less abundant proteins** | | | | | |
| B Cell Receptor Signaling Pathway | 12 | 199 | 14.66 | 4.83E-11 | 1.69E-09 |
| IL-5 Signaling Pathway | 8 | 80 | 24.31 | 1.59E-09 | 2.78E-08 |
| Pentose Phosphate Pathway | 4 | 8 | 121.5 | 1.92E-08 | 2.24E-07 |
| Proteasome Degradation | 6 | 59 | 24.72 | 1.68E-07 | 1.47E-06 |
| Regulation of Actin Cytoskeleton | 8 | 156 | 12.46 | 3.04E-07 | 1.77E-06 |
| EGFR1 Signaling Pathway | 9 | 213 | 10.27 | 2.83E-07 | 1.77E-06 |
| Kit Receptor Signaling Pathway | 6 | 70 | 20.83 | 4.71E-07 | 2.21E-06 |
| IL-6 Signaling Pathway | 7 | 114 | 14.92 | 5.06E-07 | 2.21E-06 |
| Type II Interferon Signaling (IFNG) | 6 | 76 | 19.19 | 7.70E-07 | 2.99E-06 |
| T Cell Receptor Signaling Pathway | 7 | 139 | 12.24 | 1.92E-06 | 6.72E-06 |

Ratio: Ratio of enrichment

Raw P-value: p value from hypergeometric test

Adjusted P-value: p value adjusted by the multiple test adjustment

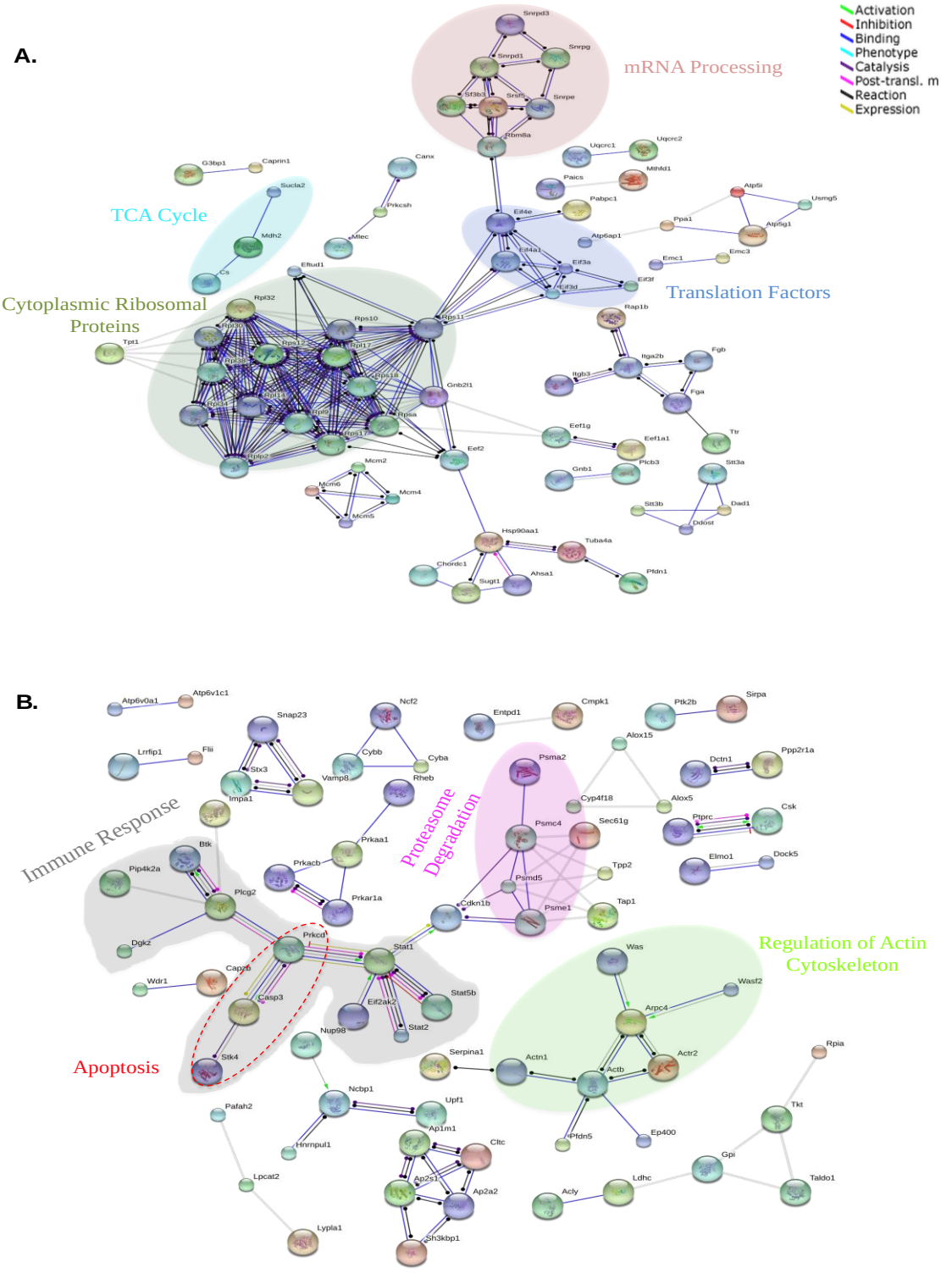


**Figure 7** A. STRING protein-protein interaction analysis of the significantly up-regulated proteins in ST rats revealing protein networks involved in mRNA processing, TCA cycle, Translation Factors, and Cytoplasmic Ribosomal proteins. B. STRING protein-protein interaction analysis of the significantly down-regulated proteins in ST rats revealing protein networks involved in Proteasome degradation, Regulation of Actin Cytoskeleton, Immune response, and Apoptosis. Color lines represent modes of interaction as detailed in the legend.

## 4.3 Large proteomic analysis of rat neutrophils

For the large proteomic analysis of rat neutrophil, we have selected 40 wistar rats after performing haematological analysis and randomly allocated into 4 groups; Control (Ctrl), Sham laparotomy (LAP), Ischemic Reperfusion (IR) and Ischemic Preconditioning (IPC). The neutrophils were isolated and the proteins extracted from the two rats of the same group were pooled to a total of 5 replicates in each group. All the 20 replicates were labelled with iTRAQ markers; Ctrl with 114, Lap with 115, IR with 116 and IPC with 117. After confirmation of iTRAQ labelling the labelled peptides were multiplexed in 1:1:1:1 ratio. HILIC fractionated samples were subjected to nLC-MS/MS analysis by LTQ orbitrap Velos (Fig. 8). The list of identified and iTRAQ labelled peptides was analyzed by using statistical software developed in R, which provided a total of 2437 protein groups in all conditions. The Principal component analysis showed that the variability among replicates was less than that among the different conditions showing relatively good reproducibility in each condition (supplementary fig. 1).

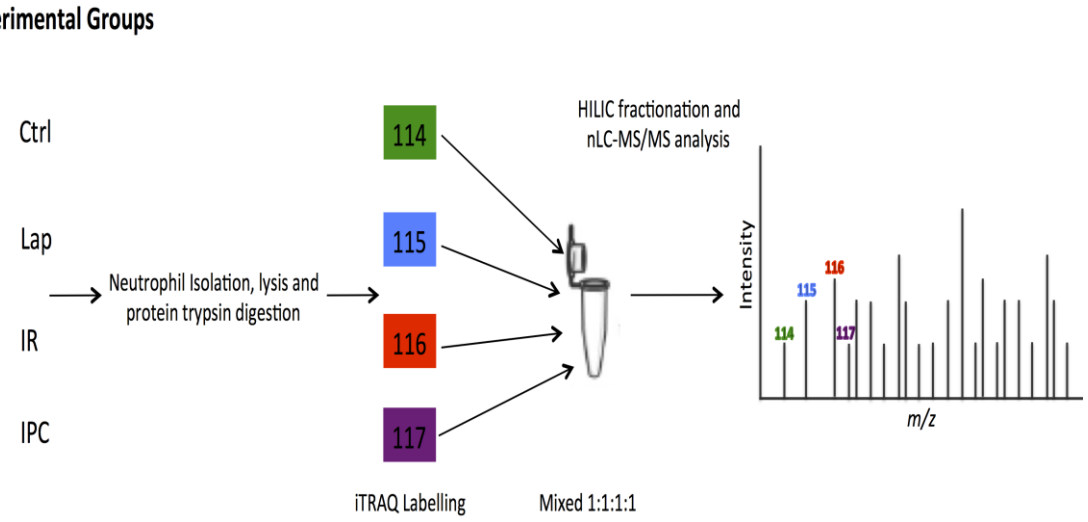


**Figure 8** Experimental workflow for the quantitative analysis of neutrophil proteome. Control (Ctrl) sample was labelled with 114, laparotomy (Lap) with 115, ischemia reperfusion (IR) with 116 and ischemic preconditioning (IPC) with 117.

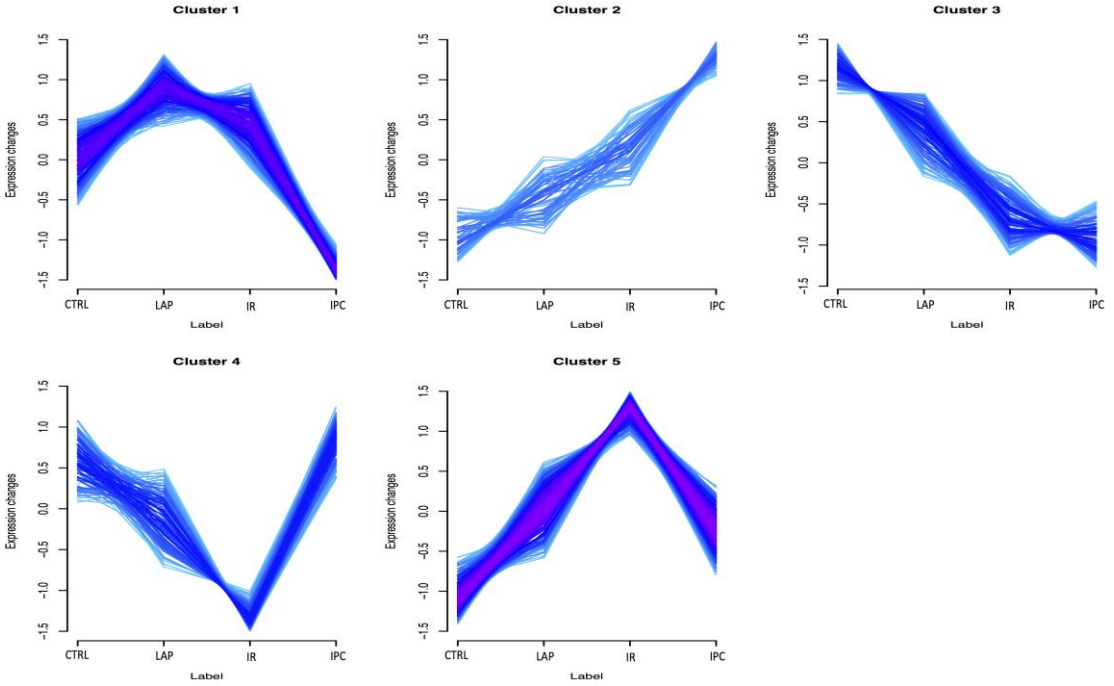


**Figure 9** Expression profile of regulated proteins during Ctrl, LAP, IR and IPC. All the identified proteins were grouped in 5 clusters.

Two validation indices minimal centroid distance (36) and Xie-Beni index (47) were subsequently applied to define and visualize the significant protein clusters. The resulting five clusters with different abundance profiles are shown in figure 9. Clusters 1-5 consisted of 570, 402, 484, 444, and 537 protein groups respectively, with no overlapping. Clusters 2 and 3 are representing the proteins with continuous increasing and decreasing relative abundance profiles respectively that can be correlated to the continuous severity in surgical procedures whereas cluster 1 showed only difference in IPC as compared to the Ctrl, Lap and IR. Fig 9 shows that a profile representing differences in relative abundance between IR and IPC groups with less difference among Ctrl, LAP and IPC groups is present in clusters 4 and 5, suggesting the two clusters with IPC responsive proteins. In that sense, proteins from clusters 4 and 5 had their abundance profile reflecting the preventive effect of IPC over IR and were chosen for a more detailed discussion. For the functional classification of the proteins in clusters 4 and 5 we used ProteinCenter for the gene ontology (GO) analysis and UniProt to retrieve enzyme activity prediction, as well as WebGestalt to find enriched pathways in the Kyoto Encyclopedia of Genes and Genomes (KEGG) database (45).

### 4.3.1 Gene ontology of protein groups from clusters 4 and 5:

Analysis of the GO terms of the protein groups from clusters 4 and 5 is shown in graph. 3. Distribution of GO terms for cellular component (Graph. 3A) showed great diversity of protein groups in their cellular localization. The major difference in relative abundance in both clusters was noticed among the proteins annotated to cytoplasm, membrane, cytoskeleton, nucleus, organelle lumen and ribosome. Graph. 3A shows 119 proteins (58 in cluster 4, 61 in cluster 5) presenting a relative abundance profile that suggests influence of the mitochondrial protein distribution pattern in preventing the IR alterations in neutrophil.

Graph. 3A shows 119 proteins (58 in cluster 4, 61 in cluster 5) presenting a relative abundance profile that suggests influence of the mitochondrial protein distribution pattern in preventing the IR alterations in neutrophil. Mostly membrane and cytoskeletal proteins from cluster 4 are downregulated in IR. The proteins from cluster 5 annotated to cytoplasm, nucleus, organelle lumen and ribosome are upregulated in IR in accordance with the activation of the transcriptional and translational machinery whereas IPC prevents such upregulation.

Graph. 3-B shows the GO slim terms for biological activity with major differences in processes like metabolic, cell communication, stimuli response and transport however GOs slim for molecular function graph. 3-C indicates that most differences are found in transcriptional and translational activity including DNA, RNA, nucleotide and metal ion binding, structural molecules and catalytic activity.

**Graph 3** GO slim terms of proteins with differential regulation level in in clusters 4 and 5. GO slim cellular component (A), Biological activity (B), and Molecular function (C). Y-axis represents the number of occurrences of each GO slim term.

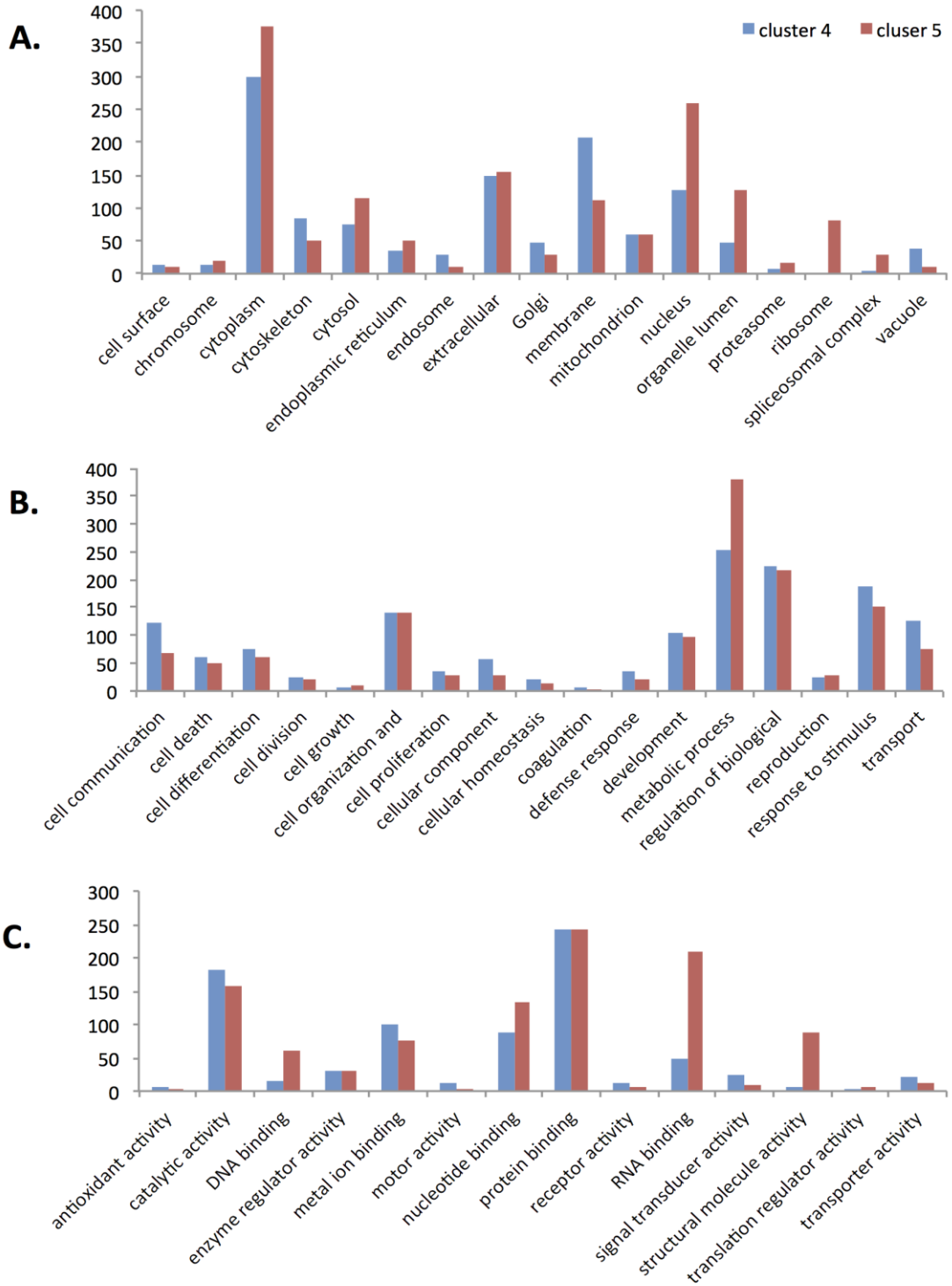

### 4.3.2 Pathway Analysis for cluster 4

All the significantly regulated proteins from cluster 4 were analyzed for the KEGG pathways for top ten functional categories (Supplementary Table - 2) and the pathways found include: regulation of actin cytoskeleton, metabolic pathways, Fc gamma R mediated Phagocytosis, chemokine signaling, focal adhesion and leukocyte transendothelial migration. Such findings are in accordance with the GO analysis. The regulation of actin cytoskeleton was classified with the highest p-value and contains 15 proteins with significant regulation. There were 54 proteins from metabolic pathways found to follow the abundance profile of cluster 4, out of which 20 were regulated, participating mainly in glycolysis/gluconeogenesis, amino sugar and nucleotide, fructose, mannose, galactose and purine metabolism (supplementary table - 2).

### 4.3.3 Pathway Analysis for cluster 5

KEGG pathway analysis of the differentially regulated proteins in cluster 5 revealed ribosome, spliceosome, RNA transport, protein processing in endoplasmic reticulum, proteasome, DNA replication, RNA transport and some metabolic pathways. Several pathways identified by KEGG analysis of regulated proteins overlapped with the GO analysis of the proteins for cluster 5 (supplementary table - 2). In particular, the ribosome pathway is the most prominent in the two analyses. This finding suggests that the response of neutrophils to IR affects the upregulation of transcription, translation, protein folding, sorting and degradation processes in cells along with the replication and metabolism. Interestingly 62 proteins out of 63 were found significantly regulated in cluster 5. All these processes are required for the inflammatory response of neutrophils during IR whereas these pathways were downregulated in neutrophils from the IPC group showing the effect of IPC on neutrophil to prevent such response.

### 4.3.4 String analysis for cluster 4 and 5

STRING v9.1 with highest confidence score (0.900) (76) was used to check for protein-protein interactions of all the proteins identified in both the clusters. Fig. 10-A and B shows the results that are in accordance with the Pathway and GO analysis

highlighting different groups of protein-protein interactions in both clusters. The Fig. 10-A shows that the most interacting proteins (i.e. the proteins that present the highest number of interactions) in cluster 4 are rac2 and Rhoa (Rho-family GTPase) are found significantly downregulated in IPC vs IR and are important regulators of motility and cell shape (77). Fig. 10-B shows analysis from cluster 5 highlighting some of the most interacting proteins Rps27, Eftud2, Hnrpd and Hsp90aa1 that are part of ribosome, spliceosome and endoplasmic reticulum processing respectively. Interestingly Rps27 and Hsp90aa1 were found regulated among all conditions, with upregulation from ctrl/lap vs IR and then downregulation from IR vs IPC, whereas Eftud2 was found also downregulated from IR vs IPC.

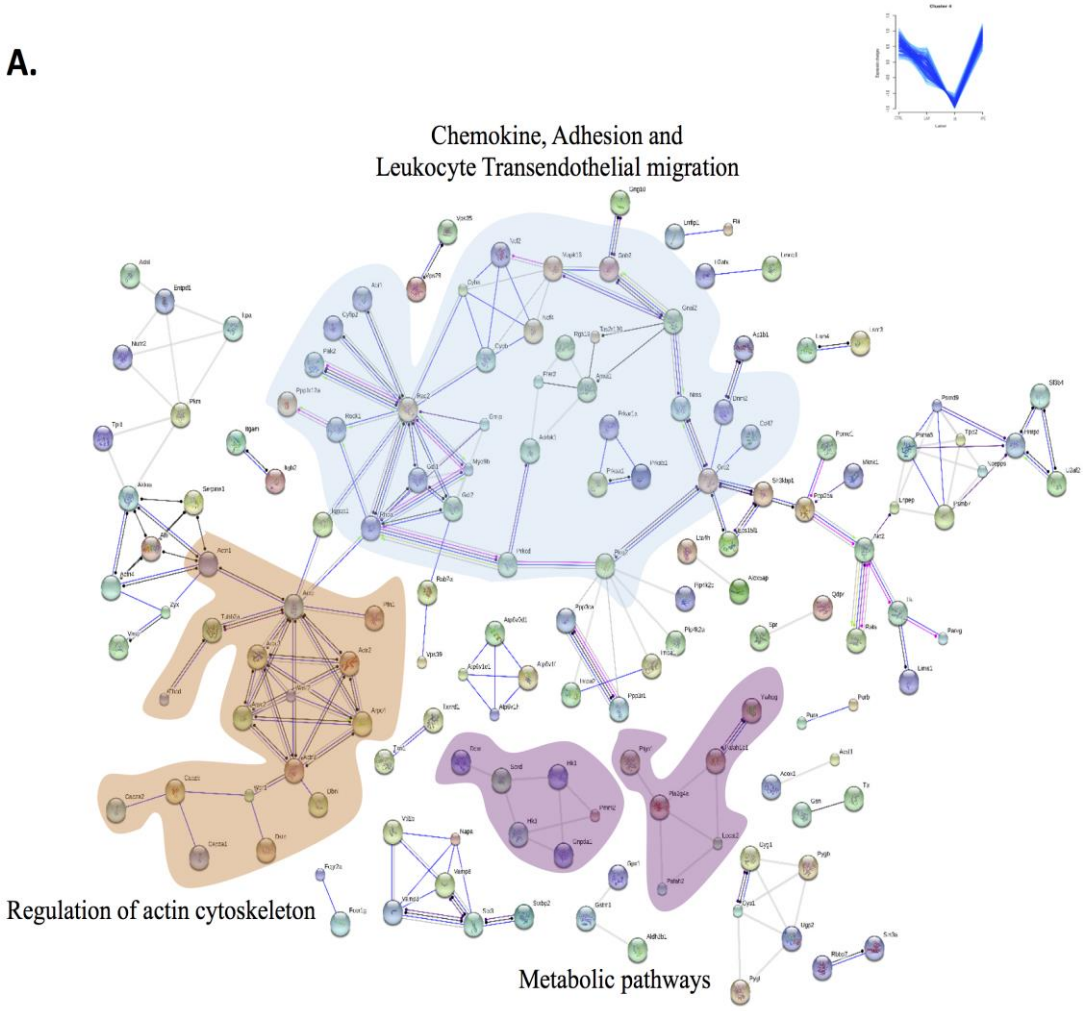

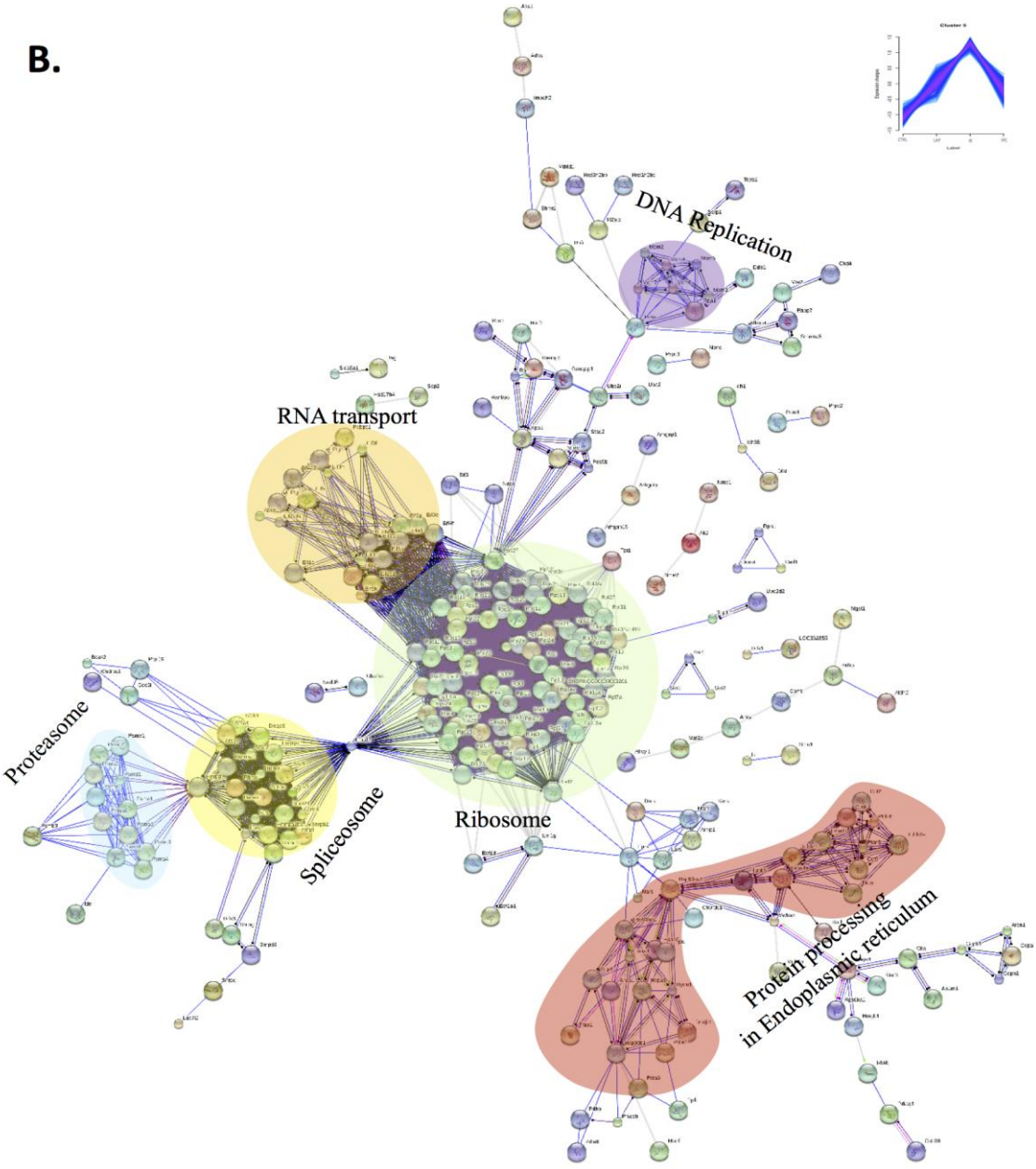


**Figure 10** (A) Protein-protein interaction analysis of cluster 4 highlighting protein networks involved in chemokine, adhesion and leukocyte transendothelial migration (blue), regulation of actin cytoskeleton (orange) and metabolic pathways (purple). (B) Protein-protein interaction analysis of cluster 5 highlighting protein networks involved in Ribosome (green), proteasome (blue), spliceosome (yellow), RNA transport (orange), DNA replication (purple), and endoplasmic reticulum (red). Thicker, blue and black lines indicate more confident binding and reaction associations respectively.

### 4.3.5 Enzyme prediction for cluster 4 and 5

To predict the enzymatic activity of the significantly regulated proteins in both clusters, Enzyme Commission numbers were retrieved from the online UniProt database service Table - 3. The proteins classified to oxidoreductases, transferases and hydrolyses were found abundant in cluster 4 and isomerases and ligases in cluster 5 respectively (Graph. 4). The predicted enzymes are involved in carbohydrate metabolism and oxidation of fatty acid and aldehydes, with some interesting antioxidants e.g; peroxiredoxin-6 (1.11.1.15), glutathione peroxidase (1.11.1.9), and methionine sulfoxide reductase (1.8.4.11) in cluster 4 and superoxide dismutase (1.15.1.1) in cluster 5.

**Table 3** Predicted enzyme activities of the quantified proteins in clusters 4 and 5.

| EC number | Protein ID | Description | Cluster | Gene symbol |
|---|---|---|---|---|
| **Oxidoreductases** | | | | |
| 1.1.1.14 | P27867 | sorbitol dehydrogenase (carbohydrate metabolism) | 4 | Sord |
| 1.1.1.271 | P23591 | GDP-L-fucose synthase (fructose and mannose metabolism) | 4 | Tsta3 |
| 1.11.1.15 | O35244 | peroxiredoxin-6 (antioxidant) | 4 | Prdx6 |
| 1.11.1.9 | P04041 | glutathione peroxidase 1 | 4 | Gpx1 |
| 1.11.1.9 | O35244 | glutathione peroxidase 1 | 4 | Prdx6 |
| 1.11.2.2 | P11247 | myeloperoxidase | 4 | Mpo |
| 1.2.1.5 | Q5XI42 | aldehyde dehydrogenase family 3 member B1 (oxidation of aldehydes) | 4 | Aldh3b1 |
| 1.3.3.6 | P07872 | peroxisomal acyl-coenzyme A oxidase 1 (fatty acid oxidation) | 4 | Acox1 |
| 1.8.4.11 | Q923M1 | mitochondrial peptide methionine sulfoxide reductase | 4 | Msra |
| 1.1.1.27 | P04642 | L-lactate dehydrogenase A chain (tissue damage) Pyruvate to lacate in absence of oxygen | 5 | Ldha |
| 1.15.1.1 | P07632 | superoxide dismutase [Cu-Zn] | 5 | Sod1 |
| 1.2.1.3 | P47738 | aldehyde dehydrogenase, mitochondrial precursor | 5 | Aldh2 |
| 1.5.1.3 | Q920D2 | dihydrofolate reductase | 5 | Dhfr |
| **Transferases** | | | | |
| 2.1.1.77 | P22062 | protein-L-isoaspartate(D-aspartate) O-methyltransferase | 4 | Pcmt1 |
| 2.3.1.67 | Q8BYI6 | lysophosphatidylcholine acyltransferase 2 fatty acid metabolism/1-acylglycerophosphocholine O-acyltransferase | 4 | Lpcat2 |
| 2.3.1.67 | Q8BYI6 | lysophosphatidylcholine acyltransferase 2 fatty acid metabolism/1-acylglycerol-3-phosphate O-acyltransferase | 4 | Lpcat2 |
| 2.3.1.67 | Q8BYI6 | lysophosphatidylcholine acyltransferase 2 lipid formation/1-alkylglycerophosphocholine O-acetyltransferase | 4 | Lpcat2 |
| 2.4.1.1 | P09811 | glycogen phosphorylase, liver form degradation of large branched glycan polymers | 4 | Pygl |
| 2.4.1.186 | O08730 | glycogenin-1 glucosylation | 4 | Gyg1 |
| 2.4.2.8 | Q64531 | Hypoxanthine-guanine phosphoribosyltransferase | 4 | Hprt1 |
| 2.7.1.1 | P27926 | hexokinase-3 | 4 | Hk3 |
| 2.7.1.149 | Q9R0I8 | phosphatidylinositol 5-phosphate 4-kinase type-2 alpha | 4 | Pip4k2a |
| 2.7.1.40 | P11980 | pyruvate kinase PKM | 4 | Pkm |
| 2.7.10.2 | Q6P6U0 | tyrosine-protein kinase Fgr Non-specific protein-tyrosine kinase | 4 | Fgr |
| 2.7.10.2 | Q63184 | interferon-induced, double-stranded RNA-activated protein kinase Non-specific protein-tyrosine kinase | 4 | Eif2ak2 |
| 2.7.11.1 | P54645 | 5'-AMP-activated protein kinase catalytic subunit alpha-1 Non-specific serine/threonine protein kinase | 4 | Prkaa1 |
| 2.7.11.1 | Q6P9R2 | serine/threonine-protein kinase OSR1 | 4 | Oxsr1 |
| 2.7.11.1 | Q9JI11 | serine/threonine-protein kinase 4 | 4 | Stk4 |
| 2.7.11.1 | Q63184 | interferon-induced, double-stranded RNA-activated protein kinase | 4 | Eif2ak2 |
| 2.7.11.1 | Q64303 | Serine/threonine-protein kinase PAK 2 | 4 | Pak2 |
| 2.7.11.13 | P09215 | protein kinase C delta type | 4 | Prkcd |
| 2.7.11.26 | P54645 | 5'-AMP-activated protein kinase catalytic subunit alpha-1 | 4 | Prkaa1 |
| 2.7.11.27 | P54645 | 5'-AMP-activated protein kinase catalytic subunit alpha-1 | 4 | Prkaa1 |
| 2.7.11.31 | P54645 | 5'-AMP-activated protein kinase catalytic subunit alpha-1 | 4 | Prkaa1 |
| 2.7.7.9 | Q91ZJ5 | UTP--glucose-1-phosphate uridylyltransferase isoform 1 | 4 | Ugp2 |
| 2.3.1.176 | P11915 | Propanoyl-CoA C-acyltransferase fatty acid metabolism | 5 | Scp2 |
| 2.3.1.97 | O70310 | glycylpeptide N-tetradecanoyltransferase 1 | 5 | Nmt1 |
| 2.4.99.18 | P07153 | dolichyl-diphosphooligosaccharide--protein glycosyltransferase subunit 1 precursor | 5 | Rpn1 |
| 2.4.99.18 | P61806 | dolichyl-diphosphooligosaccharide--protein glycosyltransferase subunit DAD1 glycoprotein | 5 | Dad1 |
| 2.5.1.18 | P08011 | microsomal glutathione S-transferase 1 detoxification | 5 | Mgst1 |
| 2.5.1.6 | P18298 | S-adenosylmethionine synthase isoform type-2 | 5 | Mat2a |
| 2.7.11.1 | Q80X41 | serine/threonine-protein kinase VRK1 isoform a non-specific serine/threonine protein kinase | 5 | Vrk1 |
| 2.7.11.10 | O88351 | Inhibitor of nuclear factor kappa-B kinase subunit beta IκB kinase/IκB kinase | 5 | Ikbkb |

Table 3 Continuous.

| EC number | Protein ID | Description | Cluster | Gene symbol |
|---|---|---|---|---|
| **Hydrolases** | | | | |
| 3.1.1.- | B2GV54 | neutral cholesterol ester hydrolase 1 | 4 | Nceh1 |
| 3.1.1.- | O35244 | peroxiredoxin-6 | 4 | Prdx6 |
| 3.1.27.- | P70709 | eosinophil cationic protein precursor | 4 | Ear11 |
| 3.1.3.16 | Q9WVR7 | protein phosphatase 1F | 4 | Ppm1f |
| 3.1.3.25 | P97697 | inositol monophosphatase 1/ inositol-phosphate phosphatase | 4 | Impa1 |
| 3.1.3.94 | P97697 | inositol monophosphatase 1/D-galactose 1-phosphate phosphatase | 4 | Impa1 |
| 3.1.6.12 | P50430 | arylsulfatase B precursor | 4 | Arsb |
| 3.2.1.114 | P28494 | Alpha-mannosidase 2 | 4 | Man2a1 |
| 3.2.1.52 | Q6AXR4 | beta-hexosaminidase subunit beta precursor | 4 | Hexb |
| 3.3.2.6 | P24527 | leukotriene A-4 hydrolase | 4 | Lta4h |
| 3.3.2.6 | P30349 | Leukotriene A-4 hydrolase | 4 | Lta4h |
| 3.4.11.14 | Q11011 | puromycin-sensitive aminopeptidase | 4 | Npepps |
| 3.4.11.3 | P97629 | leucyl-cystinyl aminopeptidase isoform 1/oxytocinase | 4 | Lnpep |
| 3.4.21.20 | P28293 | cathepsin G preproprotein | 4 | Ctsg |
| 3.4.21.76 | Q61096 | Myeloblastin | 4 | Prtn3 |
| 3.5.3.15 | O88807 | protein-arginine deiminase type-4 | 4 | Padi4 |
| 3.5.3.18 | O08557 | N(G),N(G)-dimethylarginine dimethylaminohydrolase 1 | 4 | Ddah1 |
| 3.6.1.5 | P97687 | ectonucleoside triphosphate diphosphohydrolase 1 | 4 | Entpd1 |
| 3.6.1.52 | Q8R2U6 | diphosphoinositol polyphosphate phosphohydrolase 2 | 4 | Nudt4 |
| 3.6.5.5 | P39052 | dynamin-2/Dynamin GTPase | 4 | Dnm2 |
| 3.2.1.51 | P17164 | Tissue alpha-L-fucosidase | 5 | Fuca1 |
| 3.4.19.12 | Q9DCH4 | eukaryotic translation initiation factor 3 subunit F | 5 | Eif3f |
| 3.4.22.36 | P43527 | Caspase-1 | 5 | Casp1 |
| 3.4.23.5 | P24268 | Cathepsin D | 5 | Ctsd |
| 3.4.25.1 | P60901 | proteasome subunit alpha type-6 | 5 | Psma6 |
| 3.5.1.- | Q5KTC7 | N-acylethanolamine-hydrolyzing acid amidase precursor | 5 | Naaa |
| 3.6.4.12 | P25206 | DNA replication licensing factor MCM3 | 5 | Mcm3 |
| 3.6.4.12 | P49717 | DNA replication licensing factor MCM4 | 5 | Mcm4 |
| 3.6.4.12 | P49718 | DNA replication licensing factor MCM5 | 5 | Mcm5 |
| 3.6.4.12 | P97310 | DNA replication licensing factor MCM2 | 5 | Mcm2 |
| 3.6.4.12 | P97311 | DNA replication licensing factor MCM6 | 5 | Mcm6 |
| 3.6.4.12 | Q61881 | DNA replication licensing factor MCM7 | 5 | Mcm7 |
| 3.6.4.12 | Q6PDQ2 | chromodomain-helicase-DNA-binding protein 4 | 5 | Chd4 |
| 3.6.4.13 | O35286 | putative pre-mRNA-splicing factor ATP-dependent RNA helicase DHX15 isoform 2 | 5 | Dhx15 |
| 3.6.4.13 | P60843 | eukaryotic initiation factor 4A-I isoform 1 | 5 | Eif4a1 |
| 3.6.4.13 | Q61656 | Probable ATP-dependent RNA helicase DDX5 | 5 | Ddx5 |
| 3.6.4.13 | Q5U216 | ATP-dependent RNA helicase DDX39A | 5 | Ddx39a |

Table 3 End.

| EC number | Protein ID | Description | Cluster | Gene symbol |
|---|---|---|---|---|
| **Lyases** | | | | |
| 4.1.2.13 | P05065 | fructose-bisphosphate aldolase A | 4 | Aldoa |
| 4.2.99.18 | P62908 | 40S ribosomal protein S3 | 5 | Rps3 |
| **Isomerases** | | | | |
| 5.3.2.1 | P30904 | macrophage migration inhibitory factor | 4 | Mif |
| 5.3.3.12 | P30904 | macrophage migration inhibitory factor | 4 | Mif |
| 5.4.2.2 | Q9D0F9 | phosphoglucomutase-2 | 4 | Pgm2 |
| 5.2.1.8 | P24368 | Peptidyl-prolyl cis-trans isomerase B/Peptidylprolyl isomerase | 5 | Ppib |
| 5.2.1.8 | Q62446 | peptidyl-prolyl cis-trans isomerase FKBP3 | 5 | Fkbp3 |
| 5.2.1.8 | Q6DGG0 | peptidyl-prolyl cis-trans isomerase D | 5 | Ppid |
| 5.3.4.1 | P04785 | Protein disulfide-isomerase | 5 | P4hb |
| 5.3.4.1 | P11598 | Protein disulfide-isomerase A3 | 5 | Pdia3 |
| 5.3.4.1 | P38659 | Protein disulfide-isomerase A4 | 5 | Pdia4 |
| 5.3.4.1 | Q63081 | Protein disulfide-isomerase A6 | 5 | Pdia6 |
| **Ligases** | | | | |
| 6.1.1.10 | Q68FL6 | methionine--tRNA ligase, cytoplasmic isoform 2 | 5 | Mars |
| 6.1.1.12 | P15178 | aspartate--tRNA ligase, cytoplasmic | 5 | Dars |
| 6.3.2.- | F1LP64 | E3 ubiquitin-protein ligase TRIP12 | 5 | Trip12 |
| 6.3.2.- | O09181 | SUMO-conjugating enzyme UBC9 | 5 | Ube2i |
| 6.3.2.- | Q9Z1F9 | SUMO-activating enzyme subunit 2 | 5 | Uba2 |
| 6.3.2.19 | P61079 | ubiquitin-conjugating enzyme E2 D3 | 5 | Ube2d3 |
| 6.3.4.5 | P09034 | argininosuccinate synthase | 5 | Ass1 |

**Graph 4** Prediction of enzyme activity for the rat neutrophil proteome. A bar chart represents the predicted enzyme activity for significantly regulated proteins from cluster 4 and 5.

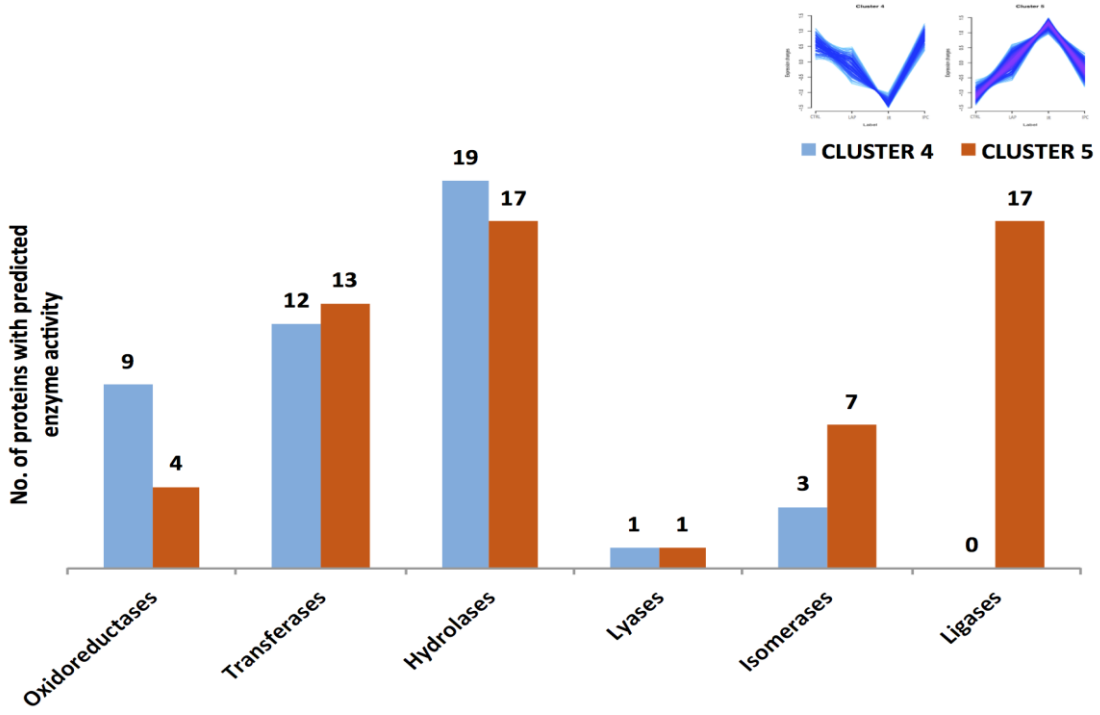


## 4.4 Phospho proteomic Analysis of rat Neutrophils.

Rat neutrophils were isolated from the four biological groups (Control, Laparotomy ischemia and Ischemic preconditioning) and proteins were extracted, digested and iTRAQ labeled. The phosphopeptides were enriched and purified. The schematic representation of methadolody utilized for this analysis is given in figure 11.

The purified peptides were analyzed in an Orbitrap Velos mass spectrometer and a total of 2151 proteins were identified out of which 549 were phosphorylated proteins (Graph 5-A). A minimum number of two peptides were selected for protein identification and for the localization of phosphorylation for the validated peptides the phosphoRS score of >95% was used. The Venn diagram for the regulated phospho proteins and phosphopeptides is shown in Graph 5-B and C. The number of phosphosites such as S/T/Y in proteins was found unique in some proteins and overlapping in others (Graph 5B) in the order S > T >Y. Similarly unique and overlapping phosphorylations were observed in phosphopeptides in the order S > T >Y as shown in Graph 5-C. The number of phosphopeptides containing Sph, Tph and Yph

showed a pattern of distribution with 75%, 22% and 3% (Graph 5D) whereas the distribution of phosphosites showed almost the same distribution as for the phosphopeptides (Graph 5-E). The most common type of phosphorylation found on these phosphoproteins was serine residue phosphorylation (Sph) followed by threonine (Tph) and tyrosine (Yph) making 60%, 33% and 7% (Graph 5-F).

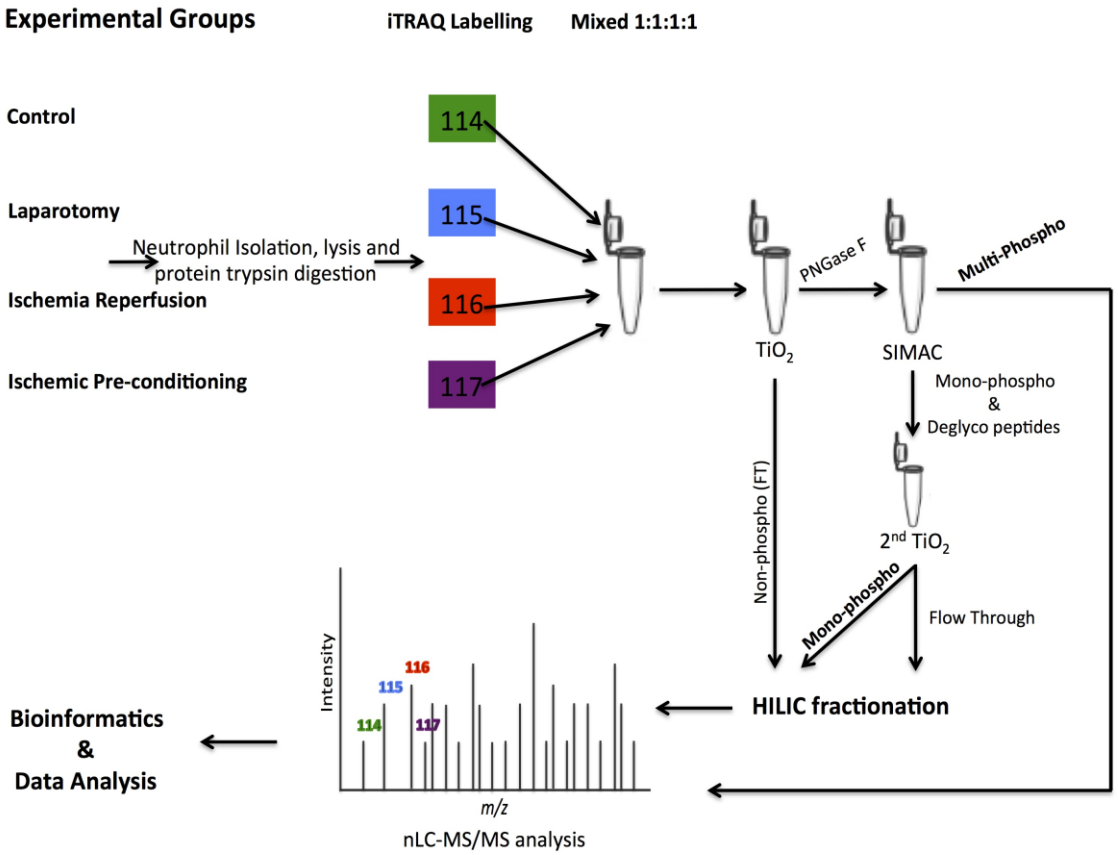


**Figure 11** Schematic presentation of experimental procedure. Neutrophils isolation by Ficoll density gradient method from Ctrl (control), Lap (laparotomy), IR (ischemia/reperfusion) and IPC (ischemic preconditioning) groups followed by protein extraction by using FASP SDS protocol. Overnight trypsin digestion 1:50 trypsin to protein ratio. iTRAQ labeling 114 for Ctrl, 115 for Lap, 116 for IR and 117 for IPC. Mono- and multi-phosphopeptides enrichment using TiSH (TiO2 SIMAC HILIC fractionation). LTQ Orbitrap MS analysis followed by bioinformatics tools.

**Graph 5** Statistical Overview of total and phosphoproteome. A. Overlap between proteome and phosphoproteome B. Overlap between Serine, threonine and tyrosine phosphoproteome C. Overlap between Serine, threonine and tyrosine phosphopeptides D. Distribution of phosphopeptides. E. Distribution of phosphosites. F. Distribution of phosphoproteins

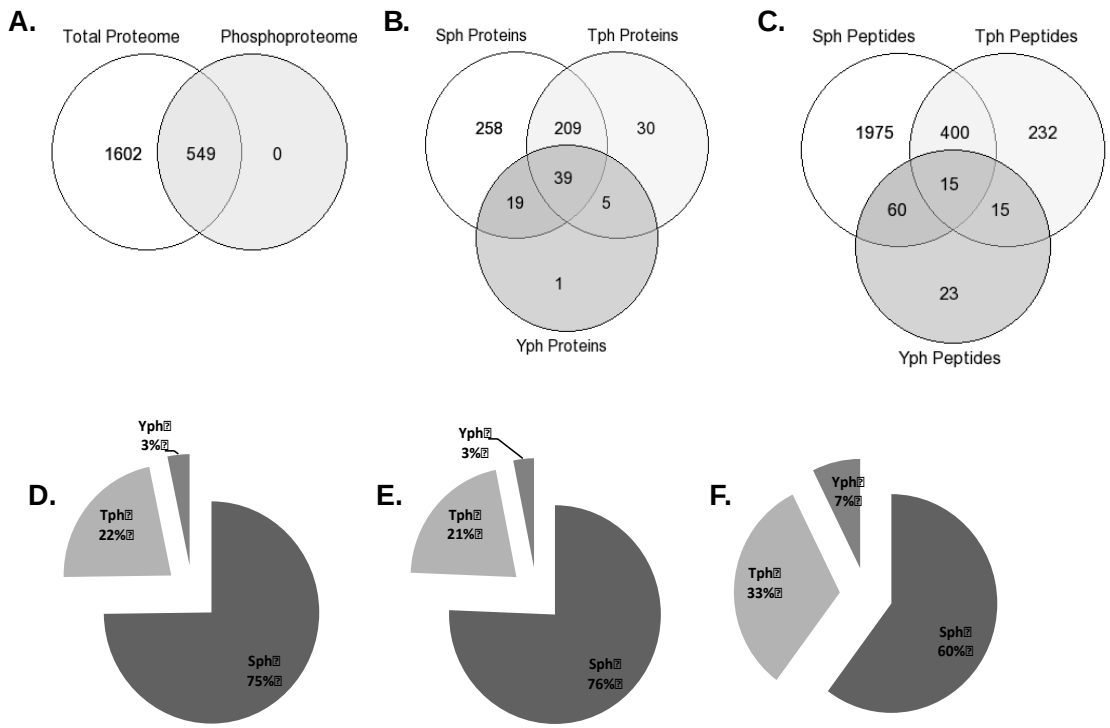


### 4.4.1 Cluster Analysis of Phosphopeptides

We have analyzed the total peptides and phosphopeptides using a script developed in the R software as described in materials and methods. Six clusters with different relative abundance profiles were obtained (Graph 6-A) in conditions: Ctrl, LAP, IR and IPC. Where clusters 1 and 6 represented a progressive up and downregulation of phosphopeptides respectively, from Ctrl to LAP to IR to IPC. This phenomenon could be related to modifications progressively induced by longer or more traumatic surgical procedures. Cluster 2 showed first an upregulation at LAP and IR followed by downregulation by IPC that can reflect the effect of IPC on proteins, possibly preventing the changes induced by IR. However, this effect is more pronounced in cluster 3 with a sharp downregulation at IR and up-regulation at IPC respectively. This could also be considered similar to the observed in cluster 5 that showed upregulation in both lap and IR followed by sharp downregulation in IPC

(Graph 6A). Whereas in cluster 4, a sharp downregulation in LAP followed by sharp upregulation in IR and then again downregulation in IPC was noticed. Most of the regulations in phosphorylation were observed in cluster 2, 3, 5 and 6. In the clusters, 378 phosphopeptides from 188 proteins were grouped in cluster 1, 621 phosphopeptides from 229 proteins in cluster 2, 541 phosphopeptides from 232 proteins in cluster 3, 565 phosphopeptides from 224 proteins in cluster 4, 754 phosphopeptides from 249 phosphoproteins in cluster 5 and 651 phosphopeptides from 251 proteins in cluster 6. Whereas the number of Sph, Tph and Yph phosphorylation sites varies among the clusters showing the highest number in cluster 5 (Graph 6B). As the number of found phosphosites in cluster 1 is 404 on 378 phosphopeptides from 188 proteins, it indicates the presence of more than one phosphosite per peptide or more than one phosphopeptide per protein.

**Graph 6** A-Cluster representation of relative abundance profiles of the identified proteins and phosphopeptides in control (Ctrl), laparotomy (Lap), ischemia reperfusion (IR), and ischemia preconditioning (IPC) from neutrophils. B. Distribution of phosphosites, phosphopeptides and phosphoproteins among the 6 clusters.

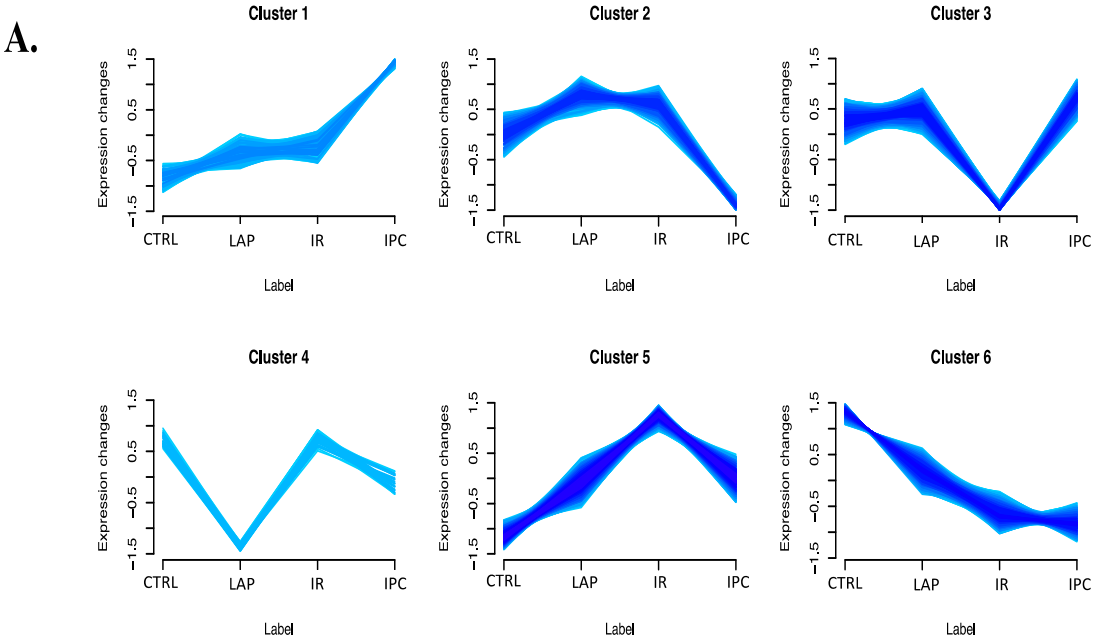


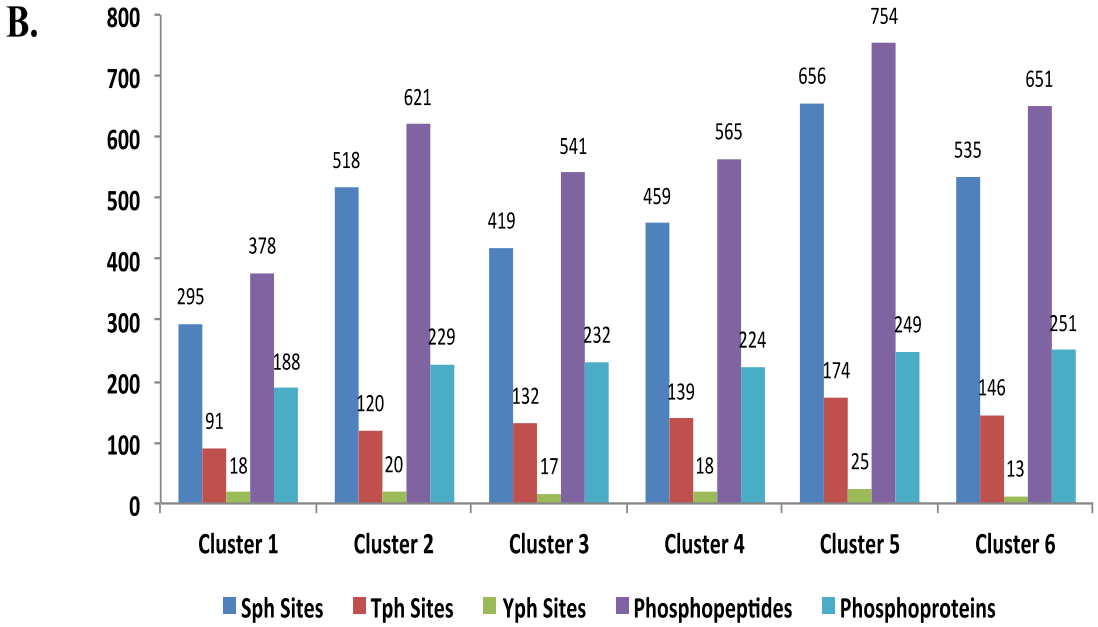

### 4.4.2 Comparison of significantly regulated phospho proteins and phosphopeptides among different conditions

The Venn diagram showing comparisons of all regulated phosphopeptides and phospho proteins is shown in the fig-12. Most of the unique regulated phosphopeptides and phosphoproteins were found in IR vs Ctrl and IR vs IPC. Similarly the number of unique phosphoproteins in both cases was 67 and 26 respectively. However there were also overlapping peptides and proteins among three conditions. The number of proteins and peptides containing phosphorylation are the highest in IR vs Ctrl, followed by IR vs IPC and IR vs LAP respectively (Fig 12A and 12B).

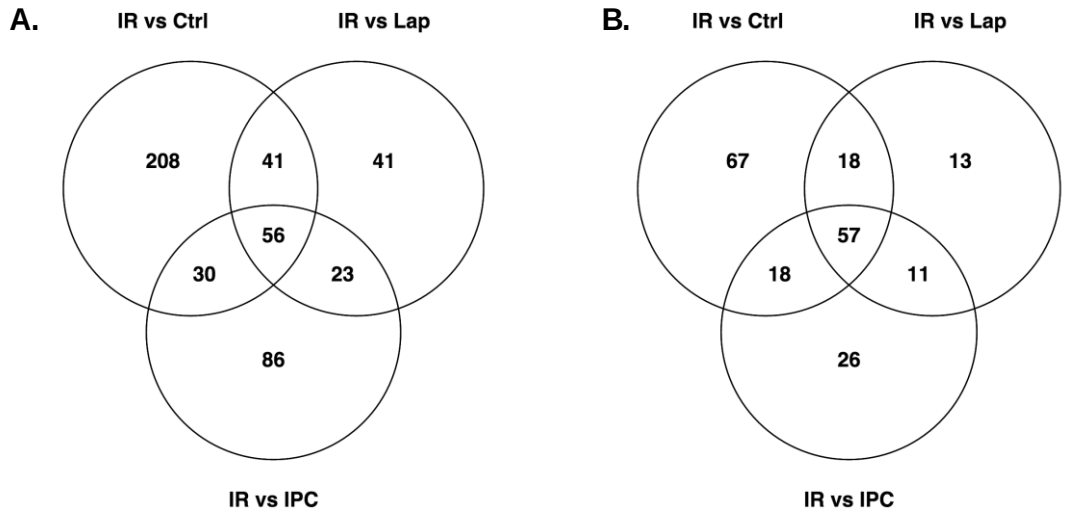


**Figure 12** Venn diagram of significantly regulated A. phophopeptides and B. phophoproteins.

### 4.4.3 Phosphorylated Kinases and phosphatases in Neutrophil

We have identified 12 protein kinases and 4 phosphatases with a significant differential phosphorylation pattern in at least one residue, and many of these proteins are potentially associated with phosphorylation in the catalytic domain (Table 4).

#### 4.4.3.1 Protein kinases with significant regulation in phosphorylation in specific domains.

Notably all of the regulated kinases belong to transferases and 5 kinases have been found significantly regulated in IR vs Ctrl while 2 kinases were found sig

regulated in IR vs IPC. Kinases and phosphatases with cluster-wise expression, number of phosphorylated peptides and their domains having significant change in the phosphorylation are given in table 4.

#### 4.4.3.1.1 Tyrosine-protein kinase

Two tyrosine-protein kinases significantly regulated in kinases were named as tyrosine-protein kinase Fgr and tyrosine-protein kinase SYK. Tyrosine-protein kinase Fgr belongs to the Scr family. It was found regulated in the cluster 2 with 7 significantly regulatory phosphosites. The important phosphorylation was found at tyr400, which is part of the catalytic domain of a subset of Src kinase-like Protein Tyrosine Kinase. The regulation in protein relative abundance was noticed in both the conditions Ctrl vs IR and IR vs IPC whereas domain phosphorylation was found only in Ctrl vs IR that can suggest a dephosphorylation event in Ctrl vs IPC. Moreover, other Tyrosine-protein kinase SYK was found with one phosphorylation out of any domain region. This downregulation was found significantly regulated in Ctrl vs IPC (cluster 2). Both kinases have enzymatic activity and belong to the transferases class (EC: 2.7.10.2).

#### 4.4.3.1.2 Beta-adrenergic receptor kinase-1, GRK2

GRKs are a family of serine-threonine kinases that participate together with arrestins in the regulation of multiple G-protein coupled receptors. We have found phosphorylation at the S670 residue in GRK2 (also known as beta-adrenergic receptor kinase-1) that was present in PH domain with binding sites for the membrane phospholipid PIP2 and free Gβγ subunits [140]. This kinase was assigned to cluster 2 (EC: 2.7.11.15) and upregulation was found in IR vs control.

#### 4.4.3.1.3 Protein Kinase C delta

PKC-delta (EC: 2.7.11.13) is another important kinase from the class of STKs found with significantly regulated phosphorylation in cluster 6 (IR vs Control) at phosphosites position S643 and S645. Phosphorylated residues were found in the catalytic domain . The phosphorylation was found downregulated but its expression was upregulated in IR and downregulated in IPC (cluster 5).

**Table 4** Identified kinases and phosphatases with significant regulation in phosphosites.

| Protein Expression Sig. Reg. | Protein ID | Description | Protein Expression Cluster | Gene Symbol | Regulated phosphopeptide in Domain | Phospho Reg. Cluster | Sig. Regulation | Phosphosite in protein | Enzyme Code | Domain containing the phosphopeptide | Domain Description |
|---|---|---|---|---|---|---|---|---|---|---|---|
| | **Kinases** | | | | | | | | | | |
| Ctrl vs IR; IR vs IPC | Q6P6U0 | Tyrosine-protein kinase Fgr | 6 | Fgr | LIVDDEYphNPQQGTKFPIK | 2 | IR vs Ctrl Sig. Reg | Y400 | EC: 2.7.10.2 | PTKc_Src_Fyn_like<br>Pkinase_Tyr | Catalytic domain of a subset of Src kinase-like Protein Tyrosine Kinases<br>Protein tyrosine kinase |
| Lap vs IPC; IR vs IPC | Q64303 | Serine/threonine-protein kinase PAK 2 | 4 | Pak2 | -- | -- | -- | -- | EC: 2.7.11.1 | -- | -- |
| | E9PTG8 | Serine/threonine-protein kinase 10 | 3 | Stk10 | -- | -- | -- | -- | EC: 2.7.11.1 | -- | -- |
| | Q63531 | Ribosomal protein S6 kinase alpha-1 | 2 | Rps6ka1 | -- | -- | -- | -- | EC: 2.7.11.1 | -- | -- |
| | Q9WUT3 | Ribosomal protein S6 kinase alpha-2 | 5 | Rps6ka2 | -- | -- | -- | -- | EC: 2.7.11.1 | -- | -- |
| | P26817 | Beta-adrenergic receptor kinase 1 | 4 | Adrbk1 | NKPRSphPVVELSK | 2 | IR vs Ctrl Sig. Reg | S670 | EC: 2.7.11.15 | PH_GRK2_subgroup | G Protein-Coupled Receptor Kinase 2 subgroup pleckstrin homology (PH) domain<br>G-beta gamma binding site |
| Lap vs IPC | Q63433 | Serine/threonine-protein kinase N1 | 1 | Pkn1 | -- | -- | -- | -- | EC: 2.7.11.13 | -- | -- |
| Ctrl vs IR; IR vs IPC | P09215 | Protein kinase C delta type | 5 | Prkcd | SPSDYSNFDPEFLNEKPQLS phFSDK | 6 | IR vs Ctrl Sig. Reg | S643 | EC: 2.7.11.13 | STKc_nPKC_delta | Catalytic domain of the Serine/Threonine Kinase, Novel Protein Kinase C delta |
| Ctrl vs IR; IR vs IPC | P09215 | Protein kinase C delta type | 5 | Prkcd | SPSDYSNFDPEFLNEKPQLS FSphDK | 6 | IR vs Ctrl Sig. Reg | S645 | EC: 2.7.11.13 | STKc_nPKC_delta | Catalytic domain of the Serine/Threonine Kinase, Novel Protein Kinase C delta |
| Ctrl vs IPC | Q64725 | Tyrosine-protein kinase SYK | 2 | Syk | -- | -- | -- | -- | EC: 2.7.10.2 | -- | -- |
| | O08815 | STE20-like serine/threonine-protein kinase | 5 | Slk | -- | -- | -- | -- | EC: 2.7.11.1 | -- | -- |
| Ctrl vs IR | Q6P9R2 | Serine/threonine-protein kinase OSR1 | 5 | Oxsr1 | -- | -- | -- | -- | EC: 2.7.11.1 | -- | -- |
| | Q91VJ4 | Serine/threonine-protein kinase 38 | 4 | Stk38 | FEGLTphAR | 1 | IR vs IPC Sig. Reg | T452 | EC: 2.7.11.1 | STKc_NDR1 | Catalytic domain of the Serine/Threonine Kinase, Nuclear Dbf2-Related kinase 1 |
| | **Phosphatases** | | | | | | | | | | |
| | P81718 | Tyrosine-protein phosphatase non-receptor type 6 | 4 | Ptpn6 | DLSphGPDAETLLK | 2 | IR vs Ctrl Sig. Reg | S12 | EC: 3.1.3.48 | SH2_N-SH2_SHP_like | N-terminal Src homology 2 (N-SH2) domain found in SH2 domain Phosphatases (SHP) proteins |
| | P97573 | Phosphatidylinositol 3,4,5-trisphosphate 5-phosphatase 1 | 5 | Inpp5d | TGIANTphLGNK | 3 | IR vs IPC Sig. Reg | T519 | EC: 3.1.3.86 | NPP5c_SHIP1-INPP5D | Catalytic inositol polyphosphate 5-phosphatase (INPP5c) domain of SH2 domain<br>Putative catalytic site<br>Putative active site<br>Putative Mg binding site<br>Putative PI/IP binding site |
| | B2GV87 | Receptor-type tyrosine-protein phosphatase epsilon precursor | 6 | Ptpre | -- | -- | -- | -- | EC: 3.1.3.48 | -- | -- |
| Ctrl vs IR; Ctrl vs IPC; IR vs IPC | P04157 | Receptor-type tyrosine-protein phosphatase C isoform 4 precursor | 5 | Ptprc | -- | -- | -- | -- | EC: 3.1.3.48 | -- | -- |

#### 4.4.3.1.4 Serine/threonine-protein kinase 38 or Non-race specific Disease Resistance 1 (NDR1)

The NDR1 (also called STK38, EC: 2.7.11.1) was significantly upregulated in IR vs IPC in cluster 1. It has also significant regulation in one phosphosite at T452 in the catalytic domain or nuclear Dbf2 related kinase 1 domain.

#### 4.4.3.1.5 Other kinases with significant regulation in phosphopeptides without domain region.

Other kinases with significant and variable number of regulation in phosphosites have also been identified, like ribosomal protein S6 kinase alpha-1 and 2 (Q63531 and Q9WUT3), Serine/threonine-protein kinase N1, Pkn1/Prk1/Pak1 (Q63433), Serine/threonine-protein kinase, Oxsr1/Osr1, (Q6P9R2), Serine/threonine-protein kinase PAK 2 (Q64303), Serine/threonine-protein kinase 10 (E9PTG8), serine/threonine-protein kinase N1 (Q63433), STE20-like serine/threonine-protein kinase (O08815), and serine/threonine protein kinase OSR1 (Q6P9R2). The phosphosites regulated in these kinases were not found in any domain region.

### 4.4.4 Phosphatases with Significant regulation in phosphorylation in the catalytic domain.

Following are the three phosphatases that showed significant regulation in the phosphosites found in their domain regions. The first phosphatase mentioned in table 1 is a tyrosine-protein phosphatase non-receptor type 6, Ptpn6/Shp-1, (P81718 EC: 3.1.3.48). Ptpn6 has one transmembrane domain and was found upregulated (IR vs Ctrl) in cluster 2 with two phosphosites. Phosphorylation on Ser12 was found upregulated in N-terminal Src homology 2 domain (N-SH2). Another phosphatase with phosphorylation found in a domain is Phosphatidylinositol 3,4,5-trisphosphate 5-phosphatase 1, Inpp5d/Ship1, (P97573). The phosphorylataion in Inpp5d (EC: 3.1.3.86) was found significantly regulated (IR vs IPC) in Cluster 3 with 4 regulated phosphosites whereas phosphorylation at T519 was in the Catalytic domain named as SH2 domain and Putative catalytic site, Putative active site, Putative Mg binding site and also in Putative PI/IP binding site.

#### 4.4.4.1 Other Phosphatases with regulation in phosphosite without domain region.

Other three phosphatase having significant regulations in phosphosites that were not present in any domain are as fallows.

Receptor-type tyrosine-protein phosphatase C isoform 4 precursor, Ptprc/CD45, (P04157) is a receptor type protein tyrosine phosphatase commonly known as CD45 or LCA (Luekocyte common antigen) showing enzymatic activity EC: 3.1.3.48. One phosphopeptide was encountered in our data set. Interestingly, its expression was found significantly regulated in cluster 5 with regulation in three conditions, Ctrl Vs IR, Ctrl vs IPC and IR vs IPC with upregulation in IR and downregulation in IPC.

The receptor-type protein tyrosine phosphatase epsilon (PTPepsilon) (B2GV87) with EC: 3.1.3.48 (cluster 6) was also among the regulated phosphatases having one phosphosite with significant regulation.

## 4.5 Motif-x enrichment analysis

Sequence motif enrichment analyses of phosphorylation sites were performed using the Motif X algorithm [78] with windows of 17 amino acids. The same Rattus norvegicus database employed previously for protein identification was used as a background file. The Venn diagram for the proteins with significant regulation in their phosphorylation sites containing serine and theronine showed the abundance for the motifs contain serine (138) as compared to theronine (8) whereas 12 proteins contain both serine and theronine in their motifs (Graph 7-A).

**Graph 7** Serine and threonine motifs along with cluster-wise distribution. **A.** The Venn diagram of phosphoproteins with significant regulation in phosphorylation carrying enriched serine and threonine motifs. **B.** Cluster-wise distribution of the enriched motifs with significantly regulated phosphorylation site.

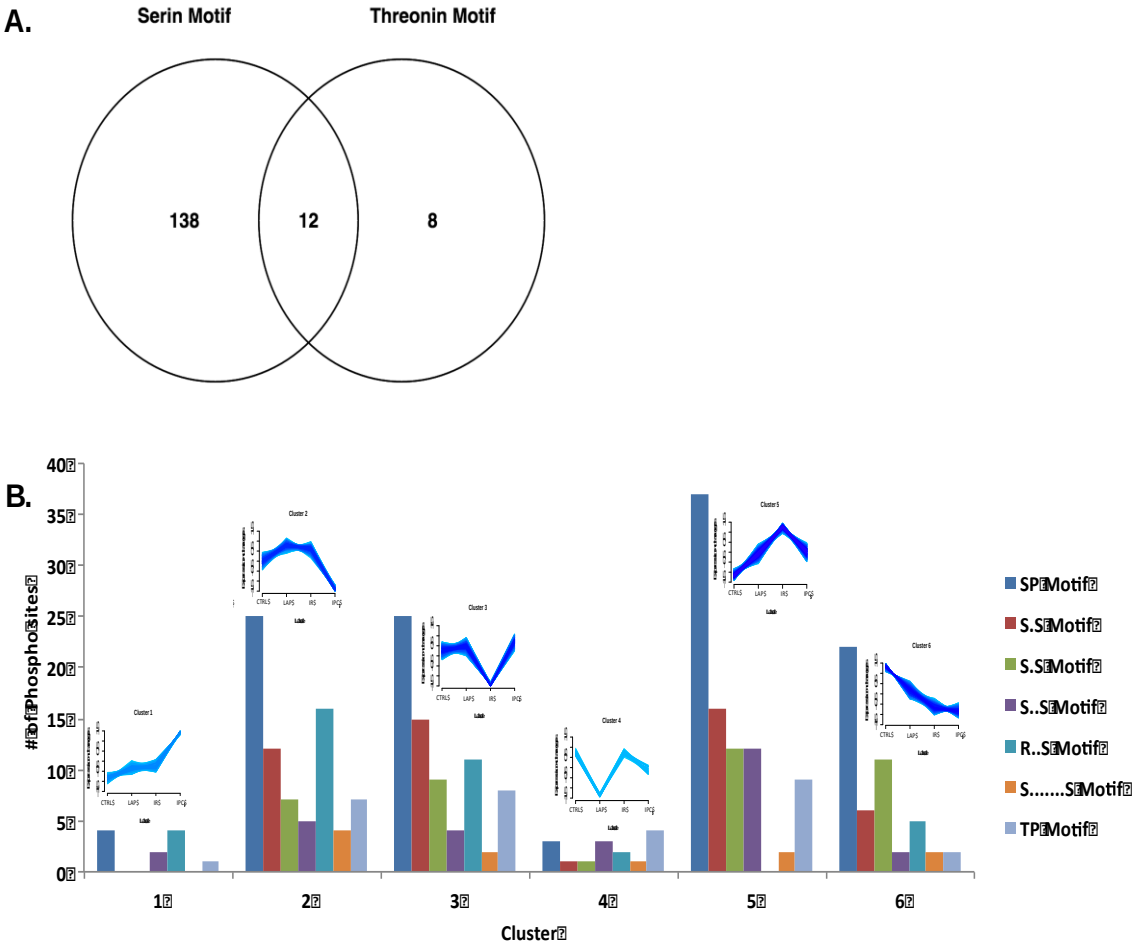


The phosphopeptides assigned to the cluster with different motifs are shown in Graph 7-B. As shown the serine containing motifs are dominant in all clusters. The abundance of the regulated phosphopeptides within the S.S motif was somewhat homogeneous throughout the four clusters (2, 3, 5 and 6) whereas the SP motif was remarkably more prominent in these four clusters. The clusters 1 and 4 contain the least motif containing peptides. However, the phosphopeptides with threonine motifs were also found in all clusters but were more prominent in cluster 2, 3 and 5. There was no enrichment for the tyrosine (y) motif as the number of tyrosine-phosphorylated peptides was low compared to serine and threonine containing peptides.

### 4.5.1 Peptides with Serine containing motifs

Table 5 Motif-x analysis of significantly regulated phopshopeptides.

| # | Motif | Motif Score | Foreground Matches | Foreground Size | Background Matches | Background Size | Fold Increase |
|---|---|---|---|---|---|---|---|
| 1 | .....SP..... | 16 | 119 | 649 | 76989 | 1084345 | 2.58 |
| 2 | .....S.S..... | 12.6 | 114 | 530 | 107004 | 1007356 | 2.02 |
| 3 | .....S.S..... | 9.95 | 86 | 416 | 90721 | 900352 | 2.05 |
| 4 | .....S..S..... | 8.24 | 68 | 330 | 80386 | 809631 | 2.08 |
| 5 | .....R..S..... | 8.21 | 44 | 262 | 46997 | 729245 | 2.61 |
| 6 | .....S.....S | 6.63 | 45 | 218 | 62838 | 682248 | 2.24 |
| 7 | .....TP..... | 10.43 | 28 | 100 | 45610 | 692616 | 4.25 |

Table 5 shows the significantly expressed motifs in all the regulated phosphopeptides. Where S represents the serine that acts as a phospho receptor and the other letters represent the single-letter code for specific amino acids, and (.) represents any amino acid in the sequence. For example, in the motif R..S an arginine exists three residues upstream of the serine phospho-acceptor site, separated from this by any two residues. In the table all motifs shown are statistically significant at the $p<0.0003$ level corresponding to the motif-x 0.000001 significance threshold that was specified for this particular run. The higher motif scores typically correspond to motifs that are more statistically significant as well as more specific (i.e., greater number of fixed positions). The SP motif was found with the highest significance and specificity. The “foreground matches” and “background matches” indicate the number of peptides containing a given motif in the data set after the removal of all peptides containing previously extracted motifs. The “foreground size” and “background size” statistics indicate the total number of peptides contained in these data sets. The “fold increase” indicates the enrichment level of the extracted motifs. Therefore motifs SP and R..S show higher enrichment level in the data set. We have found two types of S..S motifs (table 5 and fig. 13-B, & C). Figure 13 showed the difference between both where in the first S..S the serine (upstream) at position 0 acts as phosphoreceptor (Fig-13B) however in second S..S serine (downstream) at position 0 acts also as phosphoreceptor (Fig-13C) whereas other serine rsidues are at positions +2 and -2 respectively. Both S..S motifs have different motif scores. The fig. 13 represents the motif results with sequence logos from MSMS

data. The positive and negative numbers represents the position of upstream and downstream amino acids from the serine phospho receptor with 17 amino acids in total.


**Figure 13** Motif-x of phosphorylated peptides. The motif results with sequence logos from MSMS data. The positive and negative numbers represents the position of upstream and downstream amino acids from the differentially phosphorylated serine (A - F) and threonine (G). Motif positions are labeled below the x-axis and residues are colored according to their chemical and physical properties. The full character height illustrates the amino acid composition of the "wildcard" positions within the motifs. Amino acids are sorted by their frequency at each position within the motif with the most frequent amino acids appearing closest to the top of the motif logo.

### 4.5.2 Peptides with Threonine containing motif

Motif analysis for the phospho peptides also showed the presence of only one threonine TP motif with threonine as the phospho receptor. Table 5 showed the motif score of 10.43 and fold increase of 4.25 for the TP motif. The motif result with sequence logos from MSMS data is shown in the fig-13G where proline was found on position +1 after threonine. The detail about all the encountered significantly regulated kinases and phosphatases with and without enriched motifs present in phosphopeptides, regulating conditions, modified position in peptides and cluster information is given in

Table 6. The S..S motif in black represented the Fig-13B motif whereas red colored is Fig-13C as discussed above.

**Table 6** Enriched motifs for the regulated phopshopeptides in identidied kinases and phosphatases.

| Class | Sig. Regulated Phospho Peptide | Significant Regulation | Modified Pos. in peptide | Data Source 1 | Pos. in Protein | Cluster | Motif |
|---|---|---|---|---|---|---|---|
| **Kinases** | | | | | | | |
| Q6P6U0 | EDVGLEGDFRSphQGAEER | IR 3 vs Ctrl | S11 | RAT | S25 | 5 | |
| | LIVDDEYphNPQQGTKFPIK | IR 3 vs Ctrl | Y7 | RAT | Y400 | 2 | |
| | SphSSISPQPISPAFLNVGNIR | IR 3 vs Ctrl | S1 | RAT | S41 | 2 | S.S |
| | SphSSISPQPISphPAFLNVGNIR | IR 3 vs Ctrl | S1 | RAT | S41 | 5 | S.S |
| | SSphSISPQPISphPAFLNVGNIR | IR 3 vs Ctrl | S2 | RAT | S42 | 5 | S.....S |
| | SSSISphPQPISphPAFLNVGNIR | IR 3 vs Ctrl | S5 | RAT | S45 | 5 | SP |
| | SSSphISphPQPISPAFLNVGNIR | IR 3 vs Ctrl | S3 | RAT | S43 | 5 | S.S |
| | SSSphISPQPISphPAFLNVGNIR | IR 3 vs Ctrl | S3 | RAT | S43 | 5 | S.S |
| | | | | | | | |
| | EDVGLEGDFRSphQGAEER | IR 3 vs Lap | S11 | RAT | S25 | 5 | |
| Q64303 | FYDSphNTVK | IR 3 vs Ctrl | S4 | RAT | S132 | 2 | |
| | | | | | | | |
| | YLSphFTPPEK | IR 3 vs Lap | S3 | RAT | S141 | 6 | |
| E9PTG8 | ILRLSphTFEK | IR 3 vs Ctrl | S5 | RAT | S13 | 6 | |
| | LSphTFEK | IR 3 vs Ctrl | S2 | RAT | S13 | 6 | |
| | | | | | | | |
| | LSphTFEK | IR 3 vs Lap | S2 | RAT | S13 | 6 | |
| | | | | | | | |
| | LSTphFEK | IR 3 vs PC | T3 | RAT | T14 | 1 | |
| Q63531 | KLPSphTTL | IR 3 vs Ctrl | S4 | RAT | S732 | 2 | |
| Q9WUT3 | LEPVLSphSSLAQR | IR 3 vs Ctrl | S6 | MOUSE | S716 | 3 | S.S |
| | | | | | | | |
| | LEPVLSphSSLAQR | IR 3 vs PC | S6 | MOUSE | S716 | 3 | S.S |
| P26817 | NKPRSphPVVELSK | IR 3 vs Ctrl | S5 | RAT | S670 | 2 | SP |
| Q63433 | SGSphLSGR | IR 3 vs Ctrl | S3 | RAT | S377 | 2 | S.S |
| P09215 | SPSDYSNFDPEFLNEKPQLSFSphDK | IR 3 vs Ctrl | S22 | RAT | S645 | 6 | S.S |
| | SPSDYSNFDPEFLNEKPQLSphFSDK | IR 3 vs Ctrl | S20 | RAT | S643 | 6 | S.S |
| | | | | | | | |
| | SPSDYSNFDPEFLNEKPQLSphFSDK | IR 3 vs Lap | S20 | RAT | S643 | 6 | S.S |
| | | | | | | | |
| | SPSDYSNFDPEFLNEKPQLSphFSDK | IR 3 vs PC | S20 | RAT | S643 | 6 | S.S |
| Q64725 | SYSphFPKPGHK | IR 3 vs Ctrl | S3 | RAT | S291 | 6 | S.S |
| O08815 | TKDSGSphVSLQETR | IR 3 vs Lap | S6 | RAT | S778 | 3 | S.S |
| Q6P9R2 | AAISQLRSphPR | IR 3 vs PC | S8 | MOUSE | S359 | 5 | SP |
| | RVPGSphSphGRLHK | IR 3 vs PC | S5 | MOUSE | S324 | 3 | |
| Q91VJ4 | FEGLTphAR | IR 3 vs PC | T5 | MOUSE | T452 | 1 | |

Table 6 End.

| Class | Sig. Regulated Phospho Peptide | Significant Regulation | Modified Pos. in peptide | Data Source 1 | Pos. in Protein | Cluster | Motif |
|---|---|---|---|---|---|---|---|
| **Phosphatases** | | | | | | | |
| P81718 | DLSphGPDAETLLK | IR 3 vs 1 Ctrl | S3 | RAT | S12 | 2 | R..S |
| | TphSSKHKEEVYENVHSK | IR 3 vs 1 Ctrl | T1 | RAT | T557 | 5 | |
| | | | | | | | |
| | DLSphGPDAETLLK | IR 3 vs 1 Lap | S3 | RAT | S12 | 2 | R..S |
| | | | | | | | |
| P97573 | DSSLGPGRGEGPPTphPPSQPPLSPK | IR 3 vs 1 Ctrl | T14 | RAT | T963 | 2 | TP |
| | GEGPPTphPPSQPPLSphPK | IR 3 vs 1 Ctrl | T6 | RAT | T963 | 5 | TP |
| | GEGPPTphPPSQPPLSphPKK | IR 3 vs 1 Ctrl | T6 | RAT | T963 | 5 | TP |
| | KEQESphPK | IR 3 vs 1 Ctrl | S5 | RAT | S1037 | 2 | SP |
| | | | | | | | |
| | KEQESphPK | IR 3 vs 1 Lap | S5 | RAT | S1037 | 2 | SP |
| | | | | | | | |
| | GEGPPTphPPSQPPLSPK | IR 3 vs 1 PC | T6 | RAT | T963 | 2 | TP |
| | TGIANTphLGNK | IR 3 vs 1 PC | T6 | RAT | T519 | 3 | |
| | | | | | | | |
| B2GV87 | SPSphGPKK | IR 3 vs 1 Ctrl | S3 | RAT | S106 | 3 | S.S |
| | | | | | | | |
| | SPSphGPKK | IR 3 vs 1 Lap | S3 | RAT | S106 | 3 | S.S |
| | | | | | | | |
| P04157 | ANSphQDKIEFHNEVDGAK | IR 3 vs 1 Lap | S3 | RAT | S1209 | 6 | |
| | KANSphQDK | IR 3 vs 1 Lap | S4 | RAT | S1209 | 6 | |
| | KANSphQDKIEFHNEVDGAK | IR 3 vs 1 Lap | S4 | RAT | S1209 | 6 | |
| | | | | | | | |
| | ANSphQDKIEFHNEVDGAK | IR 3 vs 1 PC | S3 | RAT | S1209 | 6 | |
| | KANSphQDK | IR 3 vs 1 PC | S4 | RAT | S1209 | 6 | |
| | KANSphQDKIEFHNEVDGAK | IR 3 vs 1 PC | S4 | RAT | S1209 | 6 | |

### 4.5.3 Prediction of Kinases Responsible for Regulated Phosphorylation Events

We used the software package GPS [141] for the prediction of *in vivo* site-specific kinase-substrate relations mainly from the phosphoproteomic data. The detail of enriched motifs for the regulated phosphopeptides in identified kinases and phosphatases is mentioned in table 7.

### 4.5.4 Predicted kinase families responsible for motifs significant phosphorylation

The pie chart representations of all the predicted kinases responsible for the significant regulation of all the phospho peptides containing motifs are shown in Graph 8. The predicted kinase families for serine phosphorylation motifs are CAMK, AGC and CMGC with higher percentages among others. However, kinases for threonine belong to CMGC family among others.

**Graph 8** Pie charts with the distribution of predicted kinases responsible for motifs. A. Serine motif and B. Threonine motifs.

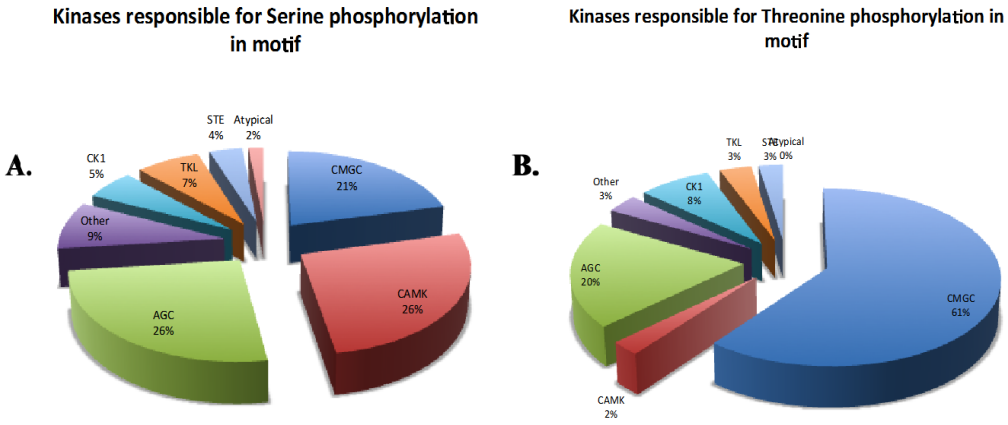


The predicted kinases responsible for the regulatory protine kinase catalysis phosphorylation specific for certain phosphosites encountered in our data set for identified kinases and phosphatases are given in the table 7 along with their phosphosites, peptides, score, and motifs. The commercially available inhibitors for these predicted kinases are listed in table 8.

**Table 7** Predicted kinases responsible for identified kinases and phosphatases phosphorylation in the catalytic domain region.

| Acc. No. | Phosphosite | Predicted Kinase | Phosphorlated Peptide | Score | Cutoff | Motif |
|---|---|---|---|---|---|---|
| **Kinases** | | | | | | |
| Q6P6U0 | Y400 | TK/Src | LIVDDEYphNPQQGTKFPIK | 24.645 | 1.63 | -- |
| | Y400 | TK/Tec* | LIVDDEYphNPQQGTKFPIK | 23.341 | 3.584 | -- |
| | Y400 | TK/Jak | LIVDDEYphNPQQGTKFPIK | 18.242 | 8.154 | -- |
| | Y400 | TK/FAK* | LIVDDEYphNPQQGTKFPIK | 14.808 | 5.968 | -- |
| | Y400 | TK/DDR* | LIVDDEYphNPQQGTKFPIK | 11 | 2.683 | -- |
| | Y400 | TK/Syk | LIVDDEYphNPQQGTKFPIK | 8.825 | 2.436 | -- |
| | Y400 | TK/Csk* | LIVDDEYphNPQQGTKFPIK | 6.778 | 4.886 | -- |
| | Y400 | TK/Abl* | LIVDDEYphNPQQGTKFPIK | 5.422 | 4.747 | -- |
| | Y400 | TK/Met* | LIVDDEYphNPQQGTKFPIK | 4.607 | 2.379 | -- |
| | Y400 | TK/VEGFR* | LIVDDEYphNPQQGTKFPIK | 4.556 | 3.654 | -- |
| | Y400 | TK/Alk | LIVDDEYphNPQQGTKFPIK | 3.667 | 3.333 | -- |
| | Y400 | TK/PDGFR* | LIVDDEYphNPQQGTKFPIK | 3.646 | 2.352 | -- |
| | Y400 | TK* | LIVDDEYphNPQQGTKFPIK | 2.516 | 0.166 | -- |
| P26817 | S670 | CMGC/MAPK | NKPRSphPVVELSK | 42.735 | 35.046 | SP |
| | S670 | AGC/PDK1 | NKPRSphPVVELSK | 5.222 | 2.257 | SP |
| | S670 | CMGC* | NKPRSphPVVELSK | 1.356 | 0.963 | SP |
| | S670 | CMGC/DYRK* | NKPRSphPVVELSK | 1.333 | 1.276 | SP |
| | S670 | AGC/PKC | NKPRSphPVVELSK | 0.384 | 0.236 | SP |
| P09215 | S643 | CAMK/RAD53* | SPSDYSNFDPEFLNEKPQLSphFSDK | 13.075 | 7.385 | S.S |
| | S643 | AGC/PKC | SPSDYSNFDPEFLNEKPQLSphFSDK | 0.905 | 0.236 | S.S |
| | S643 | Atypical/PDHK* | SPSDYSNFDPEFLNEKPQLSphFSDK | 4.405 | 3.075 | S.S |
| | S645 | CAMK/CAMK1* | SPSDYSNFDPEFLNEKPQLSFSphDK | 3.259 | 2.488 | S.S1 |
| | S645 | TKL/STKR* | SPSDYSNFDPEFLNEKPQLSFSphDK | 2.938 | 2.562 | S.S2 |
| Q91VJ4 | T452 | TKL* | FEGLTphAR | 4.648 | 4.354 | -- |
| | T452 | AGC/PKC | FEGLTphAR | 0.608 | 0.236 | -- |
| **Phosphatases** | | | | | | |
| P81718 | S12 | CAMK/PHK* | DLSphGPDAETLLK | 22.269 | 9.527 | R..S |
| | S12 | CMGC/CK2* | DLSphGPDAETLLK | 12.467 | 9.894 | R..S |
| | S12 | CMGC/CLK* | DLSphGPDAETLLK | 5.375 | 4.3 | R..S |
| P97573 | T519 | Other/TLK* | TGIANTphLGNK | 6.25 | 5.775 | -- |
| | T519 | Other/TTK* | TGIANTphLGNK | 5.188 | 5.009 | -- |

Predicted Kinases with * shows the absence of inhibitors in the database

**Table 8** List of commercially available inhibitors for the predicted kinases mentioned in table 7.

| Kinase | Inhibitor | Molecular Formula | MW | Reference | Reference 2 | Patent | Commercial Vendor | PubChem CID |
|---|---|---|---|---|---|---|---|---|
| | | | | | | | | |
| Src | 1NA-PP1 (PP1 Analog) | C19H19N5 | 317.4 | Bishop A.C. (2000) Nature 407 395 | Bishop A.C. (1999) J. Am. Chem. Soc. 121 627 | WO2003082341 | Merck (Calbiochem) | 4877 |
| Src | 1NM-PP1 (PP1 Analog II) | C20H21N5 | 331.4 | Ira G. (2004) Nature 431 1011 | Papa F.R. (2003) Science 302 1533 | WO2000042042 | Merck (Calbiochem) | 5154691 |
| Src | Bosutinib | C26H29Cl2N5O3 | 530.45 | Vultur A. Mol Cancer Ther. (2008) 7 185-94 | | WO2013024144 | Cayman Chemical | 5328940 |
| Src | Dasatinib | C22H26ClN7O2S | 487 | Kantarjian H. N Engl J Med. (2010) 362 260-70 | | WO2009094556 | Cayman Chemical | 3062316 |
| Src | PP1 | C16H19N5 | 281.36 | Hanke (1996) J. Biol. Chem. 271 695 | Liu (1999) Chem. Biol. 6 671 | WO2012109732 | Enzo (Alexis) | 1400 |
| Src | PP2 | C15H16ClN5 | 301.77 | Kirihara T. (2013) Exp Eye Res. 50014 | | WO2006068760 | Merck (Calbiochem) | 4878 |
| Src | PP3 | C11H9N5 | 211.22 | Hou (2007) Neurosci Lett 420 235 | | | Tocris | 4879 |
| Src | Saracatinib (AZD0530) | C27H32ClN5O5 | 542.03 | Hennequin Laurent (2006) J. Med. Chem. 49 (22) 6465-6488 | | | Selleck | 10302451 |
| Src | SRC Inhibitor I | C22H19N3O3 | 373.4 | Tian G. (2001) Biochemistry 40 7084 | | | Merck (Calbiochem) | 1474853 |
| Src | SU-6656 | C19H21N3O3S | 371.5 | Bowman T. (2001) Proc. Natl. Acad. Sci. USA 98 7319 | Blake R.A. (2000) Mol. Cell. Biol. 20 9018 | | Sigma | 5312137 |
| | | | | | | | | |
| JAK | AG490 | C17H14N2O3 | 294.3 | Jaleel M. (2004) Biochemistry 43 8247 | Eriksen K.W. (2001) Leukemia 15 787 | WO2004052359 | Merck (Calbiochem) | 5328779 |
| JAK | CP-690550 (Tasocitinib) | C16H20N6O | 312.38 | Manshouri T. (2008) Cancer Sci. 99 (6) 1265-73 | | | Selleck | 9926791 |
| JAK | Ruxolitinib (INCB18424) | C17H18N6 | 306.37 | Lawrence J. Wilson (2010) Expert Opinion on Therapeutic Patents May 20 (5) 609-623 | | WO2008157208 | Selleck | 25126798 |
| | | | | | | | | |
| Syk | BAY 61-3606 | C20H18N6O3 ·xHCl ·yH2O | 390.4 | Yamamoto N. (2003) J. Pharmacol. Exp. Ther. 306 1174-1181 | | | Sigma | 10200390 |
| Syk | ER-27319 | C20H22N2O5 | 370.4 | Moriya K. (1997) Proc. Natl. Acad. Sci. USA 94 12539-12544 | | | Tocris | 9799508 |
| Syk | Piceatannol | C14H12O4 | 244.2 | Wang B.H. (1998) Planta Med. 64 195 | Keely P.J. and Parise L.V. (1996) J. Biol. Chem. 271 26668 | WO2012021964 | Merck (Calbiochem) | 667639 |
| Syk | PRT062607 | C19H23N9O | 393.45 | Spurgeon S.E. (2013) J. Pharmacol Exp Ther. 2013 Feb. 344 (2) 378-387 | | | Axon | |
| Syk | R-406 | C23H24FN5O5 | 469.46 | Braselmann S. (2006) J Pharmacol Exp Ther. 319 (3) 998-1008 | | | Selleck | 11213558 |
| Syk | SYK Inhibitor I | C18H15N3O3S | 353.4 | Lai Z.Y. (2003) Bioorg. Med. Chem. Lett. 13 3111 | | | Merck (Calbiochem) | 6419747 |
| Syk | SYK Inhibitor II | C14H15F3N6O ·Ûc2HCl ·Ûc2H2O | 449.3 | Hisamichi H. (2005) Bioorg. Med. Chem. 13 4936 | | | Merck (Calbiochem) | 16760670 |
| Syk | SYK Inhibitor III | C9H7NO4 | 193.2 | Wang W.Y. (2006) Mol. Pharmacol. 70 1380 | | | Merck (Calbiochem) | 672296 |
| Syk | SYK Inhibitor IV (BAY 61-3606) | C20H18N6O3 ·Ûc2HCl ·Ûc2H2O | 444.9 | Yamamoto N. (2003) J Pharmacol Exp Ther 306 1174 | | | Merck (Calbiochem) | 11784504 |
| | | | | | | | | |
| ALK5 | A-83-01 | C25H19N5S | 421.52 | Tojo (2005) Cancer Sci. 96 791 | | | Tocris | 16218924 |
| ALK | SB-431542 | C22H16N4O3 ·xH2O | 384.39 | Inman et al (2002) Mol. Pharmacol. 62 65 | | | Sigma | 4521392 |
| ALK | SB-505124 | C20H21N3O2 ·xHCl ·yH2O | 335.4 | Byfield (2004) Mol. Pharmacol. 65 744 | | | Sigma | 9858940 |
| NPM-ALK | TAE684 | C30H40ClN7O3S | 614.22 | Zhang J. (2012) Bioorg. Med. Chem. Lett. 22 1864-ÛÔ1869 | Galkin A.V. (2007) Proc. Natl. Acad. Sci. USA 104 (1) 270-275 | | Axon | 16038120 |
| | | | | | | | | |
| p38 MAPK | BIRB-0796 (Doramapimod) | C31H37N5O3 | 527.66 | Regan J. (2002) J. Med. Chem 45 2994-3008 | | WO2004014387 | Axon | 156422 |
| MAPKAPK2 | PF3644022 | C21H18N4OS | 374.46 | Mourey (2010) J. Pharmacol. Exp. Ther. 333 797 | | | Tocris | |
| p38 MAPK | SB-202190 | C20H14FN3O | 331.3 | Davies S.P. (2000) Biochem. J. 351 95 | Ajizian S.J. (1999) J. Infect. Dis. 179 939 | | Merck (Calbiochem) | 5353940 |
| p38 MAPK | SB-203580 | C21H16N3OSF | 377.4 | Powell D.J. (2003) Mol. Cell Biol. 23 7794 | Davies S.P. (2000) Biochem. J. 351 95 | | Merck (Calbiochem) | 176155 |
| p38 MAPK | VX-745 | C19H9Cl2F2N3OS | 436.26 | Tsai Y R Epub 2013 Jan 21 Eur J Pharmacol. 2013 Feb 15 701 (1-3) 96-105 | | WO1998027098 | Selleck | 3038525 |
| | | | | | | | | |
| PDK1 | BX-320 | C23H31BrN8O3 | 547.45 | Feldman R.I. (2005) Journal of Biological Chemistry 280 19867-19874 | | WO2004048343 | SuperNova Life Science | 657138 |
| PDK1 | BX-517 | C15H14N4O2 | 282.3 | Islam I. (2007) Bioorganic and Medicinal Chemistry Letters 17 3814-3818 | | CN102639566 | EMD Millipore | 11161844 |
| PDK1 | BX-517 Analog (compound 7b) | C19H15N5O2 | 345.35 | Islam I. (2007) Bioorganic and Medicinal Chemistry Letters 17 3819-3825 | | | | 11588244 |
| PDK1 | BX-795 | C23H26IN7O2S | 591.47 | Feldman R.I. (2005) Journal of Biological Chemistry 280 19867-19874 | | WO2004048343 | Axon | 10077147 |
| PDK1 | GSK2334470 | C25H34N8O | 462.59 | Najafov A. (2011) Biochem. J. 433 357-69 | | | Tocris | 46215815 |
| PDK1 | Merck 7 (PDK1) | C28H22F2N4O4 | 516.5 | Nagashima K. (2011) J. Biol. Chem. 286 5433-6448 | | | | |
| PDK1 | OSU-03012 | C26H19F3N4O | 460.45 | Zhu J. (2004) Cancer Res. 64 (12) 4309-18 | | | Selleck | 10027278 |
| PDK1 | Wyeth PDK1 Inhibitor Compound 1 | C19H22Cl4N4O2 | 480.21 | Gopalsamy A. (2007) Journal of Medicinal Chemistry 50 (23) 5547-5549 | | | | |
| | | | | | | | | |
| PKC | Chelerythrine Chloride | C21H18NO4Cl | 383.8 | Kandasamy R.A. (1995) J. Biol. Chem. 270 29209 | Jarvis W.D. (1994) Cancer Res. 54 1707 | WO2003077917 | Merck (Calbiochem) | 72311 |
| PKC | EGCG (Epigallocatechin Gallate) | C22H18O11 | 458.4 | Dell'Aica I. (2004) EMBO Rep. 5 418-422 | Tachibana H. (2004) Nat. Struct. Mol. Biol. 11 380 | WO2001051048 | Merck (Calbiochem) | 65064 |
| PKC | GF 109203X (Go 6850) | C25H24N4O2 | 412.5 | Hers I. (1999) FEBS Lett. 460 433 | Ku W.-C. (1997) Biochem. Biophys. Res. Commun. 241 730 | US7067144 | Merck (Calbiochem) | 2396 |
| PKC | Gö 6976 | C24H18N4O | 378.4 | Gschwendt M. (1996) FEBS Lett. 392 77 | Wenzel-Seifert K. (1994) Biochem. Biophys. Res. Commun. 200 1536 | WO2003009809 | Merck (Calbiochem) | 3501 |
| PKC | Gö 7874 | C27H26N4O4 ·Ûc HCl | 507 | Kleinschroth J. (1995) Bioorg. Med. Chem. Lett. 5 55 | | US20080153903 | Merck (Calbiochem) | 5327863 |
| PKC | LY333531 (Ruboxistaurin) | C28H28IN4O3 ·CH4O3S | 582.73 | Jirousek M.R. (1996) J. Med. Chem. 39 2664 | Tang S. (2008) Proteins 72 (1) 447-60 | WO2000053013 | Axon | 153999 |
| PKC | RO-31-8220 | C25H23N5O2S ·Ûc CH4O3S | 553.7 | Trapp J. (2006) J. Med. Chem. 49 7307-16 | Powell D.J. (2003) Mol. Cell Biol. 23 7794 | | Merck (Calbiochem) | 11628205 |
| PKC | Rottlerin | C30H28O8 | 516.5 | Villalba M. (1999) J. Immunol. 163 5813 | Gschwendt M. (1994) Biochem. Biophys. Res. Commun. 199 93 | | Merck (Calbiochem) | 5281847 |
| PKC | UCN-01 | C28H26N4O4 | 482.5 | Reinhardt H.C. (2007) Cancer Cell 11 175 | Jiang K. (2004) Mol. Cancer Ther. 3 1221 | | Sigma | 72271 |

### 4.5.5 iGPS prediction analysis for kinase substrate interaction.

For 176 significantly regulated phosphopeptides found from mouse database in all the ctrl vs IR, LAP vs IR and IPC vs IR a total of 406 kinases were predicted. Out of these 12 predicted kinase substrate interactions, 2 kinases along with 2 predicted substrates were also identified in our data. Kinases were also encountered in our analysis with significantly regulated phosphorylation. These substrates were further found by network analysis to interact with more proteins (substrate) where 4 proteins were found in our study for each substrate as below (Fig 14A and B).

iGpS analysis for the identification of substrate in our data showed the presence of phopho regulataion of P62754/Rps6/40S ribosomal protein S6 Substrate for the kinase RSK1/Q9WUT3/ Rps6ka2/Ribosomal protein S6 kinase alpha-2. The significant phospho regulation was found at serine 242 and phosphopeptide was assign to cluster 3. However, four more substrate were also found in the data set for the Rps6 as shown in the fig-14A named as Poly(rC)-binding protein 1 /Pcbp1/ P60335, Rps3/ P62908/40S ribosomal protein S3, Eif4b/Q8BGD9/Eukaryotic translation initiation factor 4B and Pdcd4/Q61823/Programmed cell death protein 4.

Second Kinase NDR1/Q91VJ4/ Serine/threonine-protein kinase 38 was found to interact with substrate found in data set Supt16h/Q920B9/ FACT complex subunit SPT16 that further interact with multiple substrates as shown in fig-14B. The significant phospho regulation was found at serine 1023 and phosphopeptide was assign to cluster 2. However the found four substrates for Supt16h/Q920B9 also highlighted in figure were McM4/P49717/ DNA replication licensing factor MCM4, H2afx/P27661/ Histone H2A, Ckap4/Q8BMK4/ Cytoskeleton-associated protein 4 and Smarca5/Q91ZW3/ SWI/SNF-related matrix-associated actin-dependent regulator of chromatin subfamily A member 5.

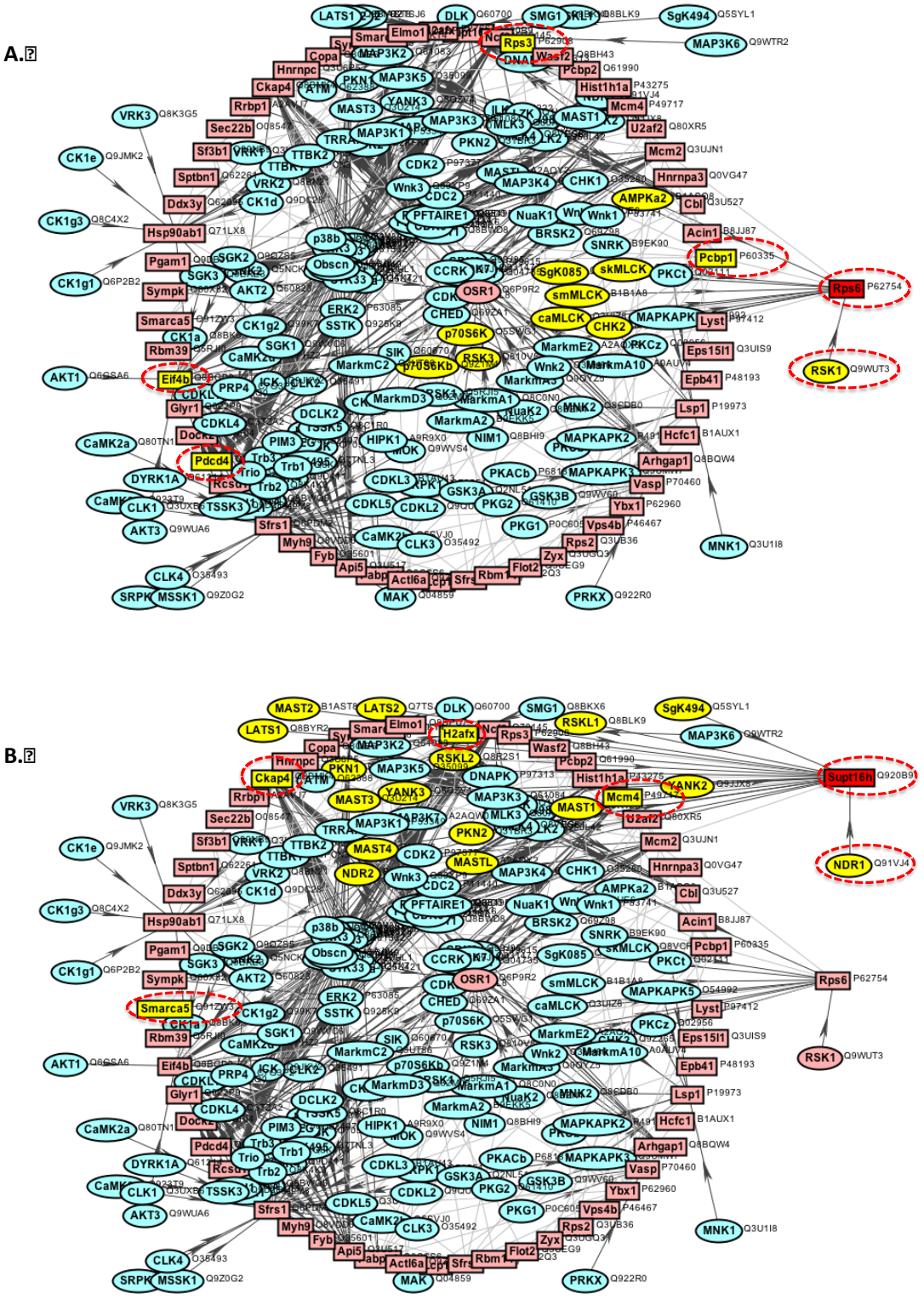


**Figure 14** A Network analysis for substrate kinase interactions A. RSK1 kinase and B. NDR1 kinase

### 4.5.6 Pathways and string analysis of significantly regulated phoshoproteins in cluster 3 and cluster 5

To find the effects of the IPC on the regulated pathways in neutrophils, we analyzed the phosphopeptides significantly regulated in any two conditions (4 conditions total) in clusters 3 and 5 for KEGG pathways analysis. The result for the pathways is shown in table 6. The most highly regulated pathway found is spliceosome with 4 proteins (u2af2, srsf2 (SR family), sf3b1 and usp39) and p-value of 0.0001. Other important signaling pathways with regulated phosphoproteins were chemokine signaling pathway, Fc-gamma R mediated phagocytosis and focal adhesion with descending p-values and 4, 3 and 3 proteins respectively. These three pathways are very interlinked therefore share some common proteins that are involved in more than one function (Table-9). These proteins have also been analyzed through an online database (STRING v10) for protein-protein interaction networks as shown in the figure-15. The interactions network confirms all the proteins mentioned in table 9. The most interacting proteins in the figure are Fgr, Pxn, Ptpn6 among others having a vital role in the first 3 most regulated pathways in the table 6 as shown below.

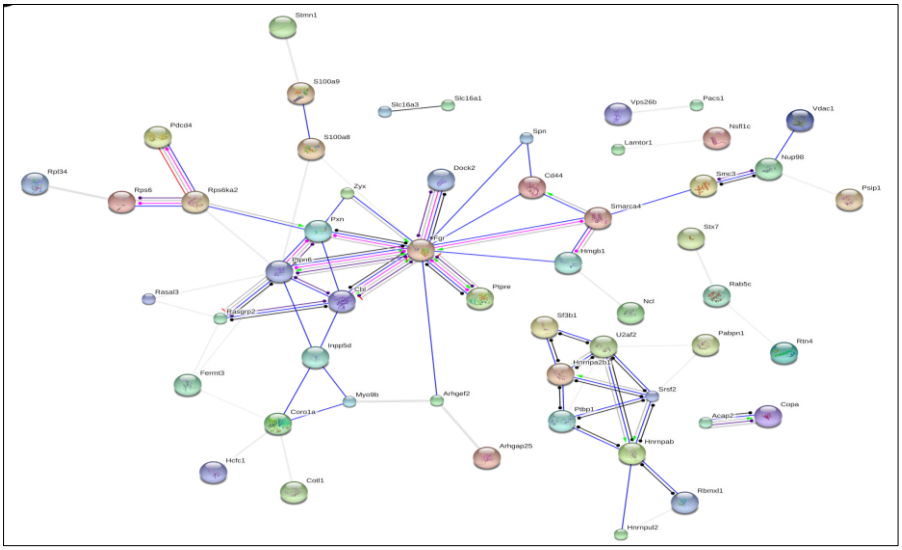


**Figure 15** String analysis of significantly regulated phosphoproteins in cluster 3 and 5.

**Table 9** KEGG pathway analysis of regulated phopshoproteins of cluster 3 and 5.

| KEGG Pathway | Asseccion No. | Gene Symbol | Description | No. of Phosphopeptides |
|---|---|---|---|---|
| **Spliceosome** *(C=135; O=4; E=0.26; R=15.49; rawP=0.0001; adjP=0.0017)* | | | | |
| | P26369 | U2af2 | U2 small nuclear ribonucleoprotein auxiliary factor (U2AF) 2 | 1 |
| | Q62093 | Srsf2 | serine/arginine-rich splicing factor 2 | 2 |
| | Q99NB9 | Sf3b1 | splicing factor 3b, subunit 1 | 2 |
| | Q3TIX9 | Usp39 | ubiquitin specific peptidase 39 | 1 |
| **Chemokine signaling pathway** *(C=178; O=4; E=0.34; R=11.75; rawP=0.0004; adjP=0.0034)* | | | | |
| | Q8C3J5 | Dock2 | dedicator of cytokinesis 2 | 4 |
| | Q66H76 | Pxn | paxillin | 2 |
| | Q6P6U0 | Fgr | Gardner-Rasheed feline sarcoma viral (v-fgr) oncogene homolog | 6 |
| | P0C643 | Rasgrp2 | RAS guanyl releasing protein 2 (calcium and DAG-regulated) | 1 |
| **Fc gamma R-mediated phagocytosis** *(C=91; O=3; E=0.17; R=17.24; rawP=0.0007; adjP=0.0040)* | | | | |
| | Q8C3J5 | Dock2 | dedicator of cytokinesis 2 | 4 |
| | P97573 | Inpp5d | inositol polyphosphate-5-phosphatase D | 2 |
| | P30009 | Marcks | myristoylated alanine rich protein kinase C substrate | 8 |
| **Insulin signaling pathway** *(C=131; O=3; E=0.25; R=11.97; rawP=0.0021; adjP=0.0089)* | | | | |
| | P22682 | Cbl | Cbl proto-oncogene, E3 ubiquitin protein ligase | 2 |
| | P62754 | Rps6 | ribosomal protein S6 | 1 |
| | P97573 | Inpp5d | inositol polyphosphate-5-phosphatase D | 2 |
| **Focal adhesion** *(C=186; O=3; E=0.36; R=8.43; rawP=0.0055; adjP=0.0134)* | | | | |
| | Q62523 | Zyx | zyxin | 1 |
| | Q10728 | Ppp1r12a | protein phosphatase 1, regulatory subunit 12A | 4 |
| | Q66H76 | Pxn | paxillin | 2 |
| **Phagosome** *(C=185; O=3; E=0.35; R=8.48; rawP=0.0055; adjP=0.0134)* | | | | |
| | O70257 | Stx7 | syntaxin 7 | 2 |
| | P35278 | Rab5c | RAB5C, member RAS oncogene family | 1 |
| | Q91ZN1 | Coro1a | coronin, actin binding protein 1A | 1 |
| **mTOR signaling pathway** *(C=51; O=2; E=0.10; R=20.50; rawP=0.0043; adjP=0.0134)* | | | | |
| | Q9WUT3 | Rps6ka2 | ribosomal protein S6 kinase polypeptide 2 | 1 |
| | P62754 | Rps6 | ribosomal protein S6 | 1 |
| **Endocytosis** *(C=230; O=3; E=0.44; R=6.82; rawP=0.0099; adjP=0.0153)* | | | | |
| | Q5FVC7 | Acap2 | ArfGAP with coiled-coil, ankyrin repeat and PH domains 2 | 1 |
| | P22682 | Cbl | Cbl proto-oncogene, E3 ubiquitin protein ligase | 2 |
| | P35278 | Rab5c | RAB5C, member RAS oncogene family | 1 |
| **B cell receptor signaling pathway** *(C=75; O=2; E=0.14; R=13.94; rawP=0.0092; adjP=0.0153)* | | | | |
| | P97573 | Inpp5d | inositol polyphosphate-5-phosphatase D | 2 |
| | P81718 | Ptpn6 | protein tyrosine phosphatase, non-receptor type 6 | 3 |
| **Long-term potentiation** *(C=69; O=2; E=0.13; R=15.16; rawP=0.0078; adjP=0.0153)* | | | | |
| | Q10728 | Ppp1r12a | protein phosphatase 1, regulatory subunit 12A | 4 |
| | Q9WUT3 | Rps6ka2 | ribosomal protein S6 kinase polypeptide 2 | 1 |

**C:** *the number of reference genes in the category*
**O:** *the number of genes in the gene set and also in the category*
**E:** *the expected number in the category*
**R:** *ratio of enrichment*
**rawP:** *p value from hypergeometric test*
**adjP:** *p value adjusted by the multiple test adjustment*

# Discussion

# 5 DISCUSSION

Ischemic preconditioning has been studied as a protective strategy against ischemia/reperfusion injury in intestinal models [19, 20]. In humans, prolonged jejunal ischemia (45 minutes), followed by reperfusion, resulted in intestinal barrier integrity loss, which is accompanied by significant translocation of endotoxins. These phenomena resulted in an inflammatory response characterized by complement activation, endothelial activation, neutrophil sequestration, and release of pro-inflammatory mediators into the circulation [24]. The comparison of the effect of IR and IPC on blood parameters has not been studied in the past using the 45 min of SMAO model in rats. Lymphocyte loss and dysfunction are well known in animal models of both SIRS and sepsis [25]. Preventing lymphocyte dysfunction, specifically preventing lymphocyte apoptosis following sepsis, has been shown to improve survival after sepsis [26]. Recently, a decrease in lymphocyte percentage has been observed following IR, local and remote IPC in a rat model with temporary supraceliac aortic clamping [27]. IPC prevented lymphocyte loss, compared with the IR group in our study.

We observed a significant increase in WBCs count after IR. Postoperative leukocytosis represents a normal physiologic response to surgery [28]. However, an augmentation in WBC count has been viewed as a predictor of ischemic stroke [29]. This increase was due to the marked elevation of leukocyte activation, as previously described in myocardial ischemia and reperfusion in dogs [30]. The increased number of granulocytes after ischemic strokes caused tissue damage, as these cells are implicated in the early responses of the hemostatic and inflammatory processes [31]. Studies have revealed that intestinal ischemia is characterized by the production of cytokines [32] and the sequestration of polymorphonuclear neutrophils (PMNs) into the ischemically damaged tissue. The complement system also contributes to the attraction of neutrophils to ischemically damaged areas [33] where neutrophil-released myeloperoxidase and other proinflammatory mediators, further contribute to IR-induced tissue damage [34]. A significant reduction in IPC circulating granulocytes in comparison with IR was noticed suggesting a protective aspect of IPC.

Except for the MCHC values, the results for RBCs, Hb, MCV, MCH, MCHC and HCT are similar to those of a study on a canine model-investigating limb IR, with or without cooling [35]. Dehydration during surgery or fluid sequestration due to edema can result into a higher hematocrit level than normal [36]. This increase was more prominent in the IR group and showed no significant difference in any other group. Similarly an increase in HCT has been observed in IR as compared to local IPC and remote IPC in a similar model using temporary supraceliac aortic clamping [27].

Studies have shown that platelets also participate in ischemic strokes [37] and IR-mediated tissue damage [38] through the generation of free radicals, proinflammatory mediators like thromboxane (TxA2), leukotrienes, serotonin, platelet factor-4 and platelet-derived growth factor (PDGF) and also modulate leukocyte function [39, 40]. Like leukocytes, the expression of P-selectin on the platelets surface helps in rolling and firm adherence to the vascular endothelium and in the interaction with leukocytes during post-ischemic reperfusion, resulting in an increased expression of the adhesion molecules, generation of superoxide and in the phagocytic activity of the leukocytes [39, 41]. Inhibition of platelet adhesion by the administration of anti-fibrinogen antibody decreased the short-term liver injury after ischemia. The platelet-derived serotonin has been found a mediator in tissue repair after hepatic normothermic ischemia in mice [42, 43]. We observed a significant decrease in platelet in IPC as compared to IR. However, the role of platelets in the progression of tissue damage after IR injury is not clear. A recent study showed that platelet-deficient mice showed significant reductions in the damage to their villi in response to IR, compared with mice with normal platelet counts [44].

The MPV was found to be higher when there was destruction of platelets in inflammatory bowel disease [45]. Another study stated that MPV was not associated with stroke severity or functional outcomes [46]. The activation of the platelets leads to morphologic changes, including pseudopodia formation and the development of spherical shape. Platelets with an increased number and size of pseudopodia differ in size, possibly affecting the PDW**.** We found an inverse relationship between PLT count and MPV value after IR and IPC. IPC is lowering the PLT count but increasing the

MPV value. Whereas a recent study in patients who underwent surgical intervention for acute mesenteric ischemia showed an increase in MPV and a decrease in PLT count in non-survival than survival [47]. In case of IR group we found an increase in PLT count and a decrease in MPV value, which is contrary to this study. The discrepancy could be attributed to different occlusion models, since AMI patients can present partial vascular occlusions lasting for less precise amount of time. We cannot correlate this change with mortality rate as the model involving 45 minutes of intestinal ischemia in rats has been considered to be free of mortality [48], whereas ischemic period and severity varies among clinical conditions, leading to higher morbidity and mortality. For example, AMI has overall mortality of 60% to 80%, and the reported incidences are increasing over time [49, 50] because the major reason is the continued difficulty in recognizing the condition [50]. The effect of IPC on these parameters with AMI needs further validation in humans.

We have identified total of 2924 rat neutrophil proteins using nLC-MS/MS analysis, 393 (13.4% of the total identified proteins) were significantly different in terms of regulation (t-test P-value < 0.05) in the surgical trauma group as compared to the control. Out of 393 proteins, 190 proteins (~6.5%) showed significant up-regulation in surgical trauma whereas 203 proteins (6.94%) presented down-regulation as compared to the control group.

The gene ontology (GO) classification of the differentially regulated proteins according to their expected subcellular localization revealed that most of the proteins belonged to cytoplasm, membrane, nucleus, cytoskeleton, organelle lumen and cytosol. The cytoskeleton, membrane, nucleus and vacuole showed higher number of down-regulated proteins and cytosol, endoplasmic reticulum, mitochondrion had higher count of up-regulated proteins, whereas ribosomal proteins were only up-regulated or non-significant. Neutrophils are highly motile defense cells and the cytoskeleton plays an important role in their motility (28). Therefore, the down-regulation of cytoskeleton proteins found in our dataset may suggest decreased neutrophil motility and low chemotaxis after surgical trauma.

We found that oxidoreductases and transferases are predominant among the down-regulated proteins whereas ligases were found more frequently within the proteins with significantly up-regulation from neutrophils after abdominal surgery in neutrophils (Table 1).

Oxidoreductases are generally involved in conversion of molecular oxygen to oxygen free radicals, superoxide, hydroperoxide, singlet oxygen and hydrogen peroxide. Downregulation of such proteins is potentially harmful, as these molecules then modify lipids, proteins, DNA and carbohydrates, increasing oxidative stress. In fact, oxidoreductases constitute the most important free radical scavenger systems (30). Lipoxygenases (LO) are oxidoreductases that introduce oxygen into unsaturated fatty acids (31). After inflammatory stimuli, arachidonic acid is liberated from the cell membrane as a result of the action of cytosolic phospholipase A2 on phospholipids (32, 33). The 12/15-LO further metabolizes arachidonic acid and liberates short-lived, peroxidized products, which are reduced, or enzymatically converted to 12-hydroxyeicosatetraenoic acid (12-HETE) as well as hepoxilins, lipoxins and others (34). Besides 12/15-LO, the lipoxygenase 5-LO also metabolizes arachidonic acid and produces leukotrienes (LTA4 /LTB4) in inflammatory cells (35). All the three lipoxygenases 12-LO, 15-LO and 5-LO, Q02759/ P48999 (EC:1.13.11.31/ 1.13.11.33 /1.13.11.34) were found down-regulated in ST among the oxidoreductases in our analysis. A study blocking the 12/15-LO in mice showed disturbance in neutrophil recruitment, possibly by alterations in the CXCL1/CXCR2 chemokine axis (36). Similarly, both CXCR2 and LTB4 receptors were found down-regulated after exposure to IL8 after trauma injury (12). Shureiqi *et al.* showed that inhibition of arachidonate 15-lipoxygenase causes cell survival and decreases apoptosis in cancer cells suggesting its role as a pro-apoptotic molecule (37) whereas another study by Tang *et al.* also reported that arachidonate lipoxygenases play an important role in cell survival and apoptosis (38). This significant down-regulation of all the three identified lipoxygenases after surgical trauma may suggest their role in down-regulation of CXCR2 and LTB4 receptors, leading to impaired chemotaxis and phagocytosis in neutrophils with a long life span.

Among the significantly up-regulated transferases the most repeatedly annotated transferases were Dolichyl-phosphate β-D-mannosyltransferase (EC: 2.4.1.83/Q9WU83) and Dolichyl-diphosphooligosaccharide protein glycotransferase (EC 2.4.99.18/ O54734, P46978, P61806, Q3TDQ1). Both participate in n-glycan biosynthesis, a process essential for maintenance of the receptor surface expression in neutrophils (39). Although not directly involved in signaling, glycosylation appears to be important in the maintenance of neutrophil responsiveness to CXC-chemokines during inflammation (40). Ten transferases significantly down-regulated in ST rats are annotated with EC: 2.7.11.1 and classified as non-specific serine/threonine protein kinases (including STE20-like and PAK 2, among others). Most of these enzymes are not well characterized with respect to their role in neutrophils after ST. One of the serine/threonine protein kinases with down-regulation is PAK2. In neutrophils, p21-activated kinase (PAK2) can be stimulated by number of chemokines (41, 42). Studies showed that PAKs are involved in a variety of cellular events such as rapid cytoskeletal responses, transcriptional events and the development of malignancy (43). Protein kinase C delta (P09215/ 2.7.11.13) was identified in our analysis with down-regulation after surgery and that has also been reported in mediating spontaneous PMN apoptosis (44).

Among the hydrolases, 6 of the proteins are annotated as DNA helicases (EC 3.6.4.12) and 3 as RNA helicases (EC 3.6.4.13) (Table 1). An important up-regulated enzyme in ST in this category is (P43527/EC 3.4.22.36) Caspase-1, which is a multifactorial enzyme. It participates in initial inflammatory response after hemorrhagic shock and peripheral tissue trauma. It is involved in maturation of cytokines IL-1β and IL-18, cell death pathways specifically in pyroptosis during infection, regulation of both glucose and lipid metabolism, and cell survival (45, 46). Along with caspase 1, neutrophil derived serine proteases, e.g. cathepsin G (CG), neutrophil elastase (NE), and proteinase 3 (PR3), are also involved in IL-1β maturation at distinct sites (47). Our results from the significantly up-regulated hydrolases included myeloblastin/proteinase 3 (Q61096/ EC 3.4.21.76), Cathepsin H (P00786/EC 3.4.22.16) and Cathepsin D (P24268/ EC 3.4.23.5) while Cathepsin C (Q64560/ 3.4.14.1) was present among down-regulated hydrolases in ST. Following abdominal surgery, up-regulation of these

enzymes in neutrophils may lead to a higher systematic production of IL-1, a cytokine involved in chronic inflammatory disease. Most of the down-regulated hydrolases are involved in the metabolism of different biomolecules, including galactose, lipids, amino acids and purines. Another interesting hydrolase found with down-regulation is (P24135/3.1.4.11) phosphoinositide phospholipase C (PLC), which produces IP3 and diacylglycerol [14] from PI-4, 5 bisphosphate (PI(4,5)P2). IP3 further mediates calcium release and DAG activates several PKC isoforms. Inhibition of PLC resulted into impaired phagocytosis in macrophages and PLC has been found accumulated at the phagocytic cup (48). Ins(1,4,5)P3 is further converted by the actions of several distinct kinases and phosphatases to a variety of inositol phosphates, that negatively regulate PtdIns(3,4,5)P3 signaling pathway (49). In this context, we have also encountered two more hydrolases with down-regulation, inositol-phosphate phosphatase (P97697/ 3.1.3.25) and diphosphoinositol-polyphosphate diphosphatase (Q8R2U6/ 3.6.1.52), which along with PLC regulates PtdIns(3,4,5)P3 signaling pathway consequently playing a critical role in controlling neutrophil function (49). Caspase 3 (P55213/3.4.22.56) was also found significantly down-regulated and its activation lead to apoptotic signals in neutrophils. Decrease in procaspases-3 was found to be associated with increased lifespan of transmigrated PMN (8, 50). Increase in systemic neutrophil life span has been known as a major cause of tissue damage after trauma (5).

Four isomerases were found with up-regulation in neutrophils after surgical trauma, interestingly three of these are annotated as EC: 5.2.1.8 (P17742/ P29117/Q62446) prolyl isomerase (Pin1), a unique cis-transprolyl isomerase, acts as regulator of TNF-α induced NADPH oxidase hyper activation in human neutrophils and thus can be an essential player in TNF-α induced inflammatory diseases (51). Another isomerase found with up-regulation is thromboxane-A synthase (P49430/ EC: 5.3.99.5), which is involved in the production of thromboxane that further induces production of superoxide in neutrophils (52).

Most of the identified ligases with differential regulation include tRNA ligases. Glutathione synthase (P46413/ EC: 6.3.2.3) that plays an important role in glutathione synthesis was found up-regulated as compared to control, which is an anti-inflammatory

and inhibits the production of several inflammatory cytokines, chemokines and their action (53).

All the presented enzyme families have essential roles in the immune response and biochemical mechanisms of the neutrophil. Our data suggest that neutrophils in rats affected by surgical trauma have critical down or upregulation of these essential enzymes, potentially causing the high life span with high ROS production and tissues damage.

It is clear from table 2 and string analysis that most of the up-regulated proteins have their role in mRNA processing, translation initiation and other translational activities. This up-regulation of translational proteins suggests higher protein expression, which is in accordance with the high neutrophil activation followed by protein secretion (54-56). Some of the up-regulated proteins in ST as compared to control were clustered in TCA cycle and oxidative phosphorylation pathways, which are crucial for energy conservation in the form of ATP. It was also found in our dataset that four significantly down-regulated proteins were assigned to the pentose phosphate pathways (PPP) and also glucose-6-phosphate dehydrogenase (g6pd), but with less significance. PPP associated proteins with down-regulation may suggest a metabolic shift from PPP in neutrophil activation after abdominal surgical trauma suggesting a low nets formation at primary stages of trauma (57).

Although neutrophils do not divide, in our study some of the proteins having their role in DNA replication and cell cycle were also identified with significantly up-regulation in ST rats. This needs attention and further studies to find out their exact role in activated neutrophils after surgical trauma.

The proteasome is an important multi-subunit enzyme complex having a central role in regulating various biological processes like apoptosis, cell cycle progression, immune response and stress related cellular responses (58). Six proteins from the proteasome degradation pathway were found significantly down-regulated in ST rats in our study. This down-regulation of proteasomal proteins was in accordance to the previous study on neonatal and adult neutrophils (59, 60) but in contrast to the recently

published work where they analyzed the human neutrophil at proteomic and RNA level from trauma patients (56). As trauma often results in MOF by activating neutrophils (7) and the participation of the proteasome in the pathogenesis of lung injury has also been investigated (61), these and our experimental findings together may suggest a time window to consider in blocking activated neutrophil proteasomal activity to avoid final injuries and later organ dysfunction after trauma.

Functional and protein-protein interaction network analysis using STRING (25) highlighted the down-regulation of proteins involved in the immune response suggesting the low immune response and high susceptibility of the trauma patients to infection as previously described (62, 63). A pro-apoptotic protein Prkcd and an important apoptotic cascade molecule Caspase-3 were found down-regulated during our analysis that supports an increased lifespan of the trauma activated neutrophils (64-67).

A group of proteins involved in regulation of actin cytoskeleton and neutrophil motility was found down-regulated, suggesting reduced directionality and migration. Butler *et al.* also proved that neutrophils from the thermally injured patients show less chemokinesis in the absence of bacterial infection (68). Another study by Kurihara *et al*. concluded defects in the directionality of the neutrophils from thermally injured rats as compared to the sham controls towards fMLP (69). Hence, this decrease in the trauma activated neutrophil motility will not only reduce the neutrophil recruitment to the site of infection but also will increase damage to the bystander tissues.

To analyse the effect of IPC on rat neutrophil proteome, in short this study Male Wistar rats (*Rattus norvegicus*), presenting no inflammatory disease, (with the mean value of granulocytes 32.1%±2.86) were selected [142]. In this way 40 rats were randomly allocated into the four groups: control, laparotomy, ischemia/reperfusion (submitted to superior mesenteric artery occlusion for 45 min followed by 120min of reperfusion), and ischemic preconditioning group (a short episode (10 minutes) of ischemia and reperfusion before the same long ischemic episode as the IR group. The choice of periods of mesenteric ischemia (45 minutes) used in this study was based on previous studies that demonstrated no mortality but presence of systemic inflammatory response

using these periods [143]. Among the many published reports which used IPC of varying duration, for example, 3 minutes, 5 minutes, also 10 minutes, it was concluded that the IPC for 10 minutes of occlusion followed by 10 minutes of reperfusion shows the best protective effect against intestinal injury by intestinal IR [144,145] compared to 2, 5, 10 and 15 minutes.

For the large proteomic analysis of rat neutrophil after IPC, the list of identified and iTRAQ labelled peptides was analyzed by using statistical software developed in R, which provided a total of 2437 protein groups in all conditions. The Principal component analysis showed that the variability among replicates was less than that among the different conditions showing relatively good reproducibility in each condition. The resulting five clusters with different abundance profiles with no overlapping showed that a profile representing differences in relative abundance between IR and IPC groups with less difference among Ctrl, LAP and IPC groups was present in clusters 4 and 5, suggesting the two clusters with IPC responsive proteins. In that sense, proteins from clusters 4 and 5 had their abundance profile reflecting the preventive effect of IPC over IR and were chosen for a more detailed discussion. For the functional classification of the proteins in clusters 4 and 5 we used ProteinCenter for the gene ontology (GO) analysis and UniProt to retrieve enzyme activity prediction, as well as WebGestalt to find enriched pathways in the Kyoto Encyclopedia of Genes and Genomes (KEGG) database (45).

Distribution of GO terms for cellular component showed great diversity of protein groups in their cellular localization. The major difference in relative abundance in both clusters was noticed among the proteins annotated to cytoplasm, membrane, cytoskeleton, nucleus, organelle lumen and ribosome. About 119 proteins (58 in cluster 4, 61 in cluster 5) presenting a relative abundance profile that suggests influence of the mitochondrial protein distribution pattern in preventing the IR alterations in neutrophil. The proteins from cluster 5 annotated to cytoplasm, nucleus, organelle lumen and ribosome are upregulated in IR in accordance with the activation of the transcriptional and translational machinery whereas IPC prevents such upregulation.

All the significantly regulated proteins from cluster 4 were analyzed for the KEGG pathways for top ten functional categories and the pathways found include: regulation of actin cytoskeleton, metabolic pathways, Fc gamma R mediated Phagocytosis, chemokine signaling, focal adhesion and leukocyte transendothelial migration (supplementary table 2). Such findings are in accordance with the GO analysis.

It is clear from the literature that the production of chemoattractant molecules (C5a, IL-8, LTB4, PAF) from inflammatory cells is altered during IR, along with the induction of various adhesion molecules onto the surface of both inflammatory cells and endothelial cells (ECs). The adhesion molecules regulating the leukocyte-endothelium interaction are the selectins, integrins b2 (CD11/CD18) expressed on neutrophils and the immunoglobulins (ICAM-1, VCAM-1, PECAM-1) on ECs (58). Integrin alpha M (P05555) and integrin β2 (P11835) were found among the regulated proteins, interestingly integrin β2 (CD11b/CD18) was found regulated in three comparisons (Ctrl vs IR, LAP vs IR and IR vs IPC). The increase in β2- integrin expression on neutrophil after hypoxia was shown by in vitro studies and later administration of anti-CD11b or anti-CD18 monoclonal antibodies in rats. Such studies also confirmed reduced infarct volumes and apoptosis with decreased accumulation of neutrophils in vivo (59, 60) however clinical studies using anti-integrin therapies with antibodies against CD11/CD18 in acute stroke patients did not show clinical improvement (61). Another protein from regulation of actin cytoskeleton pathway also found regulated in three comparisons was the IQ motif containing GTPase activating protein 1 (IQGAP1/Q9JKF1), a major scaffolding protein involved in cytoskeletal organization and signaling. It is an essential component of the CXCR2 “chemosynapse” in human neutrophils and the knock-down of IQGAP1 inhibited CXCR2 mediated chemotaxis (62). Other regulated proteins in this pathway are p21 protein (Cdc42/Rac)-activated kinase 2 (Pak2), profilin 1 (Pfn1), cytoplasmic FMR1 interacting protein 2 (Cyfip2), Nonmuscle myosin IIA (Myh9/14), actinin (Actn1), neuroblastoma ras oncogene (Nras), Rho-family GTPases like Rac2 and RhoA, phosphatidylinositol-5-phosphate 4-kinase (Pip4k2a), WAS protein family (Wasf2) and ras2 Kirsten rat sarcoma viral oncogene homolog (Kras). Most of these are important players of other pathways like

Fc gamma R mediated Phagocytosis, chemokine signaling, focal adhesion and leukocyte trans-endothelial migration. For example p21-activated kinase (PAK2) inhibition altered the subcellular localization of active RhoA, loss of directionality, increased spreading and decreased migration speed (63). The deficiency of non-muscle myosin IIA (MYH9) in T-cells decreased interstitial migration, caused over adherence to high endothelial venules and inefficient completion of recirculation through lymph nodes (64) whereas its upregulation in neutrophils suggests a functional role in the directional migration of immune cells (65). Rac2 is a member of the Rho family of GTPases that regulates the actin cytoskeleton and superoxide production. Decreased levels of Rac2 are associated with the immunodeficiency syndrome in male patients (66). Many studies investigating the role of intestinal IPC showed attenuated neutrophil sequestration and endothelial cell apoptosis, decrease in the production of inflammatory mediators like tumor necrosis factor (TNF)-α and interleukin-1, with decreased expression of adhesion molecules as ICAM-1 and VCAM-1 on ECs (67). However, the effect of IPC on the neutrophil proteome was not characterised. Pathway analysis for cluster 4 showed that most of the proteins regulated are involved in modulation of phagocytosis, morphological changes in neutrophils, cytoskeletal machinery, adhesion, and directional migration. This can further cause multiple tissue infiltration of these neutrophils in any organ leading to immunodeficiency with higher infection rate, acute lung injury (ALI) and multiple organ failure (MOF) after IR. However, the regulation of such proteins by IPC could improve neutrophil function.

There were 54 proteins from metabolic pathways found to follow the abundance profile of cluster 4, out of which 20 were regulated, participating mainly in glycolysis/gluconeogenesis, amino sugar and nucleotide, fructose, mannose, galactose and purine metabolism (supplementary table 2). In response to an underlying pathological condition and metabolic stress, neutrophils change bioenergetics in accordance with the changes in their biological functions (68). Normally glycolysis provides energy requirements for neutrophil chemotaxis (50). However, little is known regarding the regulatory role of glycolysis under normal and pathological conditions in these cells. Glycolytic enzyme, hexokinase 3 (*HK3*), was significantly down and upregulated after IR and IPC respectively. It was also significantly decreased in acute

myeloid leukemia patients as compared to normal granulocytes suggesting a role in neutrophil differentiation (69). Two proteins that belong to the family of lysophosphatidylcholine acyltransferases (P0C1Q3) involved in phospholipid metabolism and platelet-activating factor (PAF) biosynthesis were found regulated in all three conditions. Ten proteins were found upregulated in IR vs IPC including peroxiredoxin-6 (EC1.11.1.15) which acts as antioxidant by reducing damage caused by ROS/H2O2 in tissues whereas its translocation to the plasma membrane during neutrophil activation was required for optimal NADPH oxidase activity (70, 71). The IPC has an important role in the modulation of neutrophils bioenergetics, which is clear from the change in regulation of many proteins involved in metabolism.

Ribosomal proteins are also fundamental components in the cellular metabolism, ribosome synthesis, cell growth and development. Some of these ribosomal proteins have some extraribosomal activities including catalytic functions replication, transcription, RNA processing, DNA repair, and even in inflammation (72). There are 18 ribosomal proteins found upregulated by IR as compared to ctrl/ lap and downregulated by IPC as compared to IR, including 40S ribosomal proteins; Rps3a, Rps3, Rps8, Rps9, Rps11, Rps15, Rps23, Rps27, Rps28, Rps29, and 60S ribosomal proteins Rpl10a, Rpl11, Rpl15, Rpl24, Rpl26, Rpl27, Rpl36a, Rpl35. Recently activated protein synthesis has been noticed in activated human PMNs after trauma (73, 74). Our findings indicate the activation of protein biosynthesis in PMNs under oxidative stress while preconditioning resulted in decreased protein synthesis (75).

The generated ROS help in pathogen clearance, however, excessively produced superoxide damages the surrounding tissues. Superoxide dismutase (SOD) converts the superoxide radical to hydrogen peroxide ($H_2O_2$) and molecular oxygen (78). $H_2O_2$ detoxified by peroxidases such as, glutathione peroxidase (GPX) (79), peroxiredoxin (PRDX) (80) and methionine sulfoxide reductase A (81). Reperfusion injury is directly related to the formation of reactive oxygen species (ROS), endothelial cell injury, increased vascular permeability, and the activation of neutrophils and platelets, cytokines, and the complement system (82). Peroxiredoxin 6 was recently found in neutrophils as a 29 KDa protein that showed an additional biochemical role having a

phospholipase A2 (PLA2) activity, and enhancing NADPH oxidase activity in phorbol myristate acetate (PMA) stimulated neutrophils (70). A decrease in antioxidant activity in IR neutrophils could lead to higher ROS production further contributing to tissue injury after IR. Our data show that IR and IPC alter the regulation of these antioxidant enzymes in neutrophils that can lead to a difference in the level of injury produced in both situations suggesting regulation of antioxidant mechanisms in neutrophils as a one of the protective players after preconditioning.

Most regulated isomerases in cluster 5 were annotated as Protein disulphide isomerase/Pin1 (5.3.4.1) and Peptidylprolyl isomerase, PPIases (5.2.1.8). Both are involved in protein modifications that have a critical role in the protein folding process, and are involved in disulphide bonds formation and cis–trans isomerization of peptide bonds. Although Pin1 and PPIases also play a critical role in regulatory mechanisms of cellular function and pathophysiology of disease *(88)*, their role in pathophysiology of IPC in the neutrophil is not clear and could be further investigated in future studies.

In cluster 5 there were 7 ligases that were regulated and mostly involved in protein modifications like ubiquitination and sumoylation. The argininosuccinate synthase (ASS) (6.3.4.5) is an enzyme of the urea and nitric oxide (NO·) cycles and its overexpression leads to enhanced NO· generation (nitrosative stress) further implicated in epithelial cell injury, apoptosis, host immune defense, and perpetuation of the inflammatory response in the liver (89). It's significant upregulation after IR could increase NO· generation by neutrophil while downregulation could be one of the protective mechanisms after IPC.

The molecular mechanism by which IPC down regulates the cytotoxic function of neutrophils and offers tissue protection is not clear. We have also done a discovery assay using phospho proteomic analysis for better understanding the neutrophil response after intestinal ischemic preconditioning in rat model. Along with pathway analysis, domain and motif analysis for significantly regulated phosho proteins was also done after IR and IPC.

Protein phosphorylation, being an essential post-translational modification affecting all cellular activities was the main focus of this study[146]. The significantly altered protein kinases and phosphatases involved in protein phosphorylation modulation were deeply analyzed.

The rat neutrophils were isolated from the blood [147] with some modifications because two step histopaque gradient technique has been shown to be more appropriate for obtaining rat neutrophils with less (10ml) blood volume used (ml) and good number of recovered cells. The isolated neutrophils were processed for proteins extraction, digestion and peptides purification. For the enrichment and purification of the mono and multi phosphopeptides the $TiO_2$, SIMAC and HILIC (TiSH) method was used. The SIMAC shows the phosphopeptide-enriching method combining both MOAC (Metal Oxide Affinity Chromatography) and IMAC [148]. It separates both multiply and singly phosphorylated peptides, as first the acidic conditions are used to elute monophosphorylated peptides from IMAC material, then the subsequent basic elution recovered the multiply phosphorylated peptides. Singly phosphorylated peptides as well as flow through peptides then pass on $TiO_2$ for a second enrichment [149]. The purified peptides were analyzed by Orbitrap Velos Mass Spectrometry as shown in figure 11. Recently, in 2015, western blotting, phosphopeptide enrichment, and mass spectrometric analyses of fMLP-treated human neutrophils sample was performed by LC–MS/MS on an LTQ Orbitrap Velos mass spectrometer. In total, 770 ± 21 proteins (≥ 1 peptide) were identified in PolyMAC-Ti-enriched samples [150]. We identified a total of 2151 proteins out of which 549 were phosphorylated proteins and our criteria for the protein identification and assignment of phosphorylation to the phosphopeptides was very stringent. We used minimum number of 2 peptides for protein identification with phosphoRS score >95% for the localization of phosphorylation to a peptide. The identification of a greater amount of phosphopeptides shows the efficiency of enrichment and purification methods used here. We have found the largest number of phosphopeptides in rat neutrophils to date.

The Cluster analysis of these phosphopeptides and proteins using R software showed the sharp changes in protein relative abundance related to IR and IPC. The

clusters that highlight the influence of IPC suggesting its effect on reversing the IR consequences and on phosphopeptides regulation were clusters 3 and 5 graph 6. Moreover, clusters 1 and 6 show a progressive behavior of regulated phosphopeptides in all conditions. These could be regulated due to some common processes or pathways taking place in all conditions, likely to be related to the complexity of the surgical procedure, since procedures that are more complex seem to induce changes that are more pronounced in protein relative abundance. The Venn diagram comparisons of all regulated phosphopeptides and phosphoproteins graph 5 found in IR vs Ctrl and IR vs IPC showed that both the events (IR and IPC) have prominently affected phosphorylation in rat neutrophils. Similarly, the numbers of unique and overlapping phosphoproteins in both cases were larger as compared to the laparotomy group. This huge difference in phosphoproteins regulation accounts for pronounced difference in the effect of IPC on the proteome of neutrophils, changing its response to IR. Or, in the other words the response of the neutrophil proteome to IR drastically affected by IPC.

For signal transduction cascades, the eukaryotic cells depend on the phosphorylation of the hydroxyl group on the side chain of serine (S), threonine (T) and tyrosine (Y) [151,152]. Different studies have reported different ratios of S/T/Y phosphorylation in different cell lines. It has furthermore been estimated that the relative abundances of phosphoserine, -threonine, and -tyrosine in the human proteome are 90%, 10%, and 0.05%, respectively [153]. The phosphosites analysis of the phosphoproteome of rat neutrophils revealed 76% phosphorylation on Serine residue (Sph), 21% on Threonine (Tph) and 3% on Tyrosine (Yph) (Graph 5D). Our relative abundance of S/T/Y phosphorylation in regulated proteins (Graph 5F) showed 60%, 33% and 7% respectively. A different proportion of tyrosine kinases and serine/threonine kinases from the expected ratio can be due to activation by different receptors resulting in to different phenotypic changes. Whereas number of the S/T/Y phosphorylation sites also varies among the clusters. The highest numbers of S/T/Y sites were found regulated in cluster 5 that is clearly related to the different phenotypic changes found in neutrophilas a result of IPC or IR.

As already mentioned, the protein kinases have broad importance in signal transduction and are among the largest families of eukaryotes genes, making up to about 2% of the genome and have been extensively studied [154-156]. The human genome contains about 518 putative protein kinases [157-159], which can be divided into two families: 428 serine/threonine (Ser/Thr) kinases (PSKs) and 90 tyrosine (Tyr) kinases (PTKs). There are about 107 putative protein Tyr phosphatases (PTPs) and very few, about 30, protein Ser/Thr phosphatases (PSPs) [159,160]. It is accepted that short linear motifs around the phosphorylation sites provide primary specificity for kinase substrate recognition [161,162].

We detected a total of 12 protein kinases and 4 phosphatases with a significant differential phosphorylation pattern in at least one residue. Notably all of the regulated kinases belong to the transferases enzyme class and 5 kinases have been found significantly regulated in IR vs Ctrl while 2 kinases were found significantly regulated in IR vs IPC with phosphoregulataion found in the catalytic domain (table-4). However other kinases had phosphoregulation but as these were not in the catalytic domain region, they were not further discussed here. The information about their regulation in relative abundance\expression along with the cluster assigned is also given in table 4. Although the main purpose of this work is to check the effect of IPC on neutrophil phosphoproteome, it is also worth to analyze and discuss the effect of IR on kinases and phosphatases.

Two tyrosine-protein kinases named as tyrosine-protein kinase Fgr and tyrosine-protein kinase SYK were found (table 4). The Fgr is a member of the Scr family, predominantly expressed in hematopoietic cells. The regulated phosphopeptide in the catalytic domain was assigned to cluster 2 with a total of 7 significantly regulatory phosphosites. There were 5 regulated phosphopeptides-containing motif regions (Table 6) however the phosphorylation found only at tyr400 was in the catalytic domain assigned to cluster 2 with upregulation after ischemia. The pY400 in the kinase domain of activation loop switches the kinase into its active conformation [163]. After activation it regulates the intrinsic neutrophil migratory ability [164] and chemokine secretion [165]. The downregulation in protein relative abundance was noticed in both the conditions Ctrl vs

IR and IR vs IPC whereas phosphorylation in the catalytic domain at Y400 was found upregulated in Ctrl vs IR that suggests activation of Fgr after phosphorylation event in neutrophil after IR. In this regard, the identification of kinase-specific p-sites and the systematic elucidation of site-specific kinase-substrate relations (ssKSRs) associated to motility and migration assays would provide a fundamental basis for understanding cell plasticity and dynamics and for dissecting the molecular mechanisms of various diseases, whereas the ultimate progress could suggest potential drug targets for future biomedical design [166]. Interestingly 5 out of 7 phosphopeptides were found regulated in cluster 5 and contained three motifs SP, S.S and S…….S making Fgr a strong candidate having multiple catalytic functions that are contributed by distinct motifs of the protein [167]. We used the software package of GPS [168] for the prediction of *in vivo* site-specific kinase-substrate relations mainly from the phosphoproteomic data shown in the table 4. The predicted kinase for Fgr shown with highest score is Proto-oncogene tyrosine-protein kinase Src, also known as proto-oncogene c-Src or simply c-Src , that phosphorylates specific tyrosine residues in other proteins [169]. The Tyrosine-protein kinase Tec is another relevant kinase that plays a major role in the responses of human neutrophils to Monosodium urate (MSU) crystals, found second in ranking with 23.341 score for the phosphosite Y400 [170]. The higher score value means, the more potential or the possibility of the residue to be phosphorylated by that kinase. Inhibition of the phosphorylation event can be helpful in controlling neutrophil induced damage after ischemia. Unfortunately, an inhibitor for Tec has not yet established but the inhibition of the phosphorylation event in Fgr using an inhibitor for Src can be helpful in controlling neutrophil induced damage after ischemia. Therefore inhibitors for Src along with other predicted kinases are also shown in table 8 for future studies.

The GRK2 (also known as beta-adrenergic receptor kinase-1)\P26817 has the C-terminal variable region containing a PH domain which gives binding specificity to G beta gamma proteins and has diverse other functions [171,172]. We have found upregulation in the phosphorylation at S670\SP motif in the PH domain with binding sites for the membrane phospholipid PIP2 and free Gβγ subunits [173]. Its higher expression in septic neutrophils and in neutrophils after cytokines plus LPS treatment suggested its role in neutrophils desensitization to chemoattractants [173]. The 5 kinases responsible for this

specific phosphorylation are shown in table-7. Of these, CMGC/MAPK was shown with the highest score (of 42.735) and inhibitors for MAPK are also available. The phosphorylation by different kinases has been shown to transmodulate different signaling pathways by enhancing (PKA, PKC, Src) or denouncing (ERK) the catalytic activity of GRK2 [174]. Similarly, the phosphorylation of GRK2 at given tyrosine or serine residues also modulated its interaction with cellular partners. The serine phosphorylation by ERK1/2 on S670 strongly impaired GRK2/Gβγ interaction and inhibit kinase translocation and catalytic activity towards receptor membrane substrates. However phosphorylation by MAPK at S670 disrupted the complex and allowed additional rounds of dynamic GRK2/GIT1 association that favor cell migration by promoting an efficient and localized activation of the Rac/PAK/MEK/ERK signaling cascade [175]. Our result showed that GRK2 phosphorylation at S670 could be because of MAPK or ERK1/2 that can alter GRK2 catalytic activity towards membrane receptor substrates in neutrophils during ischemia resulting into activation of different signaling cascades through GPCR signaling.

Other significantly downregulated kinase with phosphorylation within a domain was the catalytic domain of the Serine/Threonine Kinase, Novel Protein Kinase C delta (P09215) that plays a role in cell cycle regulation, programmed cell death in many cell types, regulation of transcription as well as immune and inflammatory responses [176]. PKCδ is a novel PKC that was found with 2 regulated phosphorylations in the catalytic domain. Recently, it has been reported that PKCδ is required for neutrophil transmigration mediated by IL-1β and fMLP (integrin-dependent), but not IL-8 (integrin-independent), by regulating the adherence of neutrophils to endothelial cells. The molecular mechanism of PKCδ's function in neutrophil chemotaxis remained unclear [177]. We found downregulation of its phosphorylation in neutrophils after ischemia (cluster 6) whereas its relative abundance was upregulated in IR and downregulated in IPC (cluster 5). The phosphorylation of Ser643 required for the catalytic maturation of PKCδ in cardiomyocytes [150] where as the exact effect of both these phosphorylation in PKC delta in neutrophil is not known. It was reported that the decreased activity of this enzyme by hypoxia enhanced EC survival [178]. The two predicted kinases for S643 and s645 shown in table-7 are CAMK/RAD53 and

CAMK/CAMK1 respectively with the highest score. The multifunctional CaMKs are a family of serine/threonine kinases sensitive to changes in intracellular $Ca^{2+}$, which coordinate a variety of cellular functions, including gene expression, cell cycle, differentiation, and ischemic tolerance [179]. Dysregulated $Ca^{2+}$ handling is prevalent during sepsis and postulated to perpetuate the aberrant inflammation underlying subsequent organ dysfunction and death. The signal transduction cascades mediating these processes are unknown in neutrophils and other cells. However CaMK1 signaling was essential to the macrophage responding to LPS and may also be operant in vivo in regulating the inflammation and organ dysfunction consequent to sepsis [180]. However inhibitors for both the predicted kinases CAMK/RAD53 and CAMK/CAMK1 were absent in the database (table-7). In neutrophil activation and phosphorylations in the catalytic domain region of PKC delta could be involve in increase or decrease in transcellular migration or survival.

The two significant phospho regulated kinases in IR vs IPC were the serine/threonine-protein kinases OSR1 and the serine/threonine-protein kinase 38 (Q91VJ4) with assignment to different clusters. Phosphopeptide regulation in the catalytic domain at T452 was found only in (Q91VJ4) the Serine/Threonine Kinase, Nuclear Dbf2-Related kinase 1 also known as non-race specific disease resistance-1 (NDR1). NDR1 (also called STK38) plays a role in proper centrosome duplication. Recently Selimoglu et al. found that under osmotic and oxidative stresses MAP4K4 kinase directly phosphorylated NDR1 on Thr444 and induced apoptosis through the RalA-MAP4K4-NDR1 pathway in this way NDR1 appeared to also act as a tumor suppressor [181]. We have found the novel site at pT452 whose role is not clear yet. The responsible predicted kinases for T452 are TKL (tyrosine kinase like) kinase with higher score and PKC. Tyrosine kinase-like kinases are serine-threonine protein kinases named so because of their close sequence similarity to tyrosine kinases. There are eight major TKL families in animals: MLK, MLKL, RAF, STKR, LRRK, LISK, IRAK and RIPK [182]. AGC kinase family, containing PKC, have crucial roles in the regulation of physiological processes that are important for cell growth, metabolism, proliferation and survival [183] but little is known about the interaction between NDR1\stk 38 and TKL kinases\AGC kinses. In neutrophils, activation of NDR1\stk 38 after phosphorylation in

catalytic domain can result into apoptosis of neutrophil after IPC that can finally lead to lower tissue damage.

Some kinases were found with significantly regulated peptides, but these were not related to any domain. Such kinases were Rps6ka1, Rps6ka2, Pak2, pkn1 (pak1), oxsr1, syk and slk. Serine/threonine-protein kinase N1, Pkn1/Prk1/Pak1, (Q63433) is a member of the protein kinase C superfamily of serine/threonine kinases which is one of the first identified effectors for RhoA-GTPase existing in an integral plasma membrane pool and a cytosolic/peripheral pool [184]. Its relative abundance was high in IPC as compared with LAP (cluster 1) as shown in table 3 whereas the single phosphor regulated peptide was assigned to cluster 2 with upregulation (Contl vs IR) and also contain S.S (fig-3C) motif as shown in table 6 that shows presence of a binding site for other proteins. The spleen tyrosine kinase (Syk, Q64725) found downregulated in Control vs IPC (cluster 2) and one regulated phosphopeptide with pS291 contained the S.S motif too. The regulated phosphopeptide was also downregulated in IR vs Ctrl (cluster 6) as shown in table-6. The signaling pathway downstream of CD18 integrins was dependent on Syk. However, the loss of Syk kinase mediated integrin signaling impaired leukocyte activation leading to reduced host defense responses [185]. Syk is a very important player of the phagocytosis pathway, as in neutrophils its inhibition decreased the phagocytosis of IgG coated particles [186]. But the exact role of Syk in this process remained unclear. Some studies show its role in the formation of the actin filament cup during FcRγ-mediated phagocytosis [2,3]. The effect of pS291in syk is not clear in neutrophil however in B cells a positive role in receptor-mediated signaling [50]. Its downregulated phosphopeptides, found in IPC as compared to control, can affect the process of formation of the actin filament or defense response after IPC.

STE20-like serine/threonine-protein kinase, Slk, exacerbates apoptosis and may regulate cell survival during injury or repair [58.] One study have also shown the apoptotic role of Slk after its overexpression induced by subjecting kidney cells to in vitro ischemia-reperfusion injury [58,187] while other study shown its affect on cytoskeletal reorganization as part of an anti-apoptotic pathway [188]. We found upregulataion in protein expression of slk in IR group, and downregulation in IPC group. The signaling

mechanisms that ensue downstream of SLK and how they regulate cytoskeletal remodeling and cell death will allow these hypotheses to be tested in neutrophil. As differential expression of slk after IR and IPC show its opposite effect in of anycase. Serine/threonine-protein kinase, Oxsr1/Osr1, (Q6P9R2) Oxsr1 is an oxidative-stress responsive 1 protein of the STE20 family. Osr1 regulates Na+/H+ exchanger activity [189,190]. The Phosphorylation at S324 and S359 with upregulation in the IR group (cluster 5, IR vs Ctrl) containing the SP motif suggested its role in ROS production and inhibition of NADPH oxidase [3]. Our quantitative proteomic analysis of the total rat neutrophil proteome, subjected to IR and IPC, showed that Pak2 was also among the 15 most regulated proteins for actin cytoskeleton regulation pathway showing its important role in directional migration [191]. Although no domain or motif was encountered in the 2 phopshopetides (S32, S41) (table-6) significantly regulated in IR neutrophils however its relative up and downregulation in conditions lap vs IPC and IR vs IPC indicates its differential effect after IPC as compared to LAP and IR.

Similarly some important protein phosphatases with and without regulation of phosphorylation events in domains have been encountered in our data mentioned in (tables 3 and 6). There are protein tyrosine phosphatases (PTPs) along with serine threonine phosphatases. The classical PTPs include transmembrane receptor like proteins (RPTPs) that have the potential to regulate signaling through ligand controlled protein tyrosine dephosphorylation. Many of the RPTPs display features of cell-adhesion molecules in their extracellular segment and have been implicated in processes that involve cell–cell and cell–matrix contact. These contain the D1 and D2 domains, that ate important for protein–protein interactions and regulate RPTP dimerization. There are also non-transmembrane, cytoplasmic PTPs. These enzymes are characterized by regulatory sequences that flank the catalytic domain and control the activity by interactions at the active site that modulate activity [21,192]. Two RPTP found here were Receptor-type tyrosine-protein phosphatase C isoform 4 precursor, Ptprc/CD45, (P04157) and receptor-type tyrosine-protein phosphatase epsilon (B2GV87). Although the regulation in a domain within the phosphopeptide was not found in both of these, the relative abundance of Ptprc/CD45, was significanty regulated in three conditions: Ctrl Vs IR, Ctrl VS IPC and IR VS IPC in cluster 5 (table 3). CD45, commonly known

as LCA (Luekocyte common antigen), was found with one phosphosite significantly regulated. CD45 plays a role in neutrophil adhesion, chemotaxis, phagocytosis, ROS production and bacterial killing [51]. Gao *et al* showed that CD45 can regulate or enhance the stimulation and function of human neutrophils mediated through Fc gamma R(s) triggering immune responses. Therefore its upregulation in IR and downregulation in IPC can lead to change in immune responding directly affecting the Fc gamma Rs in the neutrophil.

A non-receptor type PTP with Tyrosine-protein phosphatase non-receptor type 6, Ptpn6/Shp-1, (P81718) Phosphorylation was found upregulated (IR vs Ctrl) in cluster 2 on Ser12n SH2_N-SH2_SHP_like, N-terminal Src homology 2 (N-SH2) domain found in SH2 domain Phosphatases (SHP) proteins. The SHP-1 is "negative" regulation of cell signaling however its mechanisms of regulation are incompletely understood. The N-terminal SH2 domain appeared to play a role as a negative regulator of SHP-1 catalytic activity by directly binding to the SHP-1 catalytic domain [193]. SHP-1 is involved in modulating apoptotic pathways in neutrophils.

Inhibitory signaling can be mediated by specialized surface immune inhibitory receptors that contain immunoreceptor tyrosine-based inhibitory motifs (ITIM) in the cytoplasmic domain [194]. Following receptor activation, tyrosine residues of the ITIM domain can be phosphorylated by *Src* family kinases, resulting in the recruitment of SH2 domain-containing tyrosine phosphatases, such as SHP-1. Their subsequent phosphorylation deactivates tyrosine kinases, leading to inhibition of survival signaling especially Fas ligand, TNF-alpha, or TRAIL, the anti-apoptotic effects of granulocyte-macrophage colony-stimulating factor (GM-CSF), granulocyte colony-stimulating factor (G-CSF), or IFN-gamma in neutrophils [195]. Therefore activation of SHP-1 in inhibition of survival signaling can lead to higher life span found in activated neutrophil after IR. We have identified phosphorylataion at serine 12 in N- SH2 domain of SHP-1 can be one of the important step in the regulation of these mechanisms.

It has been also proposed that SHP1 binds to multiple kinases, such as Jak2, Jak3, TAK1, ERK1/2, p38, JNK, IL-1R-associated kinase 1, and Lyn, through a novel phosphorylation-independent kinase tyrosyl inhibitory motif [196]. The regulated

phosphosites in SHP-1 contained the R..S motif for binding to other predicted kinases (CAMK, CMGC family) as mentioned in table 7. There is absence of inhibitors for the kinases regulating the phosphorylation events at S12 in Ptpn6/Shp-1. The kinases CAMK/PHK and CMGC/CK2 were predicted for this S12 phosphorylation. Recently PTPN6 was found positively regulating TCR signaling in T cell and regulated by CAMK, calcium and calmodulin regulated kinases and CMGC kinases [197] however the role of CAMKs in neutrophil in regulation of other phosphatses like PTPN6 needs further investigation. Therefore exploring the role of Ptpn6/Shp-1 in neutrophil after IR can open new windows.

The only phosphatse found with phospho upregulation in IR vs IPC shown in table-3 was Phosphatidylinositol 3,4,5-trisphosphate 5-phosphatase 1, Inpp5d/Ship, (P97573). It was found in cluster 3 with 4 regulated phosphorylation sites in the catalytic inositol polyphosphate 5-phosphatase (INPP5c) domain of SH2 domain, putative catalytic site, putative active site, putative Mg binding site, and putative PI/IP binding site. SHIP1 (Inpp5d) SHIP converts phosphatidylinositol 3, 4, 5 triphosphate to phosphatidyl 3, 4 biphosphate. Also it is responsible for the majority of phosphatidylinositol 5′-phosphatase activity in neutrophils that are important for efficient polarization and directed migration of neutrophils. However it might get activated during neutrophil spontaneous death, leading to down-regulation of Akt too[198,199]. SHIP1 has been established as a key negative regulator of the immune system. SHIP1 is known to negatively regulate various cellular processes, such as phagocytosis, cell migration, degranulation, cell survival, proliferation, differentiation, and sensitivity to chemokines [200,201]. The signaling downstream PI3K, following GPCR stimulation, plays important role in infection and inflammation whereas SHIP1 negativly regulate PtdIns(3,4,5)P3 formation, preventing the formation of top-down PtdIns(3,4,5)P3 polarity and facilitating normal cell attachment and detachment during chemotaxis [202]. The downregulated expression in cluster 5 but up regulataed phosphorylation in catalytic domain of SHIP in cluster 3 might negatively regulate the neutrophil-dependent inflammatory processes, such as found in acute lung injury [203] leading to spontaneous death, normal adhesion\chemotaxix followed by directed migration after IPC Therefore activation of SHIP can be important step in protection found associated

with IPC against IR injury. The GPS predicted TLK for this phosphosite. Tousled-like kinases (TLKs) constitute a family of serine/threonine kinases conserved in plants and animals that act in cell cycle progression through the regulation of chromatin dynamics [47] however its interaction and regulation for phosphatidylinositol 3,4,5-trisphosphate 5-phosphatase 1 is not clear yet.

As the substrate found in the our data set for the Rps6 regulated by Rps6ka2 in cluster 3 as shown in the fig-14A The found substrate were named as Poly (rC)-binding protein 1 Pcbp1/ P60335, Rps3/ P62908 (40S ribosomal protein S3), Eif4b/Q8BGD9 (Eukaryotic translation initiation factor 4B) and Pdcd4/Q61823 (Programmed cell death protein 4). Generally Rps6 play an important role in controlling cell growth and proliferation through the selective translation of particular classes of mRNA. But here it seems to affect binding proteins in neutrophil as nucleic acid binding protein, DNA repairing protein, mRNA and ribosome binding protein, and translation inhibiting protein respectively. Ribosomal protein (rp) S6 is a component of the 40S ribosomal subunit that becomes phosphorylated at serine residues but the exact molecular mechanisms regulating its phosphorylation and the function of phosphorylated rpS6 is poorly understood in neutrophils. RSK has been known to interact mTOR-independent pathway linking the Ras/ERK signaling cascade to the translational machinery in hela cells [203].

Similarly another Kinase NDR1/Q91VJ4/ Serine/threonine-protein kinase 38 was found to interact with substrate found in data set Supt16h/Q920B9/ FACT complex subunit SPT16 as shown in fig-14B. However the found four substrates for Supt16h/Q920B9 also highlighted in figure were found to be involved in binding of nucleosome/ Transcription initiation complex specifically with RNA and DNA binding proteins [178]. Therefore, Translation and transcription machinery were found to be regulated by these both the kinases.

We have also analyzed the effects phosphopeptides significantly regulated in any two conditions (4 conditions total) in cluster 3 and 5 on the regulated pathways in neutrophils. The result for pathways is shown in table 9. The most highly regulated pathway found was spliceosome with 4 proteins (u2af2, srsf2 (SR family), sf3b1 and

usp39) and p-value of 0.0001. Other important signaling pathways with regulated phosphoproteins were chemokine signaling pathway, Fc-gamma R mediated phagocytosis and focal adhesion with descending p-values and 4, 3 and 3 proteins respectively. Alternative splicing (AS) is an ubiquitous mechanism for gene expression regulation resulting into variable mRNAs from a given gene due to different arrangements of exons, introns, or portions. In the past much focus was given to post-transcriptional mechanisms of gene regulation as important regulators of immune cell function, particularly, alternative pre-mRNA splicing (2). In humans, approximately 200 spliceosomal and splicing-associated proteins regulate alternative splicing (3). AS can result into down-regulation of gene expression by creating unstable or nonfunctional proteins and mRNA isoforms, altering cytokine signaling (interleukins and their receptors) and modulating protein function (4). Alternative pre-mRNA splicing can also regulate protein expression in a cell-specific or tissue-specific manner in response to precise environmental or developmental cues [179]. However, the knowledge about the gene expression regulation by spliceosome in neutrophils is incomplete. Some information about changes in protein expression of spliceosome in T-cell after activation is available (5). The appropriate effector response in an immune cell depends on the regulation and ability of the spliceosome. It is an enzymatic complex de novo built on pre-mRNA transcripts through sequential interactions between the substrate and subunits of the spliceosome. The major subunits of the spliceosome are five snRNPs, each containing a single non-coding RNA (snRNA) and (100-300) multiple proteins (6). The SR (serine/arginine) proteins regulate AS in spliceosome because of the presence of RNA binding domains (RBDs) that interacts with intronic and exonic splicing enhancers (ISEs and ESEs, respectively) present in transcripts (7). However, in healthy cells posttranslational modifications as the methylation, acetylation, or phosphorylation of SR proteins alters their ability to bind ISEs and ESEs. SR proteins can be phosphorylated by topoisomerase I, and members of the SRPK (SR protein kinase) and CLK (Cdc2-like kinase) families. Amiloride, an epithelial Na+ channel blocker has decreased SRSF1 phosphorylation (8), and chlorhexidine, has inhibited the activity of CLK family members (9).

Some of the proteins with phosphorylated peptides regulation found here were u2af2, srsf2 (SR family), sf3b1 and usp39. Mutation in these proteins was found associated with myeloid malignancy (u2af2) (10), clinical monoclonal B-cell lymphocytosis (cMBL) (Sf3b1) (11), prostate cancer (USP39) (12). Whereas SRSF2 contains N-terminal RRM type RNA binding motifs and a C-terminal domain rich in Arg-Ser dipeptides. It was found in regulation of CD45 (exon 5) in stimulated T cells. Interestingly, along with SRSF2 several SR proteins were also altered (both increased and decreased) (13). The phosphorylation of these proteins can be an important event in the regulation of alternate splicing of mRNA leading to change in neutrophil phenotype. Neutrophils have been linked to enhanced tissue damage in various injury models, including IR in the myocardium, liver, and intestine, where elevated expression of various chemoattractant genes (Cxcl2 and Cxcl1) by MyD88 signaling in intestinal EC resulted into neutrophil recruitment (14). Neutrophils in the blood sense the chemoattractant gradient and traverse the vascular endothelium to reach the intestinal epithelium within minutes and upon reaching the inflammatory site, neutrophils selectively release monocyte chemoattractants, such as CAP18, cathepsin G, and azurocidin (15). Neutrophils also produce matrix metalloproteases (MMPs) that can cleavage chemokine precursors. For example: MMP-8 produced by PMN and macrophages cleaves and activate CXCL-5 and CXCL-8 (16, 17). The second most regulated signaling pathway after IR and IPC was chemokine signaling pathway with a p-value of 0.0004 and contained 4 regulated phosphoproteins in cluster 3 and 5. A Vav family member, dock2, has dominant role after chemokine depend activation in F-actin polymerization at the leading edge of cell migration (18), also affecting chemotaxis, superoxide production, and extracellular trap formation (19). Another protein of chemokine-regulated pathway was paxillin that was found tyrosine phosphorylated in adhesion, due to a domain interacting with the C-terminus of focal adhesion kinase FAK (20). The neutrophil activation as a result of tyrosine phosphorylation in the Fgr $^{204}$ domain was already discussed in the kinase section leading to respiratory burst and F-actin polymerization (21). Similarly, in 2011, the E-selectin dependent slow rolling and leukocyte recruitment was found associated with rasgrp2 (22). Our results confirm the involvement of phosphorylation events in Dock2, Fgr, paxilllin and rasgrp2 in

neutrophil activation that require further deep understanding of the underlying processes involved.

The interaction of Fc receptor with Ig ligands triggers phagocytosis, a process called antibody-dependent cell-mediated cytotoxicity (ADCC), that leads to the release of proinflammatory mediators, and production of cytokines (23). The regulated phosphorylated proteins in both clusters that belong to the Fc-gamma R mediated phagocytosis were dock2, Innp5d and marcks. The dock2 already discussed above was shown associated with F-actin polymerization (18) and Inpp5d was already discussed in the phosphatase section of this work that was found with phospho upregulation in IR vs IPC shown in table 3. It has a clear role in the neutrophil migration and motility (24). MARCKS (myristoylated alanine-rich C kinase substrate), a PKC target that cross-links actin filaments, is involved in macrophage phagocytosis, as this process was prevented in marcks deficient mice (25).

The proteins affecting the focal adhesion are also very important in PMNs. Intravital microscopic studies of tissues following IR showed an acute inflammatory response due to increased protein efflux and PMNs adhesion in postcapillary venules (26). It was shown that after IR of the mouse intestine, both P- and E-selectins were overexpressed on neutrophils and ECs respectively. Blocking of P-selectins has reduced PMN rolling and adhesion so attenuating the injury (27). In severely injured patients, primed neutrophils characterized by the formation of focal adhesion-like structures participate in regulation of neutrophil function. A large number of adhesion-associated components including proteins linked to actin (e.g., talin, vinculin, α actinin, zyxin) among others (28). Hence it is clear that regulation in adhesion and migration related phosphoproteins are a major event occurring within PMNs after IR and IPC.

# Conclusions

# 6 CONCLUSIONS

The hematological results showed that IPC before intestinal IR has provoked significant alterations in hematimetric parameters like a decrease in granulocytes count and in the plateletcrit and an increase in the lymphocytes count and in the mean platelet volume was most pronunced.

The comparative high throughput proteomic approach revealed the changes at regulation level in the rat neutrophil proteome at the early stages after surgical trauma. The enzyme prediction and functional pathways analysis of regulated proteins upon trauma confirm that surgical trauma results in higher expression of mRNA processing and protein synthesis increased life span and decreased neutrophil recruitment, directional motility and immune response. These protein regulations suggest that neutrophils in ST have lower activity and this causes higher susceptibility of the trauma patients to infection and bystander tissues damage, resulting in multiple organs dys functioning.

The large set of proteins was found diferentially regulated through most comprehensive proteomic analysis revealing the effect of ischemic preconditioning on the proteome of neutrophils activated by ischemia/reperfusion The neutrophils showed disruption in the cytoskeletal machinery leading to altered adhesion, directional migration, and phagocytosis after IR. This can further cause multiple tissue infiltration of these neutrophils in any organ leading to immunodeficiency with higher infection rate, acute lung injury (ALI) and multiple organ failure (MOF) after IR. However, the prevention of such regulation by IPC could improve neutrophil function. Similarly, the activation of protein biosynthesis in PMNs under oxidative stress was found upregulated by preconditioning resulted in decrease in protein synthesis by affecting the ribosome, spliceosome, RNA transport, protein processing in endoplasmic reticulum, proteasome and RNA transport. Enzymatic activity prediction suggested the importance of some antioxidant enzymes like peroxiredoxin-6, glutathione peroxidase, methionine sulfoxide reductase, superoxide dismutase, some non-specific serine/threonine protein tyrosine kinases, dynamin GTPase, protein disulphide isomerase, peptidylprolyl isomerase, and argininosuccinate synthase that could be key players modulating

changes in PMNs after IPC. It will be very useful to check the functional role of these proteins through further experimental and clinical tests that can help to find a way to reduce the injury caused by neutrophils after IR and further elucidate the effect of IPC on neutrophil biology.

Through phospho proteomics analysis of rat neutrophil after IR and IPC, we have uncovered many phosphorylation events occurring in domains and motifs of some important kinases and phosphatases mostly regulating migration and apoptosis in neutrophils. Our data confirmed the involvement of some already studied kinases in neutrophil biology along with some new players being identified for the first time here. The investigation of the specific role of these kinases along with their regulatory pathways can help to mimic the tissue injury caused by neutrophils after IR. Similarly, the changes in neutrophil behavior observed after IPC can be due to changes in expression or phosphorylation events in PKCδ, NDR1\stk 38 and INPP5c\SHIP. The Future exploration of their role can help to understand the change in neutrophil behavior after IPC. The most important predicted kinases regulating other kinases in neutrophils from IR and IPC belong to CAMK, CMGC families. The understanding of interaction between these and use of inhibitors can also be helpful.

# References

# 7 REFERENCES

1. Hietbrink F, Koenderman L, Althuizen M, Leenen LP. Modulation of the innate immune response after trauma visualised by a change in functional PMN phenotype. Injury 2009;40:851-5.

2. Hollmann MW, Gross A, Jelacin N, Durieux ME. Local anesthetic effects on priming and activation of human neutrophils. Anesthesiology 2001;95:113-22.

3. Brown GE, Silver GM, Reiff J, Allen RC, Fink MP. Polymorphonuclear neutrophil chemiluminescence in whole blood from blunt trauma patients with multiple injuries. The Journal of trauma 1999;46:297-305.

4. Teles LM, Aquino EN, Neves AC, et al. Comparison of the neutrophil proteome in trauma patients and normal controls. Protein and peptide letters 2012;19:663-72.

5. Plytycz B, Seljelid R. Stress and immunity: minireview. Folia biologica 2002;50:181-9.

6. Savitha D, Rao KR, Girish SP. Effect of surgical stress on neutrophil function. Indian journal of physiology and pharmacology 2008;52:302-6.

7. Power CP, Wang JH, Manning B, et al. Bacterial lipoprotein delays apoptosis in human neutrophils through inhibition of caspase-3 activity: regulatory roles for CD14 and TLR-2. Journal of immunology (Baltimore, Md : 1950) 2004;173:5229-37.

8. Yamamoto S, Tanabe M, Wakabayashi G, Shimazu M, Matsumoto K, Kitajima M. The role of tumor necrosis factor-alpha and interleukin-1beta in ischemia-reperfusion injury of the rat small intestine. The Journal of surgical research 2001;99:134-41.

9. Jassem W, Fuggle SV, Rela M, Koo DD, Heaton ND. The role of mitochondria in ischemia/reperfusion injury. Transplantation 2002;73:493-9.

10. Lefer AM, Lefer DJ. The role of nitric oxide and cell adhesion molecules on the microcirculation in ischaemia-reperfusion. Cardiovascular research 1996;32:743-51.

11. Guneli E, Cavdar Z, Islekel H, et al. Erythropoietin protects the intestine against ischemia/ reperfusion injury in rats. Molecular medicine (Cambridge, Mass) 2007;13:509-17.

12. Mojzis J, Hviscova K, Germanova D, Bukovicova D, Mirossay L. Protective effect of quercetin on ischemia/reperfusion-induced gastric mucosal injury in rats. Physiological research / Academia Scientiarum Bohemoslovaca 2001;50:501-6.

13. Bradbury AW, Brittenden J, McBride K, Ruckley CV. Mesenteric ischaemia: a multidisciplinary approach. The British journal of surgery 1995;82:1446-59.

14. Heys SD, Brittenden J, Crofts TJ. Acute mesenteric ischaemia: the continuing difficulty in early diagnosis. Postgraduate medical journal 1993;69:48-51.

15. Souza DG, Cara DC, Cassali GD, et al. Effects of the PAF receptor antagonist UK74505 on local and remote reperfusion injuries following ischaemia of the superior mesenteric artery in the rat. British journal of pharmacology 2000;131:1800-8.

16. Ceppa EP, Fuh KC, Bulkley GB. Mesenteric hemodynamic response to circulatory shock. Current opinion in critical care 2003;9:127-32.

17. Xiao F, Eppihimer MJ, Young JA, Nguyen K, Carden DL. Lung neutrophil retention and injury after intestinal ischemia/reperfusion. Microcirculation (New York, NY : 1994) 1997;4:359-67.

18. Wang Q, Meyer TA, Boyce ST, et al. Endotoxemia in mice stimulates production of complement C3 and serum amyloid A in mucosa of small intestine. The American journal of physiology 1998;275:R1584-92.

19. Zamir O, Hasselgren PO, Higashiguchi T, Frederick JA, Fischer JE. Effect of sepsis or cytokine administration on release of gut peptides. American journal of surgery 1992;163:181-4; discussion 4-5.

20. Meyer TA, Wang J, Tiao GM, Ogle CK, Fischer JE, Hasselgren PO. Sepsis and endotoxemia stimulate intestinal interleukin-6 production. Surgery 1995;118:336-42.

21. Granger DN, Korthuis RJ. Physiologic mechanisms of postischemic tissue injury. Annual review of physiology 1995;57:311-32.

22. Stark ME, Szurszewski JH. Role of nitric oxide in gastrointestinal and hepatic function and disease. Gastroenterology 1992;103:1928-49.

23. Mangino MJ, Anderson CB, Murphy MK, Brunt E, Turk J. Mucosal arachidonate metabolism and intestinal ischemia-reperfusion injury. The American journal of physiology 1989;257:G299-307.

24. Panes J, Granger DN. Leukocyte-endothelial cell interactions: molecular mechanisms and implications in gastrointestinal disease. Gastroenterology 1998;114:1066-90.

25. Zou L, Attuwaybi B, Kone BC. Effects of NF-kappa B inhibition on mesenteric ischemia-reperfusion injury. American journal of physiology Gastrointestinal and liver physiology 2003;284:G713-21.

26. Massberg S, Gonzalez AP, Leiderer R, Menger MD, Messmer K. In vivo assessment of the influence of cold preservation time on microvascular reperfusion injury after experimental small bowel transplantation. The British journal of surgery 1998;85:127-33.

27. Sisley AC, Desai T, Harig JM, Gewertz BL. Neutrophil depletion attenuates human intestinal reperfusion injury. The Journal of surgical research 1994;57:192-6.

28. Riaz AA, Wan MX, Schaefer T, et al. Fundamental and distinct roles of P-selectin and LFA-1 in ischemia/reperfusion-induced leukocyte-endothelium interactions in the mouse colon. Annals of surgery 2002;236:777-84; discussion 84.

29. Carden DL, Smith JK, Korthuis RJ. Neutrophil-mediated microvascular dysfunction in postischemic canine skeletal muscle. Role of granulocyte adherence. Circulation research 1990;66:1436-44.

30. Weiss SJ. Tissue destruction by neutrophils. The New England journal of medicine 1989;320:365-76.

31. Bagge U, Amundson B, Lauritzen C. White blood cell deformability and plugging of skeletal muscle capillaries in hemorrhagic shock. Acta physiologica Scandinavica 1980;108:159-63.

32. Willerson JT. Pharmacologic approaches to reperfusion injury. Advances in pharmacology (San Diego, Calif) 1997;39:291-312.

33. Nalini S, Mathan MM, Balasubramanian KA. Oxygen free radical induced damage during intestinal ischemia/reperfusion in normal and xanthine oxidase deficient rats. Molecular and cellular biochemistry 1993;124:59-66.

34. Murry CE, Jennings RB, Reimer KA. Preconditioning with ischemia: a delay of lethal cell injury in ischemic myocardium. Circulation 1986;74:1124-36.

35. Downey GP, Worthen GS, Henson PM, Hyde DM. Neutrophil sequestration and migration in localized pulmonary inflammation. Capillary localization and migration across the interalveolar septum. The American review of respiratory disease 1993;147:168-76.

36. Yellon DM, Hausenloy DJ. Myocardial reperfusion injury. The New England journal of medicine 2007;357:1121-35.

37. Pang CY, Yang RZ, Zhong A, Xu N, Boyd B, Forrest CR. Acute ischaemic preconditioning protects against skeletal muscle infarction in the pig. Cardiovascular research 1995;29:782-8.

38. Heurteaux C, Lauritzen I, Widmann C, Lazdunski M. Essential role of adenosine, adenosine A1 receptors, and ATP-sensitive K+ channels in cerebral ischemic preconditioning. Proceedings of the National Academy of Sciences of the United States of America 1995;92:4666-70.

39. Matsuyama K, Chiba Y, Ihaya A, Kimura T, Tanigawa N, Muraoka R. Effect of spinal cord preconditioning on paraplegia during cross-clamping of the thoracic aorta. The Annals of thoracic surgery 1997;63:1315-20.

40. Turman MA, Bates CM. Susceptibility of human proximal tubular cells to hypoxia: effect of hypoxic preconditioning and comparison to glomerular cells. Renal failure 1997;19:47-60.

41. Hotter G, Closa D, Prados M, et al. Intestinal preconditioning is mediated by a transient increase in nitric oxide. Biochemical and biophysical research communications 1996;222:27-32.

42. Du ZY, Hicks M, Winlaw D, Spratt P, Macdonald P. Ischemic preconditioning enhances donor lung preservation in the rat. The Journal of heart and lung transplantation : the official publication of the International Society for Heart Transplantation 1996;15:1258-67.

43. Li Y, Roth S, Laser M, Ma JX, Crosson CE. Retinal preconditioning and the induction of heat-shock protein 27. Investigative ophthalmology & visual science 2003;44:1299-304.

44. Lloris-Carsi JM, Cejalvo D, Toledo-Pereyra LH, Calvo MA, Suzuki S. Preconditioning: effect upon lesion modulation in warm liver ischemia. Transplantation proceedings 1993;25:3303-4.

45. Jenkins DP, Pugsley WB, Alkhulaifi AM, Kemp M, Hooper J, Yellon DM. Ischaemic preconditioning reduces troponin T release in patients undergoing coronary artery bypass surgery. Heart (British Cardiac Society) 1997;77:314-8.

46. Clavien PA, Selzner M, Rudiger HA, et al. A prospective randomized study in 100 consecutive patients undergoing major liver resection with versus without ischemic preconditioning. Annals of surgery 2003;238:843-50; discussion 51-2.

47. Aksoyek S, Cinel I, Avlan D, et al. Intestinal ischemic preconditioning protects the intestine and reduces bacterial translocation. Shock (Augusta, Ga) 2002;18:476-80.

48. Bolli R. The late phase of preconditioning. Circulation research 2000;87:972-83.

49. Cohen P. The regulation of protein function by multisite phosphorylation--a 25 year update. Trends in biochemical sciences 2000;25:596-601.

50. Kharbanda RK, Peters M, Walton B, et al. Ischemic preconditioning prevents endothelial injury and systemic neutrophil activation during ischemia-reperfusion in humans in vivo. Circulation 2001;103:1624-30.

51. Chouker A, Martignoni A, Schauer R, et al. Beneficial effects of ischemic preconditioning in patients undergoing hepatectomy: the role of neutrophils. Archives of surgery (Chicago, Ill : 1960) 2005;140:129-36.

52. Nayak AR, Kashyap RS, Kabra D, Purohit HJ, Taori GM, Daginawala HF. Time course of inflammatory cytokines in acute ischemic stroke patients and their relation to

inter-alfa trypsin inhibitor heavy chain 4 and outcome. Annals of Indian Academy of Neurology 2012;15:181-5.

53. Erling N, de Souza Montero EF, Sannomiya P, Poli-de-Figueiredo LF. Local and remote ischemic preconditioning protect against intestinal ischemic/reperfusion injury after supraceliac aortic clamping. Clinics 2013;68:1548-54.

54. Taha MO, Miranda-Ferreira R, Chang AC, et al. Effect of ischemic preconditioning on injuries caused by ischemia and reperfusion in rat intestine. Transplantation proceedings 2012;44:2304-8.

55. Fabian TC, Croce MA, Stewart RM, Dockter ME, Proctor KG. Neutrophil CD18 expression and blockade after traumatic shock and endotoxin challenge. Annals of surgery 1994;220:552-61; discussion 61-3.

56. Becker M, Moritz A, Giger U. Comparative clinical study of canine and feline total blood cell count results with seven in-clinic and two commercial laboratory hematology analyzers. Veterinary clinical pathology / American Society for Veterinary Clinical Pathology 2008;37:373-84.

57. Corrigan R. Fundamentals of Veterinary Clinical Pathology, 2nd edition: Can Vet J. 2011 Feb;52(2):161.

58. Tahir M, Arshid S, Heimbecker AM, et al. Evaluation of the effects of ischemic preconditioning on the hematological parameters of rats subjected to intestinal ischemia and reperfusion. Clinics 2015;70:61-8.

59. Fessler MB, Malcolm KC, Duncan MW, Worthen GS. Lipopolysaccharide stimulation of the human neutrophil: an analysis of changes in gene transcription and protein expression by oligonucleotide microarrays and proteomics. Chest 2002;121:75s-6s.

60. Piubelli C, Galvani M, Hamdan M, Domenici E, Righetti PG. Proteome analysis of rat polymorphonuclear leukocytes: a two-dimensional electrophoresis/mass spectrometry approach. Electrophoresis 2002;23:298-310.

61. Lippolis JD, Reinhardt TA. Proteomic survey of bovine neutrophils. Veterinary immunology and immunopathology 2005;103:53-65.

62. Lominadze G, Powell DW, Luerman GC, Link AJ, Ward RA, McLeish KR. Proteomic analysis of human neutrophil granules. Molecular & cellular proteomics : MCP 2005;4:1503-21.

63. Feuk-Lagerstedt E, Movitz C, Pellme S, Dahlgren C, Karlsson A. Lipid raft proteome of the human neutrophil azurophil granule. Proteomics 2007;7:194-205.

64. Nebl T, Pestonjamasp KN, Leszyk JD, Crowley JL, Oh SW, Luna EJ. Proteomic analysis of a detergent-resistant membrane skeleton from neutrophil plasma membranes. The Journal of biological chemistry 2002;277:43399-409.

65. Fessler MB, Malcolm KC, Duncan MW, Worthen GS. A genomic and proteomic analysis of activation of the human neutrophil by lipopolysaccharide and its mediation by p38 mitogen-activated protein kinase. The Journal of biological chemistry 2002;277:31291-302.

66. Greenlee KJ, Corry DB, Engler DA, et al. Proteomic identification of in vivo substrates for matrix metalloproteinases 2 and 9 reveals a mechanism for resolution of inflammation. Journal of immunology (Baltimore, Md : 1950) 2006;177:7312-21.

67. Liu KX, Li YS, Wang ZX, Li C, Liu JX, Huang WQ. [Proteomics study of intestinal mucosa after ischemic preconditioning against intestinal ischemic reperfusion injury in rats]. Zhonghua wei chang wai ke za zhi = Chinese journal of gastrointestinal surgery 2009;12:598-602.

68. Liu KX, Li C, Li YS, et al. Proteomic analysis of intestinal ischemia/reperfusion injury and ischemic preconditioning in rats reveals the protective role of aldose reductase. Proteomics 2010;10:4463-75.

69. Manning G, Plowman GD, Hunter T, Sudarsanam S. Evolution of protein kinase signaling from yeast to man. Trends in biochemical sciences 2002;27:514-20.

70. Hunter T, Sefton BM. Transforming gene product of Rous sarcoma virus phosphorylates tyrosine. Proceedings of the National Academy of Sciences of the United States of America 1980;77:1311-5.

71. Zhang ZY. Protein tyrosine phosphatases: structure and function, substrate specificity, and inhibitor development. Annual review of pharmacology and toxicology 2002;42:209-34.

72. Cohen P. The role of protein phosphorylation in human health and disease. The Sir Hans Krebs Medal Lecture. European journal of biochemistry / FEBS 2001;268:5001-10.

73. Cutillas PR, Jorgensen C. Biological signalling activity measurements using mass spectrometry. The Biochemical journal 2011;434:189-99.

74. Hurley JH, Dean AM, Thorsness PE, Koshland DE, Jr., Stroud RM. Regulation of isocitrate dehydrogenase by phosphorylation involves no long-range conformational change in the free enzyme. The Journal of biological chemistry 1990;265:3599-602.

75. Miller ML, Jensen LJ, Diella F, et al. Linear motif atlas for phosphorylation-dependent signaling. Science signaling 2008;1:ra2.

76. Bollen M, Peti W, Ragusa MJ, Beullens M. The extended PP1 toolkit: designed to create specificity. Trends in biochemical sciences 2010;35:450-8.

77. Garaud M, Pei D. Substrate profiling of protein tyrosine phosphatase PTP1B by screening a combinatorial peptide library. Journal of the American Chemical Society 2007;129:5366-7.

78. Chou MF, Schwartz D. Biological sequence motif discovery using motif-x. Current protocols in bioinformatics / editoral board, Andreas D Baxevanis [et al] 2011;Chapter 13:Unit 13.5-24.

79. Schulze WX, Usadel B. Quantitation in mass-spectrometry-based proteomics. Annual review of plant biology 2010;61:491-516.

80. Whiteaker JR. The increasing role of mass spectrometry in quantitative clinical proteomics. Clinical chemistry 2010;56:1373-4.

81. Bantscheff M, Schirle M, Sweetman G, Rick J, Kuster B. Quantitative mass spectrometry in proteomics: a critical review. Analytical and bioanalytical chemistry 2007;389:1017-31.

82. Ong SE, Blagoev B, Kratchmarova I, et al. Stable isotope labeling by amino acids in cell culture, SILAC, as a simple and accurate approach to expression proteomics. Molecular & cellular proteomics : MCP 2002;1:376-86.

83. Gygi SP, Rist B, Gerber SA, Turecek F, Gelb MH, Aebersold R. Quantitative analysis of complex protein mixtures using isotope-coded affinity tags. Nature biotechnology 1999;17:994-9.

84. Ross PL, Huang YN, Marchese JN, et al. Multiplexed protein quantitation in Saccharomyces cerevisiae using amine-reactive isobaric tagging reagents. Molecular & cellular proteomics : MCP 2004;3:1154-69.

85. Choe L, D'Ascenzo M, Relkin NR, et al. 8-plex quantitation of changes in cerebrospinal fluid protein expression in subjects undergoing intravenous immunoglobulin treatment for Alzheimer's disease. Proteomics 2007;7:3651-60.

86. Washburn MP, Wolters D, Yates JR, 3rd. Large-scale analysis of the yeast proteome by multidimensional protein identification technology. Nature biotechnology 2001;19:242-7.

87. Morris HRFaGE. Quantitative Proteomics Using iTRAQ Labeling and Mass Spectrometry. Integrative Proteomics 2012;Dr. Hon-Chiu Leung (Ed.).

88. Thingholm TE, Palmisano G, Kjeldsen F, Larsen MR. Undesirable charge-enhancement of isobaric tagged phosphopeptides leads to reduced identification efficiency. Journal of proteome research 2010;9:4045-52.

89. Beausoleil SA, Jedrychowski M, Schwartz D, et al. Large-scale characterization of HeLa cell nuclear phosphoproteins. Proceedings of the National Academy of Sciences of the United States of America 2004;101:12130-5.

90. Pinkse MW, Uitto PM, Hilhorst MJ, Ooms B, Heck AJ. Selective isolation at the femtomole level of phosphopeptides from proteolytic digests using 2D-NanoLC-ESI-MS/MS and titanium oxide precolumns. Analytical chemistry 2004;76:3935-43.

91. Negroni L, Claverol S, Rosenbaum J, Chevet E, Bonneu M, Schmitter JM. Comparison of IMAC and MOAC for phosphopeptide enrichment by column chromatography. Journal of chromatography B, Analytical technologies in the biomedical and life sciences 2012;891-892:109-12.

92. Sun S, Ma H, Han G, Wu R, Zou H, Liu Y. Efficient enrichment and identification of phosphopeptides by cerium oxide using on-plate matrix-assisted laser desorption/ionization time-of-flight mass spectrometric analysis. Rapid communications in mass spectrometry : RCM 2011;25:1862-8.

93. Wang WH, Bruening ML. Phosphopeptide enrichment on functionalized polymer microspots for MALDI-MS analysis. The Analyst 2009;134:512-8.

94. Li QR, Ning ZB, Tang JS, Nie S, Zeng R. Effect of peptide-to-TiO2 beads ratio on phosphopeptide enrichment selectivity. Journal of proteome research 2009;8:5375-81.

95. !!! INVALID CITATION !!!

96. Jensen SS, Larsen MR. Evaluation of the impact of some experimental procedures on different phosphopeptide enrichment techniques. Rapid communications in mass spectrometry : RCM 2007;21:3635-45.

97. Enzymes. British journal of pharmacology 2011;164:S279-S324.

98. Wang ZG, Lv N, Bi WZ, Zhang JL, Ni JZ. Development of the affinity materials for phosphorylated proteins/peptides enrichment in phosphoproteomics analysis. ACS applied materials & interfaces 2015;7:8377-92.

99. Thingholm TE, Jensen ON, Robinson PJ, Larsen MR. SIMAC (sequential elution from IMAC), a phosphoproteomics strategy for the rapid separation of monophosphorylated from multiply phosphorylated peptides. Molecular & cellular proteomics : MCP 2008;7:661-71.

100. Rampitsch C, Subramaniam R, Djuric-Ciganovic S, Bykova NV. The phosphoproteome of Fusarium graminearum at the onset of nitrogen starvation. Proteomics 2010;10:124-40.

101. Fila J, Honys D. Enrichment techniques employed in phosphoproteomics. Amino acids 2012;43:1025-47.

102. Gilar M, Olivova P, Daly AE, Gebler JC. Orthogonality of separation in two-dimensional liquid chromatography. Analytical chemistry 2005;77:6426-34.

103. McNulty DE, Annan RS. Hydrophilic interaction chromatography reduces the complexity of the phosphoproteome and improves global phosphopeptide isolation and detection. Molecular & cellular proteomics : MCP 2008;7:971-80.

104. McLeish KR, Merchant ML, Klein JB, Ward RA. Technical note: proteomic approaches to fundamental questions about neutrophil biology. Journal of Leukocyte Biology 2013;94:683-92.

105. Powell DW, Rane MJ, Joughin BA, et al. Proteomic identification of 14-3-3zeta as a mitogen-activated protein kinase-activated protein kinase 2 substrate: role in dimer formation and ligand binding. Molecular and cellular biology 2003;23:5376-87.

106. Singh S, Powell DW, Rane MJ, et al. Identification of the p16-Arc subunit of the Arp 2/3 complex as a substrate of MAPK-activated protein kinase 2 by proteomic analysis. The Journal of biological chemistry 2003;278:36410-7.

107. Lominadze G, Rane MJ, Merchant M, Cai J, Ward RA, McLeish KR. Myeloid-related protein-14 is a p38 MAPK substrate in human neutrophils. Journal of immunology (Baltimore, Md : 1950) 2005;174:7257-67.

108. Kettritz R, Xu YX, Faass B, et al. TNF-alpha-mediated neutrophil apoptosis involves Ly-GDI, a Rho GTPase regulator. Journal of Leukocyte Biology 2000;68:277-83.

109. Pacquelet S, Johnson JL, Ellis BA, et al. Cross-talk between IRAK-4 and the NADPH oxidase. The Biochemical journal 2007;403:451-61.

110. Boldt K, Rist W, Weiss SM, Weith A, Lenter MC. FPRL-1 induces modifications of migration-associated proteins in human neutrophils. Proteomics 2006;6:4790-9.

111. Dang PM, Stensballe A, Boussetta T, et al. A specific p47phox -serine phosphorylated by convergent MAPKs mediates neutrophil NADPH oxidase priming at inflammatory sites. The Journal of clinical investigation 2006;116:2033-43.

112. Fukuda M. Versatile role of Rab27 in membrane trafficking: focus on the Rab27 effector families. Journal of biochemistry 2005;137:9-16.

113. Ortega-Perez I, Cano E, Were F, Villar M, Vazquez J, Redondo JM. c-Jun N-terminal kinase (JNK) positively regulates NFATc2 transactivation through phosphorylation within the N-terminal regulatory domain. The Journal of biological chemistry 2005;280:20867-78.

114. Muschter S, Berthold T, Bhardwaj G, et al. Mass spectrometric phosphoproteome analysis of small-sized samples of human neutrophils. Clinica chimica acta; international journal of clinical chemistry 2015;451:199-207.

115. Jensen LJ, Jensen TS, de Lichtenberg U, Brunak S, Bork P. Co-evolution of transcriptional and post-translational cell-cycle regulation. Nature 2006;443:594-7.

116. Neduva V, Russell RB. Linear motifs: evolutionary interaction switches. FEBS letters 2005;579:3342-5.

117. Richardson JS. The anatomy and taxonomy of protein structure. Advances in protein chemistry 1981;34:167-339.

118. Murzin AG, Brenner SE, Hubbard T, Chothia C. SCOP: a structural classification of proteins database for the investigation of sequences and structures. Journal of molecular biology 1995;247:536-40.

119. Orengo CA, Michie AD, Jones S, Jones DT, Swindells MB, Thornton JM. CATH--a hierarchic classification of protein domain structures. Structure (London, England : 1993) 1997;5:1093-108.

120. Holland TA, Veretnik S, Shindyalov IN, Bourne PE. Partitioning protein structures into domains: why is it so difficult? Journal of molecular biology 2006;361:562-90.

121. Jorgensen C, Linding R. Directional and quantitative phosphorylation networks. Briefings in functional genomics & proteomics 2008;7:17-26.

122. Lim WA, Pawson T. Phosphotyrosine signaling: evolving a new cellular communication system. Cell 2010;142:661-7.

123. Schwartz D, Gygi SP. An iterative statistical approach to the identification of protein phosphorylation motifs from large-scale data sets. Nature biotechnology 2005;23:1391-8.

124. Wendell Lim BM, Tony Pawson. Cell Signaling: principles and mechanisms. science 2014.

125. Van den Steen PE, Proost P, Wuyts A, Van Damme J, Opdenakker G. Neutrophil gelatinase B potentiates interleukin-8 tenfold by aminoterminal processing, whereas it degrades CTAP-III, PF-4, and GRO-alpha and leaves RANTES and MCP-2 intact. Blood 2000;96:2673-81.

126. Tahir M, Arshid S, Heimbecker AMC, et al. Evaluation of the effects of ischemic preconditioning on the hematological parameters of rats subjected to intestinal ischemia and reperfusion. Clinics 2015;70:61-8.

127. Koike K, Moore FA, Moore EE, Poggetti RS, Tuder RM, Banerjee A. Endotoxin after gut ischemia/reperfusion causes irreversible lung injury. The Journal of surgical research 1992;52:656-62.

128. Jacome DT, Abrahao MS, Morello RJ, Martins JL, Medeiros AC, Montero EF. Different intervals of ischemic preconditioning on small bowel ischemia-reperfusion injury in rats. Transplantation proceedings 2009;41:827-9.

129. Wang SF, Li GW. Early protective effect of ischemic preconditioning on small intestinal graft in rats. World journal of gastroenterology : WJG 2003;9:1866-70.

130. E. M. S R-C, Dept. of Biochemistry FoM, A. E. C. S A, et al. Comparative Study of Four Isolation Procedures to Obtain Rat Neutrophils. Comp Clin Path 2014;11:71-6.

131. Hunter T. Protein kinases and phosphatases: the yin and yang of protein phosphorylation and signaling.

132. Schlessinger J. Cell signaling by receptor tyrosine kinases.

133. Hunter T Fau - Sefton BM, Sefton BM. Transforming gene product of Rous sarcoma virus phosphorylates tyrosine.

134. Caenepeel S, Charydczak G, Sudarsanam S, Hunter T, Manning G. The mouse kinome: discovery and comparative genomics of all mouse protein kinases. Proceedings of the National Academy of Sciences of the United States of America 2004;101:11707-12.

135. Manning G, Whyte Db Fau - Martinez R, Martinez R Fau - Hunter T, Hunter T Fau - Sudarsanam S, Sudarsanam S. The protein kinase complement of the human genome.

136. Zhu H, Klemic JF, Chang S, et al. Analysis of yeast protein kinases using protein chips. Nature genetics 2000;26:283-9.

137. Johnson SA, Hunter T. Kinomics: methods for deciphering the kinome. Nature methods 2005;2:17-25.

138. Lander ES, Linton LM, Birren B, et al. Initial sequencing and analysis of the human genome. Nature 2001;409:860-921.

139. Jurkowska M, Bal J. [Biomedical science in the era of complete sequence of human genome]. Medycyna wieku rozwojowego 2001;5:197-212.

140. Shi Y. Serine/threonine phosphatases: mechanism through structure. Cell 2009;139:468-84.

141. Kobe B, Kampmann T, Forwood JK, Listwan P, Brinkworth RI. Substrate specificity of protein kinases and computational prediction of substrates. Biochimica et biophysica acta 2005;1754:200-9.

142. Tesmer JJ, Tesmer VM, Lodowski DT, Steinhagen H, Huber J. Structure of human G protein-coupled receptor kinase 2 in complex with the kinase inhibitor balanol. Journal of medicinal chemistry 2010;53:1867-70.

143. Arraes SM, Freitas MS, da Silva SV, et al. Impaired neutrophil chemotaxis in sepsis associates with GRK expression and inhibition of actin assembly and tyrosine phosphorylation. Blood 2006;108:2906-13.

144. Penela P, Ribas C, Mayor F, Jr. Mechanisms of regulation of the expression and function of G protein-coupled receptor kinases. Cellular signalling 2003;15:973-81.

145. Elorza A, Penela P, Sarnago S, Mayor F, Jr. MAPK-dependent degradation of G protein-coupled receptor kinase 2. The Journal of biological chemistry 2003;278:29164-73.

146. Lodowski DT, Pitcher JA, Capel WD, Lefkowitz RJ, Tesmer JJ. Keeping G proteins at bay: a complex between G protein-coupled receptor kinase 2 and Gbetagamma. Science 2003;300:1256-62.

147. Madhusudan, Akamine P, Xuong NH, Taylor SS. Crystal structure of a transition state mimic of the catalytic subunit of cAMP-dependent protein kinase. Nature structural biology 2002;9:273-7.

148. Yang J, Cron P, Good VM, Thompson V, Hemmings BA, Barford D. Crystal structure of an activated Akt/protein kinase B ternary complex with GSK3-peptide and AMP-PNP. Nature structural biology 2002;9:940-4.

149. Xu X, Jin T. The Novel Functions of the PLC/PKC/PKD Signaling Axis in G Protein-Coupled Receptor-Mediated Chemotaxis of Neutrophils. Journal of immunology research 2015;2015:817604.

150. Rybin VO, Sabri A, Short J, Braz JC, Molkentin JD, Steinberg SF. Cross-regulation of novel protein kinase C (PKC) isoform function in cardiomyocytes. Role of PKC epsilon in activation loop phosphorylations and PKC delta in hydrophobic motif phosphorylations. The Journal of biological chemistry 2003;278:14555-64.

151. Shizukuda Y, Helisch A, Yokota R, Ware JA. Downregulation of protein kinase cdelta activity enhances endothelial cell adaptation to hypoxia. Circulation 1999;100:1909-16.

152. Soderling TR. The Ca-calmodulin-dependent protein kinase cascade. Trends in biochemical sciences 1999;24:232-6.

153. Zhang X, Guo L, Collage RD, et al. Calcium/calmodulin-dependent protein kinase (CaMK) I $\alpha$ mediates the macrophage inflammatory response to sepsis. Journal of Leukocyte Biology 2011;90:249-61.

154. Selimoglu R BA, Joffre C, Meunier B, Parrini MC et al. RalA GTPase and MAP4K4 Function through NDR1 Activation in Stress Response and Apoptotic Signaling. J Cell Biol Cell Metab 2014;1:1.

155. http://kinase.com/wiki/index.php/Kinase_Group_TKL.

156. Hergovich A, Stegert MR, Schmitz D, Hemmings BA. NDR kinases regulate essential cell processes from yeast to humans. Nature reviews Molecular cell biology 2006;7:253-64.

157. Zhu Y, Stolz DB, Guo F, et al. Signaling via a novel integral plasma membrane pool of a serine/threonine protein kinase PRK1 in mammalian cells. FASEB journal : official publication of the Federation of American Societies for Experimental Biology 2004;18:1722-4.

158. Van Ziffle JA, Lowell CA. Neutrophil-specific deletion of Syk kinase results in reduced host defense to bacterial infection. Blood 2009;114:4871-82.

159. Raeder EM, Mansfield PJ, Hinkovska-Galcheva V, Shayman JA, Boxer LA. Syk activation initiates downstream signaling events during human polymorphonuclear leukocyte phagocytosis. Journal of immunology (Baltimore, Md : 1950) 1999;163:6785-93.

160. Cox D, Chang P, Kurosaki T, Greenberg S. Syk tyrosine kinase is required for immunoreceptor tyrosine activation motif-dependent actin assembly. The Journal of biological chemistry 1996;271:16597-602.

161. Paris LL, Hu J, Galan J, et al. Regulation of Syk by Phosphorylation on Serine in the Linker Insert. The Journal of biological chemistry 2010;285:39844-54.

162. Luhovy AY, Jaberi A Fau - Papillon J, Papillon J Fau - Guillemette J, Guillemette J Fau - Cybulsky AV, Cybulsky AV. Regulation of the Ste20-like kinase, SLK: involvement of activation segment phosphorylation.

163. Cybulsky AV, Takano T, Papillon J, et al. Renal expression and activity of the germinal center kinase SK2. American journal of physiology Renal physiology 2004;286:F16-25.

164. Cybulsky AV, Takano T, Guillemette J, Papillon J, Volpini RA, Di Battista JA. The Ste20-like kinase SLK promotes p53 transactivation and apoptosis. American journal of physiology Renal physiology 2009;297:F971-80.

165. Hao W, Takano T Fau - Guillemette J, Guillemette J Fau - Papillon J, Papillon J Fau - Ren G, Ren G Fau - Cybulsky AV, Cybulsky AV. Induction of apoptosis by the

Ste20-like kinase SLK, a germinal center kinase that activates apoptosis signal-regulating kinase and p38.

166. Hoffmann EK, Lambert IH, Pedersen SF. Physiology of cell volume regulation in vertebrates. Physiological reviews 2009;89:193-277.

167. Lang F, Ritter M, Woll E, et al. Altered cell volume regulation in ras oncogene expressing NIH fibroblasts. Pflugers Archiv : European journal of physiology 1992;420:424-7.

168. Pedersen SF. The Na+/H+ exchanger NHE1 in stress-induced signal transduction: implications for cell proliferation and cell death. Pflugers Archiv : European journal of physiology 2006;452:249-59.

169. Henderson LM, Chappell JB, Jones OT. Internal pH changes associated with the activity of NADPH oxidase of human neutrophils. Further evidence for the presence of an H+ conducting channel. The Biochemical journal 1988;251:563-7.

170. Arshid ST, M. Fontes, B. Montero, E. F. S. Castro, M. S. Sidoli, S. Schwämmle, V. Roepstorff, P.Fontes,W., . Neutrophil proteomic analysis reveals the participation of antioxidant enzymes, motility and ribosomal proteins in the prevention of ischemic effects by preconditioning. Journal of Proteomics 2016 (submitted).

171. Felberg J, Johnson P. Characterization of recombinant CD45 cytoplasmic domain proteins. Evidence for intramolecular and intermolecular interactions. The Journal of biological chemistry 1998;273:17839-45.

172. Streuli M, Krueger NX, Thai T, Tang M, Saito H. Distinct functional roles of the two intracellular phosphatase like domains of the receptor-linked protein tyrosine phosphatases LCA and LAR. The EMBO journal 1990;9:2399-407.

173. Zhu JW, Doan K, Park J, et al. Receptor-like tyrosine phosphatases CD45 and CD148 have distinct functions in chemoattractant-mediated neutrophil migration and response to S. aureus. Immunity 2011;35:757-69.

174. Pei D, Lorenz U, Klingmuller U, Neel BG, Walsh CT. Intramolecular regulation of protein tyrosine phosphatase SH-PTP1: a new function for Src homology 2 domains. Biochemistry 1994;33:15483-93.

175. Ravetch JV, Lanier LL. Immune inhibitory receptors. Science 2000;290:84-9.

176. Yousefi S, Simon HU. SHP-1: a regulator of neutrophil apoptosis. Seminars in immunology 2003;15:195-9.

177. Abu-Dayyeh I, Shio MT, Sato S, Akira S, Cousineau B, Olivier M. Leishmania-induced IRAK-1 inactivation is mediated by SHP-1 interacting with an evolutionarily conserved KTIM motif. PLoS neglected tropical diseases 2008;2:e305.

178. Nishio M, Watanabe K, Sasaki J, et al. Control of cell polarity and motility by the PtdIns(3,4,5)P3 phosphatase SHIP1. Nature cell biology 2007;9:36-44.

179. Webb PR, Wang KQ, Scheel-Toellner D, Pongracz J, Salmon M, Lord JM. Regulation of neutrophil apoptosis: a role for protein kinase C and phosphatidylinositol-3-kinase. Apoptosis : an international journal on programmed cell death 2000;5:451-8.

180. Leung WH, Tarasenko T, Bolland S. Differential roles for the inositol phosphatase SHIP in the regulation of macrophages and lymphocytes. Immunologic research 2009;43:243-51.

181. Mondal S, Subramanian KK, Sakai J, Bajrami B, Luo HR. Phosphoinositide lipid phosphatase SHIP1 and PTEN coordinate to regulate cell migration and adhesion. Molecular Biology of the Cell 2012;23:1219-30.

182. Lam PY, Yoo SK, Green JM, Huttenlocher A. The SH2-domain-containing inositol 5-phosphatase (SHIP) limits the motility of neutrophils and their recruitment to wounds in zebrafish. Journal of cell science 2012;125:4973-8.

183. Luo HR, Mondal S. Molecular control of PtdIns(3,4,5)P3 signaling in neutrophils. EMBO Reports 2015;16:149-63.

184. Strassheim D, Kim JY, Park JS, Mitra S, Abraham E. Involvement of SHIP in TLR2-induced neutrophil activation and acute lung injury. Journal of immunology (Baltimore, Md : 1950) 2005;174:8064-71.

185. Carrera P, Moshkin YM, Gronke S, et al. Tousled-like kinase functions with the chromatin assembly pathway regulating nuclear divisions. Genes & development 2003;17:2578-90.

186. Black DL. Mechanisms of alternative pre-messenger RNA splicing. Annual review of biochemistry 2003;72:291-336.

187. Altintoprak F, Arslan Y, Yalkin O, Uzunoglu Y, Ozkan OV. Mean platelet volume as a potential prognostic marker in patients with acute mesenteric ischemia-retrospective study. World journal of emergency surgery : WJES 2013;8:49.

188. Lindemann S, Klingel B, Fisch A, Meyer J, Darius H. Increased platelet sensitivity toward platelet inhibitors during physical exercise in patients with coronary artery disease. Thrombosis research 1999;93:51-9.

189. Pak S, Kondo T, Nakano Y, et al. Platelet adhesion in the sinusoid caused hepatic injury by neutrophils after hepatic ischemia reperfusion. Platelets 2010;21:282-8.

190. Russell J, Cooper D, Tailor A, Stokes KY, Granger DN. Low venular shear rates promote leukocyte-dependent recruitment of adherent platelets. American journal of physiology Gastrointestinal and liver physiology 2003;284:G123-9.

191. Kubes P, Jutila M, Payne D. Therapeutic potential of inhibiting leukocyte rolling in ischemia/reperfusion. The Journal of clinical investigation 1995;95:2510-9.

192. Hierholzer C, Kalff JC, Audolfsson G, Billiar TR, Tweardy DJ, Bauer AJ. Molecular and functional contractile sequelae of rat intestinal ischemia/reperfusion injury. Transplantation 1999;68:1244-54.

193. Savill JS, Wyllie AH, Henson JE, Walport MJ, Henson PM, Haslett C. Macrophage phagocytosis of aging neutrophils in inflammation. Programmed cell death in the neutrophil leads to its recognition by macrophages. The Journal of clinical investigation 1989;83:865-75.

194. Buttenschoen K, Fathimani K, Buttenschoen DC. Effect of major abdominal surgery on the host immune response to infection. Current opinion in infectious diseases 2010;23:259-67.

195. Lawrence T. The Nuclear Factor NF- $\kappa$ B Pathway in Inflammation. Cold Spring Harbor Perspectives in Biology 2009;1.

196. Dienz O, Rud JG, Eaton SM, et al. Essential role of IL-6 in protection against H1N1 influenza virus by promoting neutrophil survival in the lung. Mucosal immunology 2012;5:258-66.

197. Wei M, Kuukasjarvi P, Laurikka J, et al. Cytokine responses in patients undergoing coronary artery bypass surgery after ischemic preconditioning. Scandinavian cardiovascular journal : SCJ 2001;35:142-6.

198. Camara-Lemarroy CR. Remote ischemic preconditioning as treatment for non-ischemic gastrointestinal disorders: beyond ischemia-reperfusion injury. World journal of gastroenterology : WJG 2014;20:3572-81.

199. Entman ML, Michael L, Rossen RD, et al. Inflammation in the course of early myocardial ischemia. FASEB journal : official publication of the Federation of American Societies for Experimental Biology 1991;5:2529-37.

200. Zhou J-Y, Krovvidi RK, Gao Y, et al. Trauma-associated Human Neutrophil Alterations Revealed by Comparative Proteomics Profiling. Proteomics Clinical applications 2013;7:10.1002/prca.201200109.

201. Nauseef WM, Volpp BD, McCormick S, Leidal KG, Clark RA. Assembly of the neutrophil respiratory burst oxidase. Protein kinase C promotes cytoskeletal and membrane association of cytosolic oxidase components. The Journal of biological chemistry 1991;266:5911-7.

202. Surve CR, Lehmann D, Smrcka AV. A chemical biology approach demonstrates G protein betagamma subunits are sufficient to mediate directional neutrophil chemotaxis. The Journal of biological chemistry 2014;289:17791-801.

203. Ku CJ, Wang Y, Weiner OD, Altschuler SJ, Wu LF. Network crosstalk dynamically changes during neutrophil polarization. Cell 2012;149:1073-83.

204. Zarbock A, Abram CL, Hundt M, Altman A, Lowell CA, Ley K. PSGL-1 engagement by E-selectin signals through Src kinase Fgr and ITAM adapters DAP12 and FcR gamma to induce slow leukocyte rolling. The Journal of experimental medicine 2008;205:2339-47.

# ANNEXES

## Supplementary Data

**Supplementary Graph 1** Distribution of hematimetric parameters in the four experimental groups. (A) Hematocrit, (B) Mean corpuscular hemoglobin concentration, (C) Red cell distribution width and (D). Plateletcrit. (**P < 0.001 to 0.01; *P < 0.01 to 0.05)

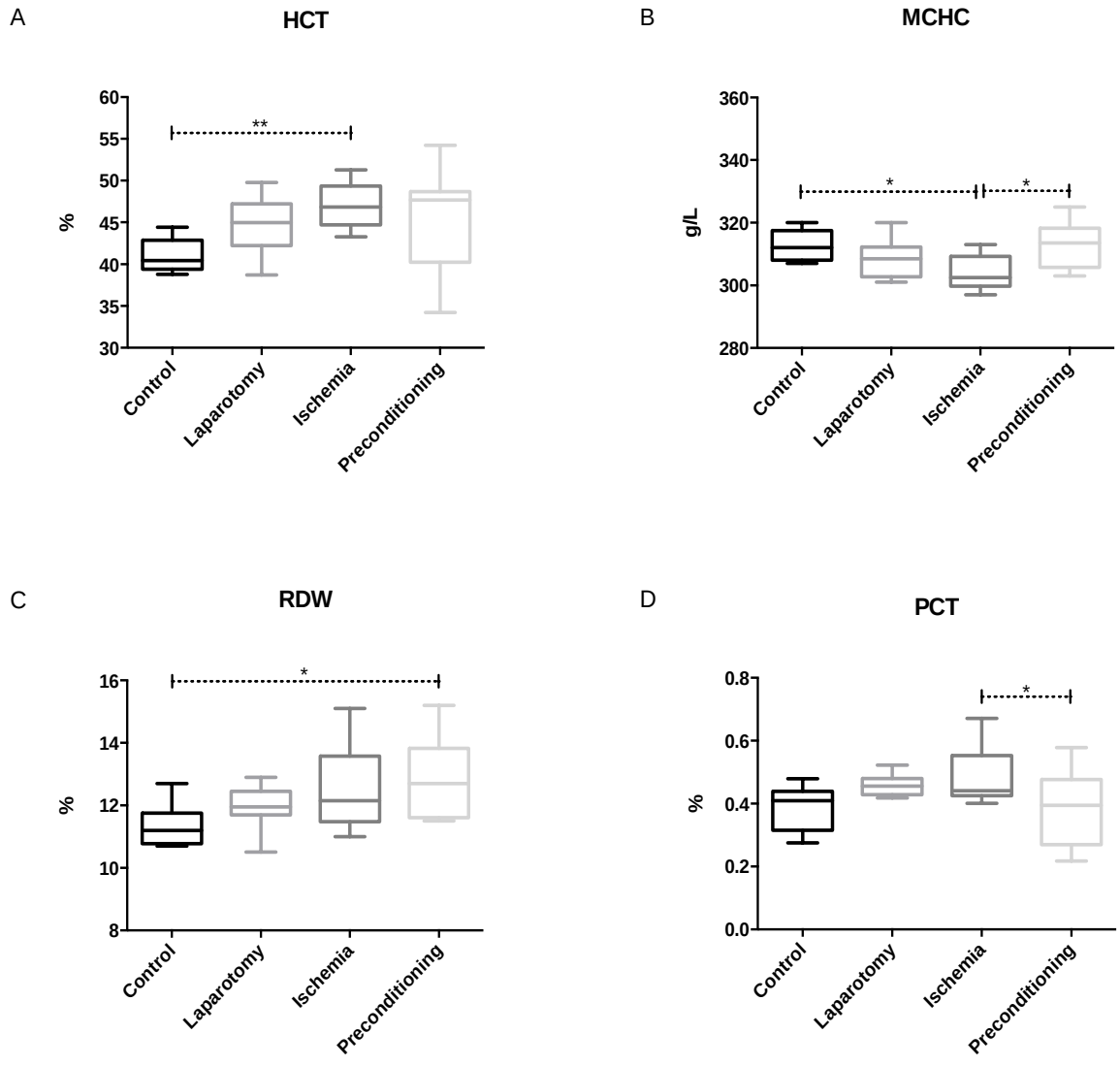

**Supplementary Graph 2** GO slim terms of proteins with differential regulation level in ST as compared to control. GO slim cellular compartment (A), biological process (B), and molecular function (C). Y-axis represents the GO terms.

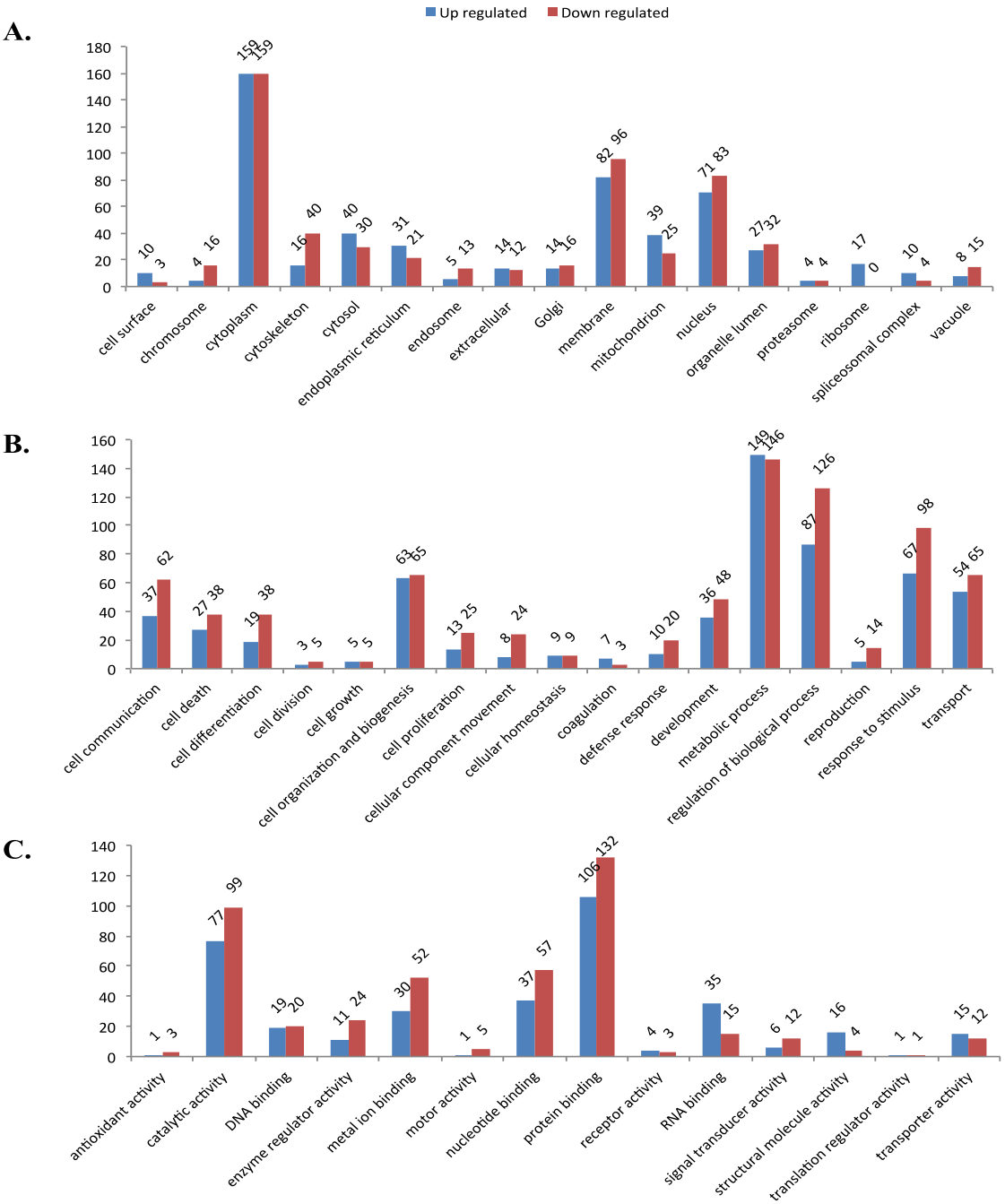

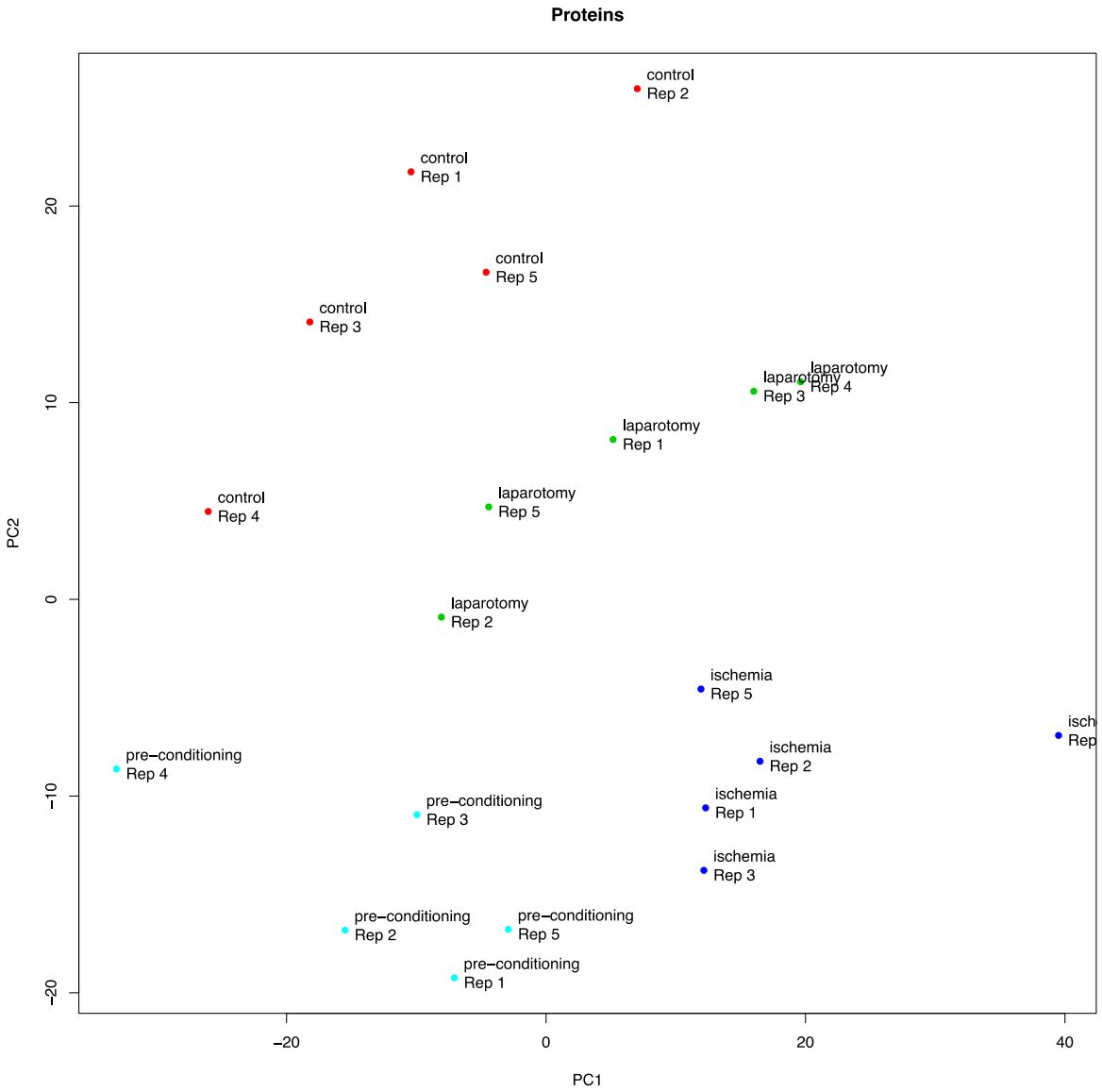


**Supplementary Figure 1** PCA analysis

Supplementary Table 1. Hematological analyses, expressed as mean ± standard deviation, median and range (min. - max.) of the four groups.

| Parameters | Control group | | | Laparotomy group | | | Ischemia/Reperfusion group | | | Preconditioning group | | |
|---|---|---|---|---|---|---|---|---|---|---|---|---|
| | Mean ± std dev | Median | Range Min - Max | Mean ± std dev | Median | Range Min - Max | Mean ± std dev | Median | Range Min - Max | Mean ± std dev | Median | Range Min - Max |
| WBC ($10^9$/L) | 10.27 ± 2.04 | 10.85 | 6.8 - 12.3 | 14.71 ± 3.4 | 15.75 | 8.6 - 18.7 | 18.13 ± 5.16 | 19.1 | 11.8 - 15.75 | 16.39 ± 4.67 | 15.7 | 8.7 - 23.2 |
| Lymphocytes ($10^9$/L) | 6.79 ± 1.59 | 7.2 | 4.1 - 8.8 | 5.6 ± 1.42 | 5.3 | 3.5 - 7.7 | 5.65 ± 1.28 | 5.65 | 3.7 - 8.8 | 5.61 ± 2.24 | 5.05 | 3.9 - 11.6 |
| Monocytes ($10^9$/L) | 0.31 ± 0.07 | 0.3 | 0.2 - 0.4 | 0.6 ± 0.28 | 0.5 | 0.3 - 1.2 | 0.71 ± 0.29 | 0.6 | 0.4 - 0.6 | 0.57 ± 0.19 | 0.6 | 0.3 - 0.8 |
| Granulocytes ($10^9$/L) | 3.17 ± 0.59 | 3.1 | 2.3 - 3.9 | 8.51 ± 2.11 | 9.15 | 4.7 - 10.7 | 13.36 ± 6.31 | 12.85 | 5 - 9.15 | 10.21 ± 3.7 | 9.85 | 4.5 - 17.6 |
| Lymphocytes (%) | 64.76 ± 2.96 | 65.1 | 60 - 70.8 | 38.26 ± 4.98 | 39.95 | 30.3 - 45.1 | 28.47 ± 5.23 | 27.35 | 22 - 70.8 | 36.33 ± 8.19 | 34.85 | 26.7 - 51.8 |
| Monocytes (%) | 3.25 ± 0.36 | 3.1 | 2.9 - 3.9 | 3.68 ± 0.6 | 3.6 | 2.9 - 4.7 | 3.36 ± 0.28 | 3.35 | 3 - 3.9 | 3.81 ± 0.43 | 3.85 | 3.2 - 4.7 |
| Granulocytes (%) | 32.1 ± 2.86 | 31.65 | 26.2 - 37.1 | 57.63 ± 4.61 | 56.75 | 51.1 - 65.9 | 67.87 ± 5.74 | 69.5 | 57.5 - 57.63 | 59.89 ± 8.25 | 61.45 | 44.5 - 69.3 |
| RBC ($10^{12}$/L) | 6.528 ± 0.55 | 6.58 | 5.49 - 7.52 | 7.38 ± 0.72 | 7.65 | 6.1 - 8.3 | 7.66 ± 0.52 | 7.665 | 6.88 - 7.65 | 7.32 ± 1.38 | 7.63 | 4.62 - 9.58 |
| Hb (g/L) | 128 ± 6.94 | 126.5 | 120 - 142 | 138.5 ± 12.03 | 138.5 | 120 - 156 | 143.3 ± 7.69 | 144 | 134 - 142 | 141 ± 20.02 | 147.5 | 107 - 167 |
| HCT (%) | 40.83 ± 1.86 | 40.45 | 38.8 - 44.4 | 44.63 ± 3.63 | 44.95 | 38.7 - 49.8 | 47.07 ± 2.61 | 46.85 | 43.3 - 44.95 | 45.14 ± 6.31 | 47.65 | 34.2 - 54.2 |
| MCV (fL) | 61.39 ± 2.46 | 61.1 | 57.2 - 65.1 | 60.41 ± 1.95 | 59.95 | 58 - 63.7 | 61.57 ± 2.34 | 61.2 | 58.2 - 65.1 | 60.8 ± 2.39 | 60.75 | 56.6 - 64.7 |
| MCH | 19.16 ± 0.75 | 19.15 | 17.6 - 20.3 | 18.6 ± 0.67 | 18.6 | 17.8 - 19.7 | 18.7 ± 0.8 | 18.8 | 17.5 - 20.3 | 18.98 ± 0.73 | 19.05 | 17.4 - 20.1 |
| MCHC (g/L) | 312.8 ± | 312.5 | 307 - | 308.7 ± | 308.5 | 301 - | 304.1 ± | 302.5 | 297 - | 312.7 ± | 313.5 | 303 - |

Suplementary Table 2 Pathway analysis for cluster 4 and 5

| Pathway | C | O | E | R | rawP | adjP | No. of Proteins | Cluster |
|---|---|---|---|---|---|---|---|---|
| | | | | | | | | |
| Regulation of actin cytoskeleton | 208 | 31 | 1.53 | 20.31 | 4.29E-31 | 5.49E-29 | 31 | 4 |
| Metabolic pathways | 1169 | 54 | 8.58 | 6.29 | 3.63E-27 | 2.32E-25 | 54 | 4 |
| Neurotrophin signaling pathway | 129 | 19 | 0.95 | 20.07 | 2.07E-19 | 7.74E-18 | 19 | 4 |
| Fc gamma R-mediated phagocytosis | 91 | 17 | 0.67 | 25.45 | 2.42E-19 | 7.74E-18 | 17 | 4 |
| Insulin signaling pathway | 131 | 18 | 0.96 | 18.72 | 6.72E-18 | 1.72E-16 | 18 | 4 |
| Chemokine signaling pathway | 178 | 19 | 1.31 | 14.54 | 1.01E-16 | 2.15E-15 | 19 | 4 |
| Focal adhesion | 186 | 19 | 1.37 | 13.92 | 2.31E-16 | 4.22E-15 | 19 | 4 |
| Leukocyte transendothelial migration | 114 | 16 | 0.84 | 19.12 | 3.32E-16 | 5.31E-15 | 16 | 4 |
| Oocyte meiosis | 115 | 16 | 0.84 | 18.96 | 3.83E-16 | 5.45E-15 | 16 | 4 |
| Long-term potentiation | 69 | 13 | 0.51 | 25.67 | 3.78E-15 | 4.84E-14 | 13 | 4 |
| Ribosome | 122 | 63 | 1.05 | 59.84 | 1.10E-97 | 1.08E-95 | 63 | 5 |
| Spliceosome | 135 | 30 | 1.16 | 25.75 | 1.59E-33 | 7.79E-32 | 30 | 5 |
| RNA transport | 156 | 23 | 1.35 | 17.09 | 1.20E-21 | 3.92E-20 | 23 | 5 |
| Protein processing in endoplasmic reticulum | 164 | 20 | 1.42 | 14.13 | 2.52E-17 | 6.17E-16 | 20 | 5 |
| Proteasome | 49 | 12 | 0.42 | 28.38 | 9.96E-15 | 1.95E-13 | 12 | 5 |
| DNA replication | 36 | 8 | 0.31 | 25.75 | 7.01E-10 | 1.14E-08 | 8 | 5 |
| Metabolic pathways | 1169 | 33 | 10.09 | 3.27 | 3.61E-09 | 5.05E-08 | 33 | 5 |
| NOD-like receptor signaling pathway | 53 | 7 | 0.46 | 15.31 | 3.70E-07 | 4.53E-06 | 7 | 5 |
| Cell cycle | 124 | 9 | 1.07 | 8.41 | 1.43E-06 | 1.56E-05 | 9 | 5 |
| Aminoacyl-tRNA biosynthesis | 61 | 6 | 0.53 | 11.4 | 1.48E-05 | 0.0001 | 6 | 5 |

**C:** *the number of reference genes in the category*
**O:** *the number of genes in the gene set and also in the category*
**E:** *the expected number in the category*
**R:** *ratio of enrichment*
**rawP:** *p value from hypergeometric test*
**adjP:** *p value adjusted by the multiple test adjustment*

1.